Nocturnal oscillations: Understanding the brain through sleep

A dissertation presented by

Chi Wing Crystal Goh

to the

Institute of Cognitive Neuroscience, *Faculty of Brain Sciences*

in fulfilment of the requirements for the degree of

Doctor of Philosophy

in the subject of

Cognitive Neuroscience

University College London

November 2013

Declaration of Authorship

I, Chi Wing Crystal Goh, declare that this thesis titled, 'Nocturnal oscillations: Understanding the brain through sleep' and the work presented in it are my own. I confirm that:

- This work was done wholly or mainly while in candidature for a research degree at this University.
- Where any part of this thesis has previously been submitted for a degree or any other qualification at this University or any other institution, this has been clearly stated.
- Where I have consulted the published work of others, this is always clearly attributed.
- Where I have quoted from the work of others, the source is always given. With the exception of such quotations, this thesis is entirely my own work.
- I have acknowledged all main sources of help.
- Where the thesis is based on work done by myself jointly with others, I have made clear exactly what was done by others and what I have contributed myself.

Signed: 

Date: 1/11/2013

UNIVERSITY COLLEGE LONDON

Abstract

Faculty of Brain Sciences
Institute of Cognitive Neuroscience

Doctor of Philosophy

Nocturnal oscillations: Understanding the brain through sleep

by Chi Wing Crystal Goh

This thesis explores the nature of sleep oscillations using behavioral and neurophysiological measures. The first experiment examines how the magnitude of different spectral frequencies in the sleep electroencephalography affect individual's subjective emotional experience of positive and negative moods, as well as the emotional detriment associated with a full night of sleep deprivation, and its recovery after a daytime nap. The change in positive and negative moods across a night's sleep is predicted by the magnitude of different oscillatory activity during rapid-eye-movement (REM) and non-REM (NREM) sleep. Experiment 2 uses EEG with simultaneous functional magnetic resonance imaging (fMRI) to examine the blood oxygen level dependent (BOLD) signal changes associated with sleep stage changes, and specifically investigates the functional connectivity changes within the basal ganglia network that occur across an early, slow-wave-rich sleep cycle. In NREM sleep, the functional connectivity of the globus pallidus and the striatum (composed of the putamen and caudate nucleus) show patterns supporting the tripartite division model, and lend support to existing studies of information processing during sleep, especially in the motor domain. Experiment 3 seeks to validate the hypothesis that different frequencies of oscillatory activity within the brain will differentially modulate the spatial profile of BOLD activity. This is achieved with applying transcranial alternating current stimulation (tACS) during fMRI acquisition, by artificially inducing oscillations of different frequencies in the brain while measuring the BOLD signal changes associated with the oscillatory activity. Stimulation to the primary visual cortex led to BOLD activity increases, relative to baseline, in different neural networks depending on the frequency of stimulation. The three experiments presented in the thesis shed light on the nature of neural network modulations caused by ongoing oscillatory activity, and bridge the gap between electrophysiological and haemodynamic findings of sleep-dependent information processing.

Acknowledgements

Thank you to British tax payers who funded my research. To my parents Dr. Lau and Dr. Goh, thank you for planting the seeds of curiosity and love, and always reminding me that the true purpose of knowledge lies in helping the world. To Professor Vincent Walsh, my dearest supervisor, mentor and friend, thank you for your patience and gift of freedom, for teaching me how, not what, for taking my concept of the Freedom Gene more seriously than others, and for always telling me that you are proud of me (and now its on paper). Thank you to the Walsh lab - a unique, international and multigenerational family unconcerned with the petty formalities of social interaction, who's complete acceptance of my true nature has served as a constant source of comfort and support that requires only presence and no words - I am grateful and blessed. Thank you to Professor Matthew Walker, for adopting me into his lab, and who's sensible expressions of scientific creativity has taught me the value of overlaying the veil of practicality onto zealous ambitions. Thank you to my student Timothy Owens, for trusting me and diving into a challenging experiment wholeheartedly. Thank you to Dr. Oliver Josephs, who's intelligence and expertise lies on a different spectrum than most humans, for his undying patience, dedication and generosity, especially at 3.00am watching six monitors simultaneously. To my dear friend and mentor Dr. Ryota Kanai, who is exempt of mammalian sleep biology and makes very difficult feats appear very easy, thank you for being a role model and for encouraging me to move beyond my limits. To Professor Jon Driver, thank you for believing in me from the very beginning. To Mu Sang Sunim, thank you for ecouraging me to keep a Zen mind in all affairs, scientific or otherwise. And to Max, simply: thank you, I love you. Lastly, I would like to thank the open source community for continuously developing and sharing amazing, powerful software for everyone.

Contents

Dedicated to all the organisms on the planet that sleep.

Chapter 1

Neuroscience of sleep

Over the last decade, research in the fields of molecular genetics, neurophysiology and the cognitive neurosciences have rapidly increased our understanding of the processes generating and maintaining sleep. We spend approximately one-third of our lives asleep, and the cognitive functions of sleep are currently the topic of extensive study and debate. The neurobiology of sleep is introduced in the following section.

1.1 Neurophysiology of sleep

1.1.1 Sleep architecture

Sleep and wake are different brain states, and specific systems of neurons determine their onset, maintenance, and termination. While wakefulness is marked by consciousness, awareness and activity, sleep is a natural state of physical inactivity that recurs periodically, characterized by the loss of consciousness and reduced responsiveness to external stimuli.

In placental mammals, sleep comprises of two distinct states - rapid eye movement (REM) sleep and non-REM (NREM) sleep - which alternate throughout a nights sleep at regular intervals (Carskadon, 2000). In humans, NREM sleep is further classified into sleep stages 1 to 4 (S1, S2, S3, S4).

Sleep architecture describes the temporal structure and pattern of REM and NREM sleep; it encompasses the amount of time spent in each sleep stage (quota), as well as the total sleep time within a 24 hour period (duration). Latency describes the time taken to reach a certain sleep stage from wakefulness, and the duration of a NREM-REM cycle is also an important aspect of sleep architecture. NREM sleep constitutes roughly 4/5 of total sleep time in most species, while the interval between REM sleep episodes - or each "sleep cycle" - varies as a function of brain size, ranging from ¡10 min cycles in rodents to 90 min cycles in humans (Zepelin & Rechtschaffen, 1974). Figure 1.1 describes a typical nights sleep of an adult human, containing five sleep cycles across approximately 7.5 hours. The amount of time spent in S3 and S4, collectively known as slow wave sleep (SWS), decreases as the night progresses, while REM quota increases towards the morning.

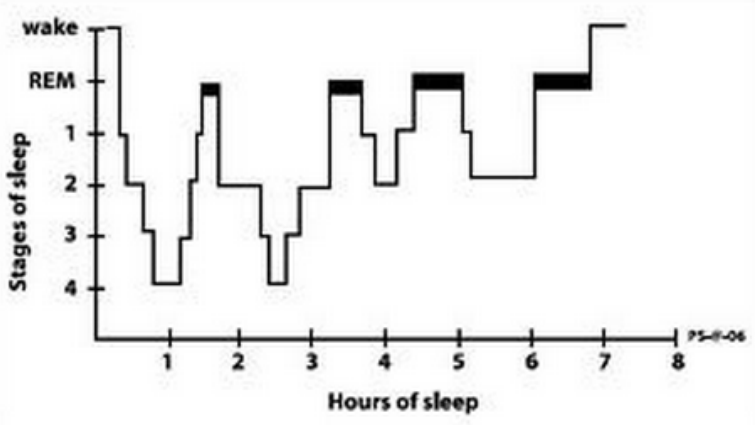

FIGURE 1.1: Hypnogram showing the typical sleep architecture of a young human adult. Black bars indicate REM sleep; five sleep cycles are shown with decreasing amounts of slow wave sleep as the night progresses.

Sleep stages are characterized by distinct scalp electroencephalography (EEG) signatures and patterns, described in detail in the following section. In general, the EEG in the waking state comprises of low voltage, high frequency signals with a dominant alpha (8-12 Hz) frequency. As sleep stages progress from S1 to SWS, the EEG displays higher levels of synchrony, reflected by higher amplitudes and lower dominant frequency patterns. In SWS, the main activity recorded is a slow delta (0.8-4 Hz) oscillation (see

Figure 1.2, bottom two traces). In REM sleep, the EEG resembles that of the waking pattern, with the exception of rapid eye movements (REMs) and a very attenuated muscle tone.

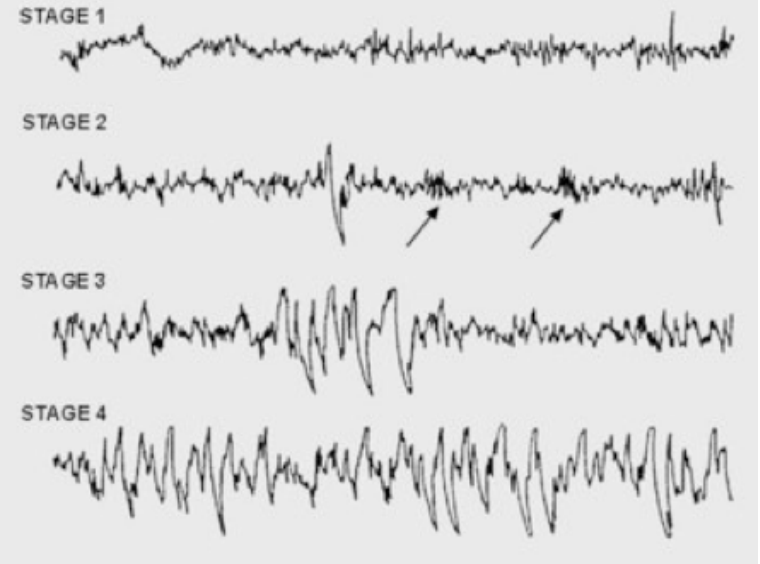

FIGURE 1.2: As NREM sleep progresses from Stage 1 to 4, the proportion of delta activity increases, indicating greater neural synchrony. Sleep spindles (arrows) are transient events in the sigma (12-15 Hz) frequency band, and characteristic of Stage 2 sleep.

1.1.2 Sleep regulation

Wakefulness is controlled by relatively diffuse structures within the ascending activating system (AAS), which stimulates activity and attentiveness throughout the entire cortex. Wakefulness requires excitatory innervation of the forebrain, and depends on the discharge activity in several parallel ascending neurotransmitter pathways that include glutamate, acetylcholine (ACh) and monoamine (serotonin and noradrenalin) systems (Jones, 2005). Figure 1.3 shows that many of the corresponding cell bodies for these systems are located in the brainstem. Electrical stimulation of the glutamatergic reticular formation (RF) of the upper brainstem produces immediate and lasting EEG desynchronization in a previously sleeping preparation (Moruzzi & Magoun, 1949), and establishes this region as the core wake-promoting center.

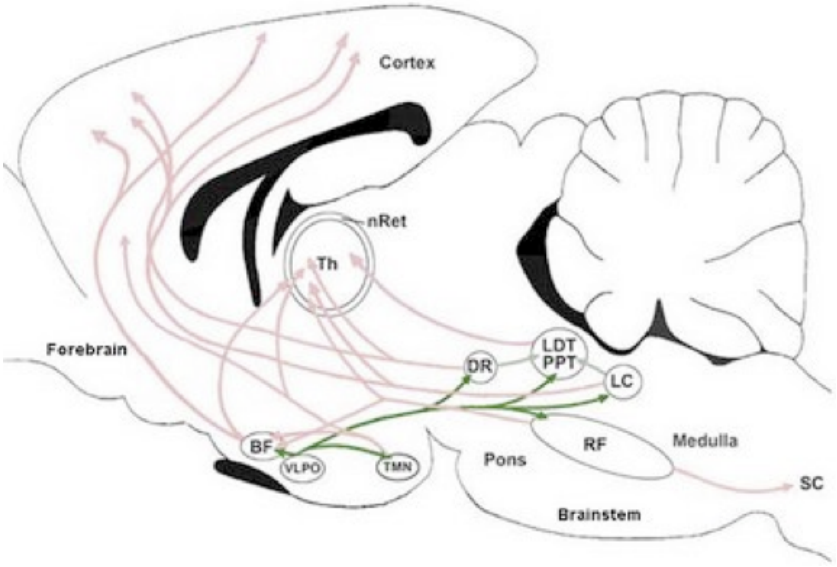

FIGURE 1.3: Sagittal schematic of the ascending activating system supporting wakefulness and sleep regulation (rodent brain). Pink arrows indicate excitatory influences, green are inhibitory. RF: reticular formation; Th: thalamus; SC: superior colliculus; LC: locus coeruleus; LDT/PPT: laterodorsal tegmentum/pedunculopontine; TMN: tuberomammillary nucleus; BF: basal forebrain; VLPO: ventrolateral preoptic area; DR: dorsal raphe.

A major component of the AAS - the thalamus - receives ascending signals from cholinergic cells in the laterodorsal tegmentum / pedunculopontine (LDT/PPT) region in the pons-midbrain junction (Steriade & McCarley, 2005). These neurons are highly active during wakefulness and REM sleep, but have low discharge rates during NREM sleep. Monoaminergic projections from the locus coeruleus (LC) and dorsal raphe (DR) contribute to the AAS via thalamic excitation (McCormick, 1989), at the same time sending widespread projections to the forebrain. These neurons show state-related changes in discharge rates, decreasing during NREM sleep and becoming virtually quiescent during REM. The histaminergic tuberomammillary nucleus (TMN) of the caudolateral hypothalamus also projects to the thalamus and forebrain, and shows similar state-related changes.

The thalamus and cortex receives a secondary ascending cholinergic projection from the basal forebrain (BF), which, like the LDT/PPT system, is a component of the AAS that is crucial for maintaining wakefulness via afferent brainstem input (see Figure 1.3,

red lines). Therefore there are two major relay pathways for cortical activation from the brainstem, one via the thalamus and the other through the BF, as well as direct projections from the LC and DR to the cortex.

Sleepiness is determined by two factors - homeostasis and circadian rhythm. Sleep homeostasis is the internal regulatory mechanism that depends on the duration since the last sleep out. The longer the time spent awake, the higher the sleep propensity, and greater the duration and intensity of subsequent sleep, indexed by the amount of EEG delta (1-4 Hz) activity. Adenosine accumulates during wakefulness, inhibiting components of the AAS (especially the BF cholinergic pathway; see Figure 1.3, green lines) and induces sleepiness (McCarley, 2007). Circadian rhythm on the other hand is independent of the amount of preceding sleep or wakefulness, and varies with a 24 hour periodicity. The suprachiasmatic nucleus (SCN) within the hypothalamus serves as a diurnal pacemaker and inhibits brainstem projection during sleep, thus shutting off the arousal system.

1.2 Sleep electrophysiology

1.2.1 Introduction

The first sleep EEG was recorded in 1929 by the German psychiatrist Hans Berger. Ever since, EEG has been the hallmark of determining, or "scoring", changes in alertness and sleep stages. EEG is used in combination with the electrooculogram (EOG) and electromyogram (EMG) to define sleep states. The polysomnography (PSG) scoring criteria originated with the Rechtschaffen and Kales (1968a) scoring manual, and now includes the American Academy of Sleep Medicine's manual for sleep scoring (Iber, 2007). Other main electrophysiological findings are derived from intracortical or unit cell recordings from animals, which are informative but not directly relevant for understanding sleep- related cognition in humans. The scoring criteria for each sleep stage are summarized below, and their putative neural mechanisms are described using recent electrophysiological evidence.

1.2.2 Wakefulness

Wakefulness is defined by a low-voltage, high frequency EEG pattern consisting of primarily beta (15-30 Hz) and low gamma (30-50 Hz) activity with the eyes open, and dominated by alpha (8-12 Hz) activity with the eyes closed. This stage is usually accompanied by relatively high tonic EMG, and the EOG trace open contains REMs and blinks.

1.2.3 Stage 1

S1 occurs in transition from wakefulness to other sleep stages, or after body movements during sleep. In nocturnal sleep, S1 duration is relatively short compared to during daytime naps, lasting between 1-7 minutes. S1 is characterized by relatively low voltage, mixed frequency EEG with prominence in the theta (4-8 Hz) band, with faster frequencies in a lower voltage than the theta activity (see Figure 1.2, top trace). The early portions of S1 contains slow eye movements, each several seconds long, as well as a general slowing of the EEG with decrease in amount, amplitude and frequency of alpha activity. The latter portions of SS1 shows the highest voltage theta activity (50-75 uV), occurring in irregularly spaced bursts. Vertex sharp waves with amplitudes as high as 200 uV can also appear in conjunction with the background high amplitude theta.

1.2.4 Stage 2

S2 is notable for the presence of spindles (Sp), which are brief waxing and waning bursts of frequencies in the sigma (12-15 Hz) band, lasting 0.5 - 1 second, occurring against a background of relatively low voltage, mixed frequency EEG activity (see Figure 1.2, arrows). Sp often co-occur with K complexes (Kc), which are EEG waveforms with a well delineated negative sharp wave immediately followed by a positive component. Kc are maximal over vertex areas (e.g. C3/4 on the International 10-20 system), and long periods of absence may intervene between their presence without the of occurrence of a stage change.

Two kinds of Sp are described in humans: slow Sp (11-13 Hz) predominate over frontal regions, whereas fast Sp (13-15 Hz) predominate over centro-parietal areas. These two spindling activities differ in their homeostatic and circadian regulations, development in infancy, pharmacological reactivity (De Gennaro & Ferrara, 2003) and also by their association with general cognitive function (Bódizs, Sverteczki, Lázár, & Halász, 2005). Source localization of the EEG scalp recordings reveal two sources: slow Sp originate from the mesial frontal region, while fast Sp arise from the precuneus (Anderer et al., 2001). It is debated, however, whether these functional differences are due to activity of different neural networks, or a consequence of differential modulation of a single generator (De Gennaro & Ferrara, 2003). It is important to note also that while Sp are most substantial during S2, they also occur during SWS in conjunction with delta waves and slow oscillations, which are described below.

1.2.5 Slow wave sleep

S3 and S4 are scored according to the proportion of delta slow waves observed (see Figure 1.2, bottom two traces). Together, they are termed slow wave sleep (SWS), where the EEG consists of waves with amplitudes >75 μV peak-to-peak. During this state, the EOG can also show gradual rolling eye movements, and there is low muscle activity.

Whether slow and delta waves differ qualitatively or quantitatively is unknown. EEG power density within the delta frequency band (1-4 Hz) declines from the first to the second NREM sleep episode through the night, while that of the slow wave frequency band (<1 Hz) does not. Animal intracellular recordings show that the slow oscillation (<1 Hz) of cortical neuron membrane potentials is the fundamental cellular phenomenon that underlies neural activity in NREM sleep (Steriade, Curró Dossi, & Contreras, 1993). The slow oscillation of SWS represents a spontaneous event where cortical neurons are alternately silent and active for a few hundred milliseconds. It consists of a "down-state", when virtually all cortical neurons are deeply hyperpolarized and remain silent. This is followed by a depolarization phase or up-state, also lasting for several hundred milliseconds, during which the membrane potential surges back to firing threshold. This

causes intense synaptic activity in the entire thalamocortical system, and neurons fire at rates even higher than during quiet wakefulness (Steriade, 2001).

The slow oscillation organizes the synchronous delta and sigma neuronal oscillations. At the cellular level, hippocampal activity is particularly influenced by and synchronized to the cortical slow oscillation (Isomura et al., 2006). These are caused by a large fraction of hippocampal pyramidal neurons firing bursts of action potentials within a 40-120 ms time window, and observed as sharp waves occurring at irregular intervals (0.02-3 s_1) (Buzsáki, 1996). Ripples - brief 200 Hz oscillations produced by hippocampal interneurons - are phase-locked to sharp waves, and are observed in association with sharp waves in hippocampal field potential recordings (Mölle, 2006).

Using high-density scalp EEG, Massimini, Huber, Ferrarelli, Hill, and Tononi (2004) captured both widespread and local slow oscillation cycles, and demonstrated that each cycle of the slow oscillation is a traveling wave. Slow oscillation cycles were defined with a negative zero-crossing onset and a subsequent positive zero-crossing separated by 0.3-1.0 seconds, and a peak-to-peak amplitude of $>140\ \mu V$. The spatial and temporal development of the slow oscillation is as follows: each wave originates at a definite site - more frequently in prefrontal-orbitofrontal regions - and propagates over the scalp in an anteroposterior direction, at an estimated speed of 1.2-7.0 m/sec (Massimini, Huber, Ferrarelli, Hill, & Tononi, 2004). The time series of slow oscillation detections were correlated with sleep stage progression, with no occurrence during wakefulness and REM sleep, sporadic detection corresponding to Kc during S1/2, and the highest detection rates in SWS - up to 1.25 per second or 0.8 Hz.

1.2.6 REM

Neuronal activity during REM sleep vs. eyes-opened-wakefulness are largely similar (Hobson & Steriade, 1986), with the fundamental difference that EMG signal is at its lowest throughout the entire sleep episode. For this reason, REM sleep is often referred to as "paradoxical sleep", and is characterized by:

1. A cortical EEG showing relatively low voltage and mixed frequencies with theta predominance (Rechtschaffen & Kales, 1968a);
2. Rapid eye movements (Aserinsky & Kleitman, 1953);
3. Autonomic activation;
4. Loss of muscle tone (R. Berger, 1961).

REM sleep further consists of two functional microstates: phasic REM and tonic REM, where the former includes bursts of phasic activity such as REMs and is characterized by a lack of reactivity to sensory stimuli due to neuronal adaptation, while the latter contains no REMs and is comparatively more sensitive to external stimuli. Sleep stages progress from wakefulness to SWS in association with subjective experience of loss of self-awareness. REM sleep is of special interest because self-awareness partial and transiently reappears during this sleep period, mainly in relation to dreams (Kubota et al., 2011). EEG desynchrony during REM sleep is one of its staging criteria, and suggests higher cortical activation relative to NREM sleep.

REM sleep in humans and other non-human primates is also characterized by high levels of ponto-geniculo-occipital (PGO) waves, which are phasic field potentials caused by bursts of neuronal firing that originate in specific pontine regions, and propagate through the lateral geniculate nucleus (of the thalamus) to the occipital cortex and other brain regions (Datta, 2000).

A recent EEG and magnetoencephalography (MEG) study examined the temporal relationship between low gamma activity and REMs in phasic REM sleep, and found increased activation and functional decoupling between the left frontal areas and posterior sensory-associated regions, as well as increased functional coupling between the right frontal and midline alerting systems (Corsi-Cabrera, Guevara, & del Río-Portilla, 2008).

A separate MEG study also demonstrated significant increase in slow wave and gamma band activity within the lep dorsomedial prefrontal cortex (PFC) and left dorsolateral PFC (DLPFC) during REM sleep, compared to the waking baseline state (Ioannides,

Kostopoulos, Liu, & Fenwick, 2009). The PFC is an important area for executive control and attentional processing, as well as consciousness generation (Duncan & Owen, 2000). These observed electrophysiological activities in the PFC during REM may explain partial reappearance of self-awareness related to dreaming, via temporal activation patterns specific to REM sleep (Muzur, Pace-Schott, & Hobson, 2002).

1.3 Sleep imaging

Combining EEG and MRI imaging methods provides insight into the spatial activation patterns that are associated with sleep stages, EEG frequency power changes, and EEG events during sleep. Older studies using positron emission tomography (PET) suggest a global decrease in cerebral and thalamic activity during NREM (Wu, Buchsbaum, Hershey, & Hazlett, 1991; Maquet et al., 1997; Nofzinger et al., 2002; Peigneux, Laureys, & Maquet, 2001), in accordance with the EEG slow potential activity. The most consistent results report that REM and NREM both display diminished brain activity in prefrontal and parietal areas relative to wakefulness. Specifically, light sleep is characterized by deactivation in the frontal and parietal cortices, and in the thalamus, compared to wakefulness. In deep sleep, additional decrease is observed in the basal ganglia. REM sleep, in contrast, is accompanied by cerebral blood flow (CBF) increase in the pons, limbic system, and the secondary visual cortex, and CBF decrease in the parietal and prefrontal regions. However, PET studies have relatively low temporal resolution compared to fMRI, and are unable to capture metabolic activity related to transient EEG events that distinctly characterise sleep electrophysiology.

The following sections will introduce findings from sleep imaging studies performed with concurrent EEG-fMRI, according to two main fMRI analysis methods:

1. modeling the effects of sleep stages and EEG events in the fMRI signal with linear regression, where regressors are derived from the EEG signal directly and indirectly;

2. examining functional connectivity - the way in which brain regions coactivate - during different sleep stages determined by the EEG signal.

1.3.1 Linear regression methods

The first concurrent EEG-fMRI sleep study was conducted by Kaufmann et al. (2006). This study defined the onsets of each sleep stage change by scoring the EEG, and convolved the boxcar onset regressors with the haemodynamic response function (HRF). The BOLD signal associated with each sleep stage was then contrasted against a waking baseline and against each other, to determine activation differences between these sleep stages.

1.3.1.1 Stage 1

Kaufmann et al. (2006) reported strong deactivations during S1 (relative to wake) in thalamic structures, the dorsal cingulate gyrus and the caudate nucleus, with other weaker deactivations in the frontal and occipital lobes. No significant differences between BOLD signal during S1 and wakefulness have since been reported. This does not necessarily indicate that there are no detectable gross cortical activation differences, but rather illustrates the need for models with higher sensitivity when using multiple regression in the fMRI analysis.

1.3.1.2 Stage 2

Kaufmann et al.'s study first reported signal decreases comprising thalamic and hypothalamic regions, the cingulate cortex, right insula and adjacent regions of the temporal lobe, the inferior parietal lobule and the inferior/middle frontal gyri. The authors suggest that these regions form a network required for a "disjunctive state" in which perception of wakefulness is discontinued, as S2 is often associated with loss of consciousness, and therefore the establishment of synchronized sleep is not likely to be explained by a single "super-structure".

Using a different analysis approach, Laufs, Walker, and Lund (2007) obtained the EEG frequency power time series in the delta, theta, alpha and sigma (12-15 Hz; the range for spindles) bands and compared the BOLD signal related to power fluctuation in each band, within each sleep stage. They found that as alpha power decreased during S2, BOLD signal increases were seen in the bilateral precuneus, posterior cingulate, prefrontal and temporoparietal cortices. This agrees with previous PET sleep data showing decreased activity in the retrosplenium and prefrontal cortices during NREM sleep, relative to wakefulness (Maquet, 2000). There is wide over- lap with regions within the default mode network (DMN) (M. E. Raichle, MacLeod, & Snyder, 2001), whose activity during resting wakefulness is higher than during sleep or active perception and action. Both alpha power and DMN activity reflect a subjects vigilance level, and may explain their correlation during S2.

Bilateral thalamic BOLD signal during S2 is also increased with decreasing alpha power, but positively correlated with sigma power changes. The thalamus plays a role in the cortico-thalamic spindle-generating loop during S2 (Steriade & McCarley, 2005). That haemodynamic changes are opposite in direction for alpha versus sigma power variation is in keeping with a decrease in alpha activity during the transition from wakefulness to sleep and the coincident occurrence of Sp.

1.3.1.3 Spindles and k-complexes

PET studies have previously shown a negative relationship between thalamic CBF and the power spectrum in the sigma band (Hofle et al., 1997). Spindles (Sp) and K-complexes (KC) are transient EEG events that open co-occur, and their associated BOLD signals have recently been studied using an event-related fMRI design. Laufs et al. (2007) reported changes in the thalamus and frontal, central, temporal and occipital cortices, reflecting synchronized activity of the primary sensorimotor, visual and auditory cortices along with the thalamus. Signal changes were opposite in direction: KC correlated with deactivation and Sp was related to activation. This is in contrast to previous PET reports of deactivation, but in line with cellular evidence (Amzica & Steriade, 1997) and observations from rat studies demonstrating that KC mark "down-to-up"

state transitions, whilst Sp activity occurs in the subsequent upstate (Mölle, Marshall, Gais, & Born, 2002; Battaglia, Sutherland, & McNaughton, 2004).

Another recent EEG-fMRI study reported activation patterns common to both fast and slow spindles, involving bilateral thalami, anterior cingulate and insula cortices, and the superior temporal gyri (Schabus et al., 2007). To further investigate whether fast and slow Sp originate from separate neural networks, the authors directly contrasted BOLD signal associated with each spindle type (as opposed to contrasting each type with wakefulness). Beyond the common activation pattern, slow spindles were found to correlate with significant activity increase in the superior frontal gyrus, whilst fast spindles recruited sensorimotor regions more strongly, as well as the hippocampus and mesial frontal cortex. These findings corroborate the existence of two types of spindles in human NREM sleep, and suggest that fast spindles are responsible for sensorimotor and mnemonic information processing (Schabus et al., 2007). Both studies point towards areas that may be involved in sensory replay or memory formation during sleep, especially in the superior and mid temporal gyri, but whether these areas are actively involved in these processes during sleep remains unconfirmed.

1.3.1.4 Slow wave sleep

Laufs et al. (2007) reported no significant associations between BOLD and EEG frequency power time courses during SWS. While one might expect correlations in the delta (1-4 Hz) and slow-wave (<1 Hz) bands, it has been shown that slow EEG oscillations during sleep are "traveling waves" (Massimini, Huber, Ferrarelli, & Hill, 2004), such that each oscillation originates frontally and travels in an anterior-posterior trajectory. While slow oscillations are readily detected by scalp EEG during S3/4, they are neither synchronized in space nor periodic in time. Thus the haemodynamic changes generated by spatially moving cortical activity are unlikely to be detected by a one-dimensional regressor derived from a single stationary electrode (e.g. theta and delta activity derived from Cz), as was the approach taken in Laufs' study.)

Spontaneous BOLD signal changes related to slow wave sleep is tracked with better precision using an event- related approach, similar to the study by Schabus et al. (2007)

on spindles. This is done specifically by time-locking the haemodynamic response function convolution to the onset of each individual slow oscillation. An important study by Dang-Vu et al. (2008) did so to identify brain areas recruited during slow waves and delta waves, operationally defined by amplitudes (rather than frequency limits) of >140 μV and 75-140 μV respectively.

Wave-onset was determined by the maximum negativity of each wave, considered to reflect the intracellularly defined slow oscillations transition from the hyperpolarized (down-state) to depolarized phase (up-state). Relative to the SWS baseline activity, which consisted mainly of small-amplitude >4 Hz oscillations, they found that both slow and delta waves were associated with activity increase in the pontine tegmentum (including the locus coeruleus), the midbrain, cerebellum, hippocampal gyrus, inferior gyrus, midfrontal gyrus, precuneus and the posterior cingulate cortex (Dang-Vu et al., 2008).

Still relative to the baseline SWS activity, slow waves were in particular related to increased activity in the pons, cerebellum and parahippocampal gyrus, while delta waves were associated with frontal increases, namely in the medial prefrontal cortex and inferior frontal gyrus. There were no differences when slow wave vs. delta wave activities were directly contrasted, and no significant decreases were associated with either wave type. The activations reported were also specifically related to the presence of the waves rather than specifically the up-state/depolarizing phase, as moving the event onsets to the consequential positive peak uncovered identical brain activation patterns.

The authors argued that SWS is characterized at the macroscopic systems level by phasic increases in regional brain activity, which are related to discrete events such as slow waves or delta waves. This particular event-related approach reveals findings of BOLD signal increases only, in contrast to earlier PET and block- design fMRI studies that report brain activity decrease during SWS (Maquet et al., 2000; Kaufmann et al., 2006). This is largely attributed to the difference in statistical contrasts used - while earlier studies compared brain activity distribution during sleep and wakefulness, the event-related design describes transient changes in regional activity associated with

discrete SWS waves relative to a baseline of low-power theta, alpha and beta activity in NREM sleep.

These cortical activities associated with SWS oscillations are widespread, but not global. They are identified in discrete cortical areas and characterize the activity consistently associated with detected slow and/or delta waves across subjects, rather than responses elicited by each individual wave, whose site of origin and propagation pattern can vary (Massimini et al., 2007). The pattern of frontal-dominant responses (including medial, orbital, inferior and mid-frontal gyri, but not the superior frontal gyri) and limited parietal and temporal association areas (precuneus only) agrees with scalp EEG recordings indicating frequent slow oscillation-initiation in the region between the DLPFC and OFC.

1.3.1.5 REM

The presence of REMs is a classical definition of REM sleep (Rechtschaffen & Kales, 1968b), signifying transient phasic activations embedded within tonic periods of sustained high-frequency EEG and muscle tone suppression (Hobson & Pace-Schott, 2002; Pace-Schott & Hobson, 2002). A recent EEG-fMRI study revealed differences in sensory processing and in thalamocortical activity patterns during the tonic vs phasic REM sleep periods in humans (Wehrle et al., 2007). The authors delivered an acoustic stimulation during REM sleep, which elicited residual activation of the auditory cortex only during tonic REM sleep back- ground. In contrast, phasic REM containing bursts of REMs was characterized by a lack of reactivity to sensory stimuli. The authors conclude that a thalamocortical network including limbic and parahippocampal regions contributed to a functionally isolated and closed intrinsic loop that was specific to phasic REM sleep only, and argue for the specific division of REM sleep into tonic and phasic functional microstates.

These results further support the activation of limbic system and memory circuits during human REM sleep, where the transient co-activation of amygdala, hippocampus, cingulate and sensory cortex form an emotional-perceptual-memory circuit. This network may also account for processing and retrieval of emotional information during

both wakefulness and sleep (Wagner, Gais, & Born, 2001; Hobson & Pace-Schott, 2002; Walker, Liston, Hobson, & Stickgold, 2002; Peigneux, 2003). The synchronous activity of the thalamus, limbic structures and hippocampus/parahippocampus during REM is also associated with generation of emotionally intense dream contents (Maquet et al., 1997; Hobson & Pace-Schott, 2002; Cantero et al., 2003). The amygdala activation strengthens phasic REM sleep elements, which may be crucial for plasticity changes on a neuronal level (Morrison, Sanford, & Ross, 2000; Datta, Mavanji, Ulloor, & Patterson, 2004). From an evolutionary perspective, REM sleep in mammals is closely linked to the development of the nervous system, and so findings from this study strengthen the supposition that REM sleep-related processes contribute to the enhancement of cortical plasticity (Maquet, 2000; Pace-Schott & Hobson, 2002).

1.3.2 Functional connectivity

Studies of functional connectivity in human sleep seek to address a different question compared to the studies mentioned above. Rather than asking which brain regions are more or less activated during specific sleep stages, it examines the way in which a specific functional network changes its dynamics across sleep.

Functional connectivity allows identification of neuroanatomical systems on the basis of correlation patterns in spontaneous BOLD signals. The spatial properties of the spontaneous BOLD signal therefore reflects regions of similar functionality, and gives insight into the fundamental functional architecture of a system. The most simple, sensitive and interpretable method is to average the BOLD time-course of all voxels within an area of interest, and correlating this signal with that of all other voxels within the brain, to uncover a pattern of coactivation (Fox & Raichle, 2007). Disadvantages of this method include the requirement of an a priori definition of a seed region, and that the extracted waveform may not be a true independent variable when assessing statistical significance. Nonetheless, this method is most widely used in functional connectivity studies. Hierarchical clustering is another method used that requires no seed region definition, and produces a correlation matrix of multi-seed time-courses; the limiting

factor in this method is determined by the clustering algorithm used for the hierarchical tree or topological map.

Much of the functional connectivity work performed during human sleep pertains to the way in which nodes within the default mode network (M. E. M. Raichle & Snyder, 2007) change their connectivity strength during different stages of sleep. Horovitz et al. (2008) found that the default mode network maintains the same pattern during light sleep as in wakefulness. Seeding the posterior cingulate cortex (PCC), the nodes of the DMN include the bilateral angular gyrus / inferior parietal lobule, the mid frontal gyrus and anterior cingulate cortex (ACC). During deep sleep, however, the reduction of consciousness was reflected in the altered correlation between the frontal nodes and the PCC. The authors attributed this change to the decrease in consciousness during sleep. However, this reduced frontal involvement within the DMN during deep sleep has subsequently not been replicated.

Studies of functional connectivity within the default mode network (Koike, Kan, Misaki, & Miyauchi, 2011), as well as other networks such as the dorsal attention system, the executive control system, as well as the visual, auditory and somatomotor systems (Larson-Prior et al., 2009), have shown that NREM sleep causes little or no change to the network dynamics. In fact, studies examining functional connectivity during sleep with EEG data have shown that coherence increases, rather than decreases, during sleep (Ferri, Rundo, Bruni, Terzano, & Stam, 2007; Dimitriadis, Laskaris, Del Rio-Portilla, & Koudounis, 2009).

Based on these findings, other studies have sought to measure the level of information integration during sleep using graph theory. Graph theoretical analysis of resting state fMRI during wake reveals a small-world organization of functional brain networks (Achard, Salvador, Whitcher, Suckling, & Bullmore, 2006). Small world topologies are characterised by dense clusters of neighboring nodes and at the same time a short path length between distant pairs of nodes (Bassett & Bullmore, 2006). Small-world models therefore support integrated processing over the entire network, as well as specialized processing in local clusters, and is befinng for large-scale brain networks. Spoormaker et al. (2010); Spoormaker, Czisch, Maquet, and Jancke (2011) have shown that small-world

properties are highest in deep NREM sleep, lowest in light NREM sleep, and intermediate during wake. Corticocortical functional connecitivty, on the other hand, was highest in light NREM sleep and lowest in deep NREM sleep. This indicates that the brains ability to integrate information across functional modules is limited both during light and deep sleep, albeit by different processes.

1.4 Conclusion

Existing evidence provides insight into the neurophysiological dynamics of sleep that may relate to the wide range of cognitive processes influenced by sleep. For example, the relationship between memory consolidation and sleep has been well documented (Diekelmann, Born, & Wagner, 2010; Stickgold & Walker, 2007; Walker, Stickgold, Alsop, Gaab, & Schlaug, 2005; Schabus et al., 2004; Diekelmann, Wilhelm, & Born, 2009; Rauchs et al., 2011; Wilhelm, Diekelmann, & Born, 2008; Rasch & Born, 2013; Diekelmann & Born, 2010; Marshall & Born, 2007; Bergmann, Mölle, Diedrichs, Born, & Siebner, 2012), lending insight to higher level processes such as creativity (Stickgold & Walker, 2004) and emotional perception (van der Helm, Gujar, & Walker, 2010; Schröder, 2010; Wagner et al., 2001; Payne & Kensinger, 2011).

Chapter 2

Experiment 1: Sleep-dependent regulation of subjective emotional experience

This study examines the effects of sleep and sleep deprivation on subjective emotional experience, as well as the relationship between sleep electrophysiology and changes in subjective emotional experience before and after sleep. Forty-seven young adults underwent a total sleep deprivation (SD) session as well as a normal sleep session under controlled laboratory conditions, separated by at least one week. Their subjective reports of mood (Positive and Negative Affect Schedule) were measured before and after sleep in the sleep session, and before and after deprivation in the SD session. Subjects' electrophysiological data were also measured during sleep. Results show that SD increases negative mood and reduces positive mood, and that a post-deprivation nap does returns the positive mood to pre-deprivation baseline, but not for negative mood. Additionally, sleep physiology influences mood changes for positive and negative affect in opposite directions. Specifically, increase in positive mood is predicted by *low* theta power in NREM sleep EEG, but increase in negative mood is predicted by *high* theta power in REM sleep, as well as delta power in Stage 2 sleep. These results are discussed in terms of

2.1 Introduction

The functional role of sleep extends beyond cognitive processes of memory consolidation. A growing body of evidence points to an intimate relationship between affective brain regulation and sleep, and is concomitant with the common observation that patients with mood disorders also experience sleep dysfunction. For example, psychiatric mood and anxiety disorders such as major depression, post-traumatic stress disorder (PTSD) abnormalities and bipolar disorder, are characterized by abnormal limbic activity / limbic-prefrontal connectivity (Ohayon & Shapiro, 2000; Adrien, 2002; Harvey, Jones, & Schmidt, 2003; De Hert, van Eyck, & De Nayer, 2006), and very often co-occur with sleep dysfunction, where similar brain regions are also affected. The symbiosis between sleep and affect is seen in adaptive benefits following the presence of sleep, in particular REM, as well as the detrimental consequences caused by the absence of sleep.

2.2 Sleep and emotion

In REM sleep, affect-related cortical regions such as the amygdala, hippocampus and "extended limbic circuit" of the mPFC show elevated activity (Nofzinger, 2005). This is paralleled by a reduction of noradrenaline levels, resulting from the suppression of activity in the locus coeruleus (Marrosu et al., 1995), leading to relatively higher levels of cholinergic activity. These anatomical and chemical systems largely overlap with systems that support emotion processing in the waking brain, and overlap with systems that are disrupted following sleep deprivation (SD).

In addition to impairments of vigilance, attention and memory, SD is often associated with emotional instability and irritability (Horne, 1985). Restricting sleep to only five hours per night for one week will increase an individual's level of emotional disturbance, as detected through mood scale questionnaires, as well as increasing the level of subjective emotional difficulties, as documented in diaries (Dinges, Pack, Williams, & Gillen, 1997). Medical residents with accumulated sleep loss also experience an amplified negative emotional response from disruptive daytime events, and are unable to feel

the benefits of positivity associated with goal-enhancing activities (Zohar, Tzischinsky, Epstein, & Lavie, 2005).

SD is also known for its temporary antidepressant benefit in patients with major depressive disorder, despite its ability to exaggerate negative mood (Gillin, Buchsbaum, Wu, Clark, & Bunney, 2001). A full night of SD also causes abnormally amplified responses to pleasure-evoking stimuli, as the threshold for emotional stimuli to be judged as "pleasant" is lowered (Gujar, Yoo, Hu, & Walker, 2011). This illustrates the detrimental effects of SD as an exaggeration of subjective emotional experience, regardless of positive or negative valence. In other words, the sleep deprived individual experiences emotions more intensely than he or she would, in the face of the same environment or stimuli that would otherwise evoke a less substantial subjective emotional response if the individual had a full night of rest.

Interestingly, SD not only increases sensitivity of subjective mood, but also causes inaccurate recognition and expression of both positive and negative emotional signals. For example, a full night of SD will impair one's ability to recognize the emotional intensity of facial expressions (van der Helm et al., 2010), especially in "Happy" and "Angry" faces, and especially in women. The authors suggest that the observed gender difference in impairment may be linked to differences in mood regulation in men and women, where women display higher levels of salivary cortisol levels after SD, reflecting higher levels of stress (Birchler-Pedross et al., 2009). The inability to accurately recognize emotions in faces has been linked to a lack of empathy, and has been well documented in developmental disorders such as autism, as well as consistently linked to social dysfunction (Itier & Batty, 2009). In addition, SD has also been shown to attenuate emotional expressiveness and even impairs the sleep deprived individual's emotional facial and vocal expression (McGlinchey et al., 2011), where sleep deprived individuals' facial expressions appear less responsive when watching emotional film clips, despite maintaining the same level of subjective emotional reaction to the film clips (Minkel, Htaik, Banks, & Dinges, 2011).

Results from these studies show that while SD *amplifies* subjective emotional arousal, it also impairs emotional recognition and *decreases* the emotional intensity of expression

in response to emotive stimuli. This unique pattern of behavior has been explained in terms of the changes in cortical activation and connectivity following SD, and its relation to emotional processing.

2.3 Sleep loss and emotional brain function

Compared to after a restful night of sleep, the sleep-deprived brain's neural responses to emotionally salient stimuli are in fact *enhanced*. fMRI studies reveal that a single night of SD induces a 60% increase in amgydala BOLD activation when faced with aversive stimuli. Furthermore, the amygdala significantly *decreases* its functional connectivity with regions responsible for its top-down regulatory control - namely the ACC and mPFC, but *increases* functional connectivity with the locus coeruleus - the fight-or-flight adrenergic-activating brainstem structure (Yoo, Gujar, Hu, Jolesz, & Walker, 2007). Additionally, excessive pupil dilation is observed during passive viewing of negative visual stimuli (Franzen, Buysse, Dahl, Thompson, & Siegle, 2009). Both neural and autonomic responses are increased following sleep loss, leading to a subjectively more intense experience of fearful or negative emotions.

The same is true for the subjective experience of positive emotions towards positive stimuli. Compared to after a restful night, the dopaminergic mesolimbic systems show significantly greater neural response to pleasure-evoking stimuli after SD, as well as lowered functional connectivity to areas responsible for its feedback-control - the medial prefrontal cortex (mPFC) and orbital prefrontal cortex (oPFC) (Gujar et al., 2011). This activation profile caused by SD is particularly promoting of reward-seeking behaviors, such as taking higher risks for monetary gains in gambling tasks (McKenna, Dickinson, Orff, & Drummond, 2007; Venkatraman, Huettel, Chuah, Payne, & Chee, 2011), or altering the willingness to exchange money for glimpses of attractive faces (Libedinsky et al., 2011).

Together, these findings support the hypothesis that SD leads to affective dysfunction, caused by a disconnection between *(i)* primary subcortical limbic and striatal affective

signals, and *(ii)* their subsequent higher-order re-representation. The weakened connectivity between brain regions responsible for affective processing, and those that in turn interpret and reciprocally control their salient signals, explains the biased increase in emotional intensity subjectively experienced after SD, regardless of emotional valence.

2.3.1 Current hypothesis

Given the intimate relationship between sleep and emotional regulation, the present study aims to investigate:

1. How changes in subjective mood, in the absence of emotional stimuli, differ across sleep vs. across SD
2. Whether a recovery nap following a full night of sleep deprivation can allow subjective mood to return to a 'pre-deprivation' baseline
3. Whether changes in subjective mood across a night of sleep can be predicted by temporal or electrophysiological markers of sleep

The effect of SD on positive and negative moods is inconsistent in the literature, and depends on the experimental paradigm. The Positive and Negative Affect Schedule (PANAS), which is a 20-item self-report measure of positive affect (PA) and negative affect (NA)(D. Watson, Clark, & Tellegen, 1988), has been shown to be a reliable and valid measure for subjective mood (Crawford & Henry, 2004). In this scale, PA and NA are treated as dispositional dimensions, where high NA reflects the presence of subjective displeasure and distress, while low NA reflects the absence of these feelings. On the other hand, the PA measure reflects the extent to which pleasurable engagement with the environment is experienced. The PANAS therefore captures NA and PA as independent measures.

2.4 Method

2.4.1 Subjects

A total of sevety-two healthy adult participants completed the study (Forty-seven experimental subjects, 21 females, 20 2.8 years; Twenty-five control subjects, 20 females, 19 2.2 years). The study was approved by the institutional review board at the University of California, Berkeley (Committee for Protection of Human Subjects), with all participants providing written informed consent.

Participants abstained from caffeine, alcohol, and naps for 72 h before and during the study, and kept a normal sleepwake rhythm and average sleep duration (7-9 h of sleep per night, morning rise time of 7:00-8:30 A.M.) for 1 week before study participation, verified by actigraphy (a wristwatch movement sensor, sensitive to wake and sleep states). The amount of sleep obtained during the period before the study did not differ between the sleep-deprivation session and the sleep-rested session in either average number of hours (mean: 7.62 and 7.10, respectively: two-sample t-test, $t(46) = 0.64$, $p = 0.37$) or variability, as assessed in standard deviation across nights (mean: 0.67 and 0.33, respectively: $t(46) = 0.81$, $p = 0.29$).

Exclusion criteria, assessed using a prescreening questionnaire (see Appendix B), were a history of sleep disorders, neurologic disorders or closed head injury, Axis I psychiatric disorders according to the DSM-IV criteria (encompassing major mental disorders including depression, anxiety disorders, bipolar disorder, attention deficit disorder, and schizophrenia), history of drug abuse, and current use of anti-depressant or hypnotic medication. No subject reported being a habitual napper (defined as napping 2 or more days per week).

2.4.2 Design

Forty-seven participants were assigned to both a sleep-deprivation and a sleep-control session. The order of sessions were counterbalanced across subjects and separated by seven days. In the sleep-control session, subjects were awake across day 1 and slept

normally at night in a lab while polysomnography (PSG) was monitored. In the sleep-deprivation session, subjects were awake across day 1 and night 1, accumulating a mean of 31.3 hours of total sleep deprivation. PANAS mood scale questionnaires were administered twice, once at the evening before sleep and once in the morning upon waking in the sleep-control session, and at the same matched time in the sleep-deprivation session.

Of the forty-seven participants, a subset of twenty-five participants underwent an additional period of sleep deprivation across day 2, followed by a nap session after the extended sleep-deprivation period. PANAS ratings were measured again after the nap session upon waking.

An additional group of twenty-five participants were assigned to a separate wake-control group, where PANAS mood ratings were measured twice, once in the morning and once in the evening, at time-points matched to the experimental group's day 2 PANAS measurement times.

Subjects in the deprivation group were continuously monitored in the laboratory throughout the enforced waking period by trained personnel, independently confirmed using actigraphy monitoring, accumulating a mean of 31.3 h (s.d. 1.87) total sleep deprivation before the morning PANAS measurement session. A standardized regimen of waking activity was conducted during the deprivation period, with subject activities limited to Internet, e-mail, and reading in a standard light environment (340 lux). Participants were allowed occasional short indoor walks around the floor of the experimental area (maximum light: 530 lux). During the deprivation period, a standard breakfast was provided to each subject (7:00 A.M.), which contained no caffeine and included yogurt or cereal, toast, a small fruit bowl, and a glass of orange juice (400 calories), and a standard lunch was provided (12:00 P.M.) containing a sandwich (variable filling, depending on subjects dietary preferences), a small bag of pretzels, and a granola bar (550 calories). Water intake was offered *ad libitum* throughout the experimental period, as were snack options of either a small box of dried raisins or bag of pretzels.

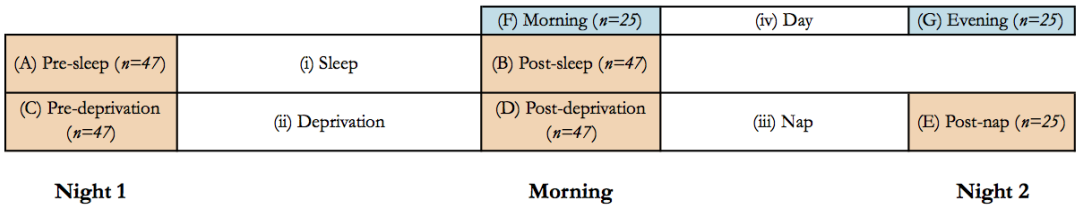

FIGURE 2.1: Mood scores were collected from subjects (n=47), using the PANAS scale, at Night 1 and Morning, corresponding to before (A) and after (B) a full night of sleep (i). The same 47 subjects underwent a full night of sleep deprivation (ii) in a separate session, during which PANAS scores were taken before (D) and after (E) deprivation, at time-points matched to Night 1 and Morning in the sleep session. Of these 47 subjects who were sleep-deprived, 25 subjects continued to also undergo a post-deprivation recovery nap (iii), and PANAS scores were collected upon waking from the recovery nap (F) at time-point Night 2. Finally, PANAS scores were collected from a separate group of 25 normal, rested control subjects (blue bars) at Morning (F) and Night 2 (G) after a normal interval across the day (iv).

2.4.3 Sleep PSG

2.4.3.1 Acquisition

Sleep in the sleep-control session was monitored in the laboratory with PSG sleep (23:30hr-07:30hr 30min) using a Grass Technologies Comet XL system (Astro-Med, Inc., West Warwick, RI). Electroencephalography (EEG) was recorded at 19 standard locations conforming to the International 10-20 System [47] (FP1, FP2, F7, F3, FZ, F4, F8, T3, C3, CZ, C4, T4, T5, P3, PZ, P4, T6, O1, O2). Electrooculography was recorded at the right and left outer canthi (right superior; left inferior). Electromyography was recorded via three electrodes (one mental, two submental). Electrocardiogram was recorded via two electrodes placed below the left and right clavicles.Reference electrodes were recorded at both the left and right mastoid (A1, A2). Data was sampled first at 800Hz by the amplifier, digitized at 400Hz. All data was stored unfiltered (recovered frequency range of 0.1100Hz), except for a 60Hz notch filter to remove mainline noise. For recording only, each channel was referenced to a forehead scalp derivation.

2.4.3.2 Preprocessing

All EEG analyses were performed in MATLAB 7.5 (The Mathworks, Natick, MA), including the add-in toolbox EEGLAB (http://sccn.ucsd.edu/eeglab/). EEG and EOG

were referenced to the contralateral mastoid, and filtered to 0.5-50 Hz. EMG used a bipolar montage filtered to 10-70 Hz and 0.1-12Hz, respectively. EKG used a bipolar montage bandpassed at 0.01-40 Hz. EEG and EOG were epoched into 5 second bins. Sleep-staging was performed in accordance with standardized techniques, using C3,C4,O1,O2, right and left EOG and EMG channels. Sleep was visually scored in 30-second epochs using the C3-A2 derivation according to standard criteria (Rechtschaffen & Kales, 1968b).

2.4.3.3 Spectral decomposition

Power spectral analysis of sleep EEG was carried out according to previously published methods(Mander, Santhanam, Saletin, & Walker, 2011). Specifically, EEG channels were re-referenced to the average of the left and right mastoid (A1, A2), with high- and low-pass Finite Impulse Response (FIR) filtering at 0.5Hz and 80Hz, respectively. The all-night recording was then visually artifact-rejected in 5-second epochs. Artifact-laden epochs were removed from subsequent analyses. Power spectral density was calculated by use of a Fast Fourier Transform (FFT) on each hamming-windowed 5-second epoch. FFT results were then sorted according to sleep stage and averaged for each respective stage. Absolute power in bands of interest was calculated by averaging across standard and custom EEG frequency band ranges: $Slow(0.7-1Hz)$, $Delta(1-4.6Hz)$, $Theta(4.6-8Hz)$, $Alpha(8-12Hz)$, $Sigma(12-15Hz)$, $Beta_A(15-20Hz)$, $Beta_B(20-25Hz)$, $Beta_C(25-30Hz)$, $Beta_D(30-35Hz)$, $Beta_E(35-40Hz)$, $Beta_{Wide}(14-35Hz)$, $Gamma(30-40Hz)$, and log-transformed.

2.5 Results

2.5.1 Behavioural data

Forty-seven subjects gave PANAS mood ratings before and after sleep in the sleep-control session, and before and after deprivation in the deprivations session. A subset of twenty-five subjects underwent further daytime deprivation following the nighttime

deprivation, proceeding with a daytime recovery nap. These twenty-five subjects then gave PANAS mood ratings upon waking after the recover nap. A separate group of twenty-five subjects served as a wake-control group, and gave PANAS mood ratings in the morning at a time matched to the morning time-point of the sleep-rested / deprivation session, and another in the evening corresponding to the post-nap time-point.

The summed PANAS scores for PA and NA were treated separately. Six subjects' PANAS scores in either the PA or NA dataset were higher than 3 standard deviations than the mean, and thus treated as outliers and removed from subsequent analysis. The remaining subjects ($n = 41$) are included in all subsequent analyses pertaining to sleep-rested and sleep-deprived sessions across nighttime between time points Night 1 and Morning, unless otherwise stated.

2.5.1.1 Rested data (compare across time points)

In the rested session, subjects' summed positive affect (PA) mood ratings increased significantly after a night's sleep ($t(40) = 3.47, p < 0.01$) (Figure 2.2, top graph, red line). Summed negative affect (NA) ratings were also found to increase after a night's sleep ($t(40) = 3.73, p < 0.001$) (Figure 2.3, red line).

2.5.1.2 Deprived data (compare across time points)

In the sleep deprivation session, subjects' summed positive mood ratings were found to decrease signficantly ($t(40) = 3.79, p < 0.001$) in the morning compared to the previous evening (Figure 2.2, blue line). In contrast, summed negative mood ratings were significantly increased following deprivation ($t(40) = -3.36, p < 0.01$) (Figure 2.3, blue line).

2.5.1.3 Nap data (compare across time points)

Following deprivation, a recovery nap in the subsequent day failed to restore positive mood, which remained significantly lower than prior to deprivation the preceding night

($t(25) = -2.09, p < 0.05$). Negative mood showed a recovery trend following the nap but was not significantly different from negative mood ratings measured in the morning after deprivation ($t(40) = 3.79, p = 0.088$).

2.5.1.4 Comparing across conditions (Rested vs. Deprived)

For both positive and negative mood ratings, baseline mood ratings at night before sleep / nighttime deprivation did not differ significantly ($Positive, p = 0.16; Negative, p = 0.066$).

Positive mood ratings in the morning were significantly lower following the deprived session, compared to after a night's sleep ($t(40) = -5.61, p < 0.001$), as well as when compared to morning positive ratings in the wake-control group ($t(64) = 4.03, p < 0.001$). For negative mood, ratings were significantly higher after deprivation, compared to after sleep ($t(40) = 2.98, p < 0.001$). Negative mood ratings in the wake-control group were also higher in the morning compared to those who had slept ($t(64) = 3.41, p < 0.001$). Of interest is that both PA and NA ratings after the recovery nap still differed significantly from mood ratings from the wake-control group ($Positive, t(24) = 2.17, p < 0.05; Negative, t(24) = 2.04, p < 0.05$).

The difference in mood ratings across time (i.e. the *change score*) for different conditions were examined. The positive change score for the rested session was significantly higher than the deprivation change score ($t(40) = 5.09, p < 0.001$), as well as higher than the change score across the day in the wake-control group ($t(64) = 7.49, p < 0.001$) (Figure 2.2, bar graph). The negative change score for the rested session was significantly lower than that of the deprivation session ($t(40) = -2.20, p < 0.05$), but significantly higher than that of the change score for the nap session ($t(64) = 3.39, p < 0.01$), as well as the wake-control change score across the day ($t(64) = 2.13, p < 0.01$) (Figure 2.3, bar graph).

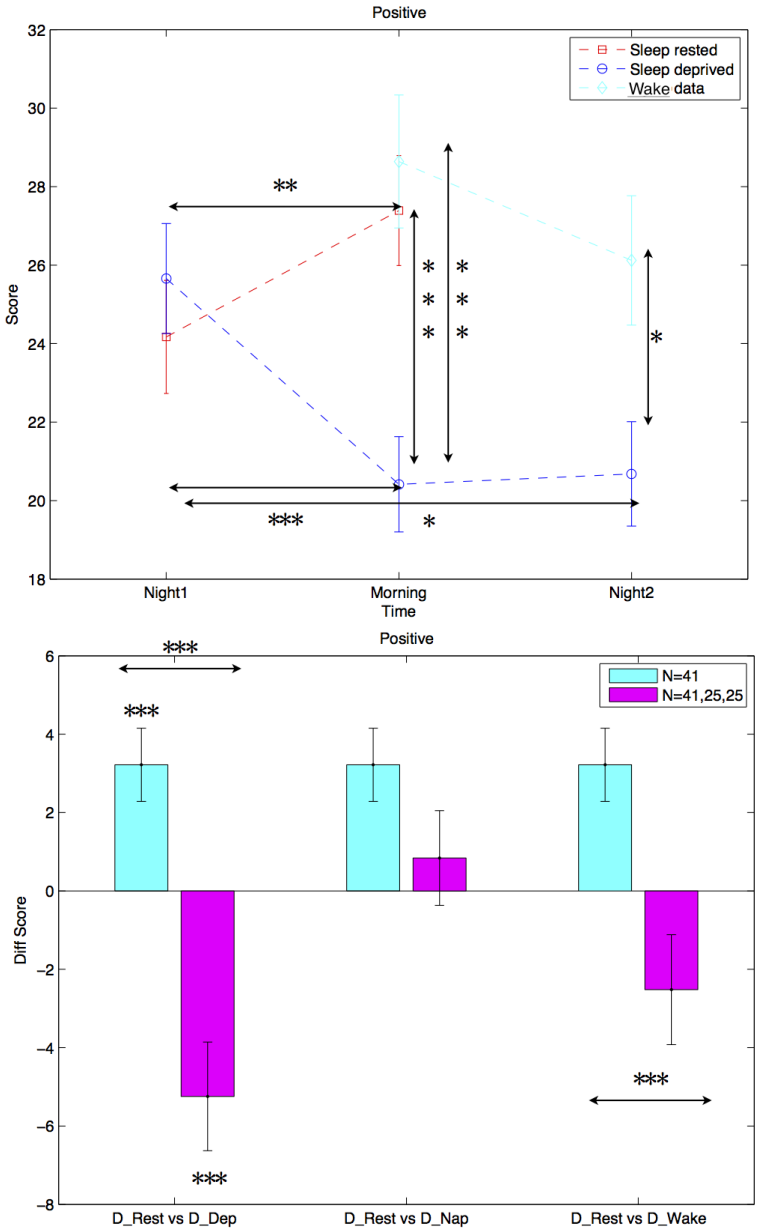

FIGURE 2.2: Positive Affect (PA) mood ratings from the PANAS scale. Top graph: Subjects' PA scores at the time points Night 1, Morning, and Night 2. Line colors indicate different conditions. Red line indicates scores taken from the Sleep Rested session ($n = 41$). Dark blue line indicates scores taken from the Sleep Deprived session ($n = 41$), and the Recovery Nap session ($n = 25$). The light blue line indicates scores taken from the control group ($n = 25$). Asterisks indicate the significance level of differences in PA score across time points, as well as across conditions. Bottom graph: Bars indicate the difference in PA score calculated across different time points. D-Rest: PA score difference between Night 1 and Morning ($n = 41$) in the Sleep Rested condition. D-Dep: PA score difference between Night 1 and Morning ($n = 41$) in the Sleep Deprived condition. D-Nap: PA score difference between Morning and Night 2 ($n = 25$) from subjects who underwent a recovery nap after sleep deprivation. D-Wake: PA score difference between Morning and Night 2 ($n = 25$) taken from control subjects who did not undergo any experimental conditions. Asterisks indicate the significance level of the "PA difference scores" (asterisks above/below error bars) and differences in the "PA difference scores" (asterisks above horizontal arrows), as a means of comparing the magnitude of PA score change across conditions. Error bars show standard error. $*$: $p < 0.05$; $**$: $p < 0.01$; $***$: $p < 0.001$

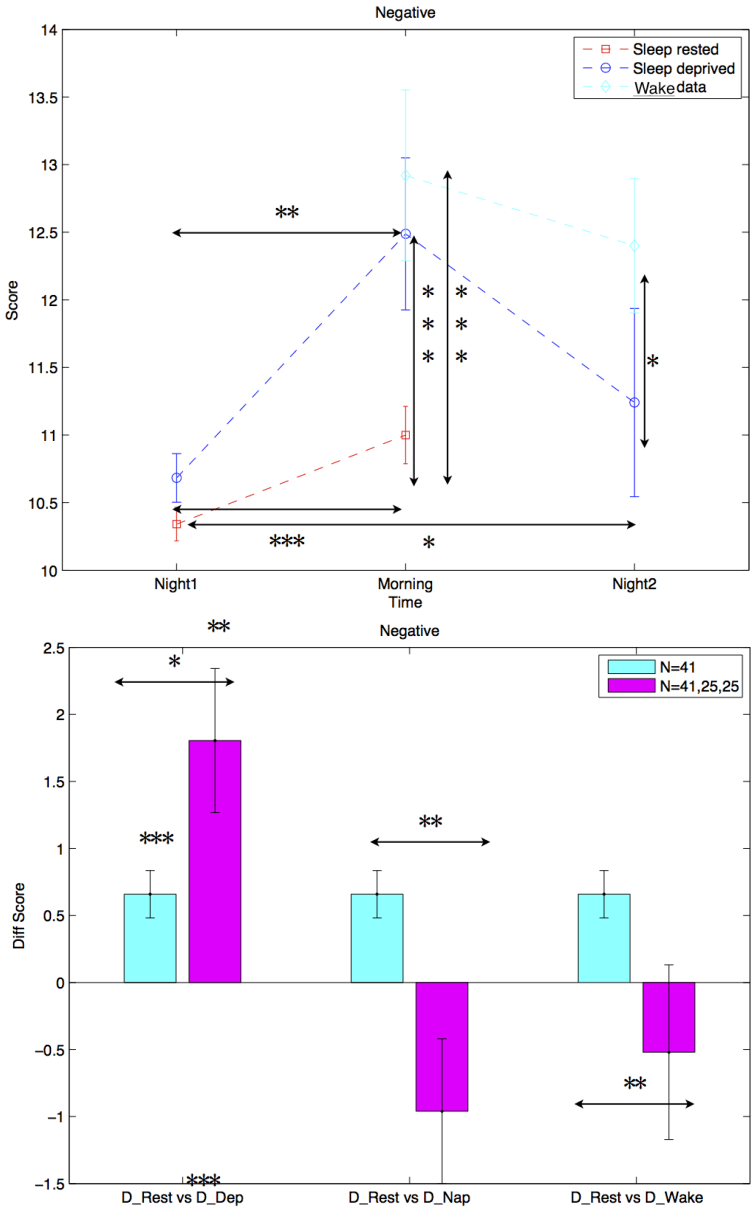

FIGURE 2.3: Negative Affect (NA) mood ratings from the PANAS scale. Top graph: Subjects' NA scores at the time points Night 1, Morning, and Night 2. Line colors indicate different conditions. Red line indicates scores taken from the Sleep Rested session ($n = 41$). Dark blue line indicates scores taken from the Sleep Deprived session ($n = 41$), and the Recovery Nap session ($n = 25$). The light blue line indicates scores taken from the control group ($n = 25$). Asterisks indicate the significance level of differences in NA score across time points, as well as across conditions. Bottom graph: Bars indicate the difference in NA score calculated across different time points. D-Rest: NA score difference between Night 1 and Morning ($n = 41$) in the Sleep Rested condition. D-Dep: NA score difference between Night 1 and Morning ($n = 41$) in the Sleep Deprived condition. D-Nap: NA score difference between Morning and Night 2 ($n = 25$) from subjects who underwent a recovery nap after sleep deprivation. D-Wake: NA score difference between Morning and Night 2 ($n = 25$) taken from control subjects who did not undergo any experimental conditions. Asterisks indicate the significance level of the "NA difference scores" (asterisks above/below error bars) and differences in the "NA difference scores" (asterisks above horizontal arrows), as a means of comparing the magnitude of NA score change across conditions. Error bars show standard error. $*$: $p < 0.05$; $**$: $p < 0.01$; $***$: $p < 0.001$

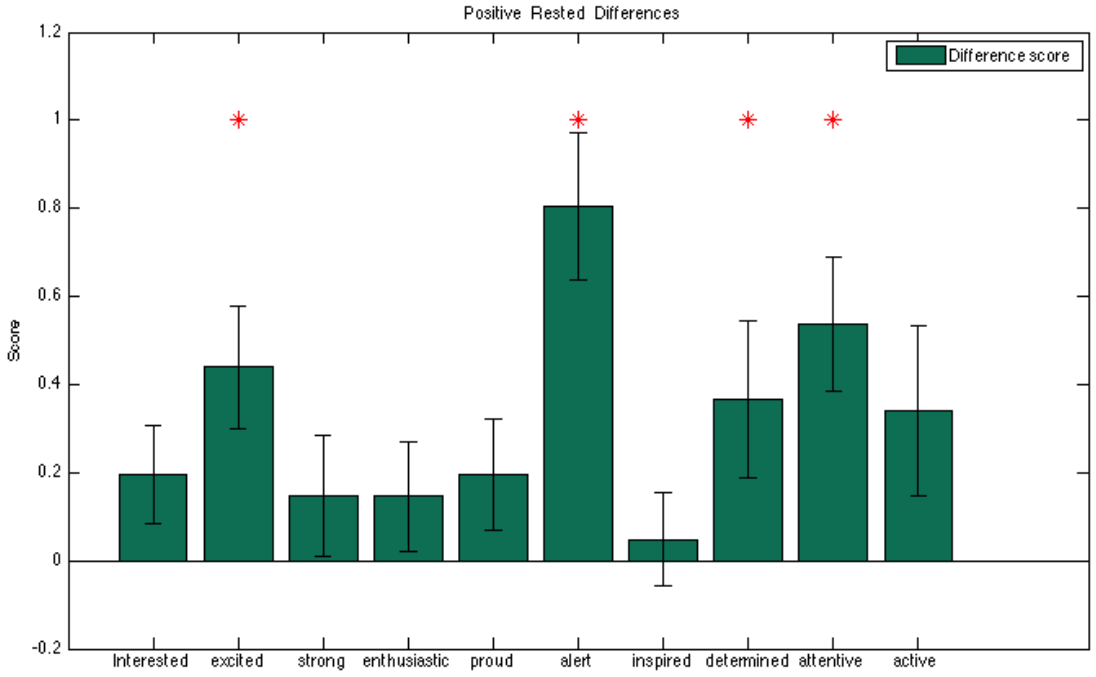

FIGURE 2.4: Bar graph showing the differences in positive mood ratings across the night after sleep (Morning *minus* Night 1), for each of the individual positive moods from the PANAS scale. Bars with asterisks indicate the positive moods that significantly increase after a night's sleep. Error bars show standard error. $*$: $p < 0.05$

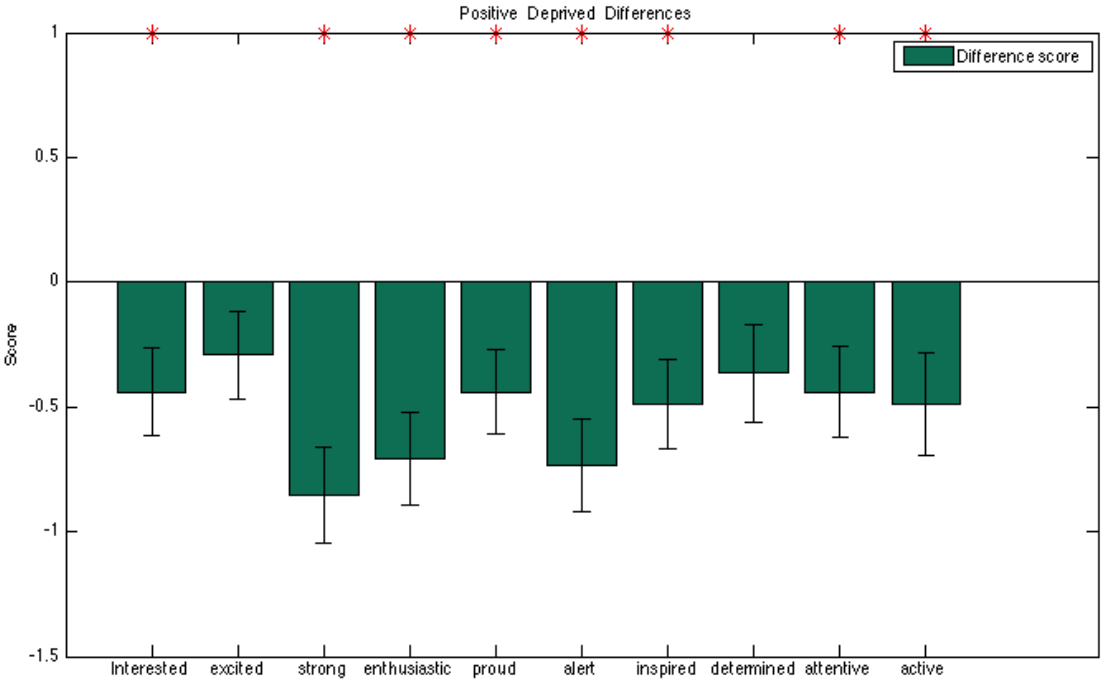

FIGURE 2.5: Bar graph showing the differences in positive mood ratings across the night after sleep-deprivation (Morning *minus* Night 1), for each of the individual positive moods from the PANAS scale. Bars with asterisks indicate the positive moods that significantly decrease after a full night's sleep-deprivation. Error bars show standard error. $*$: $p < 0.05$

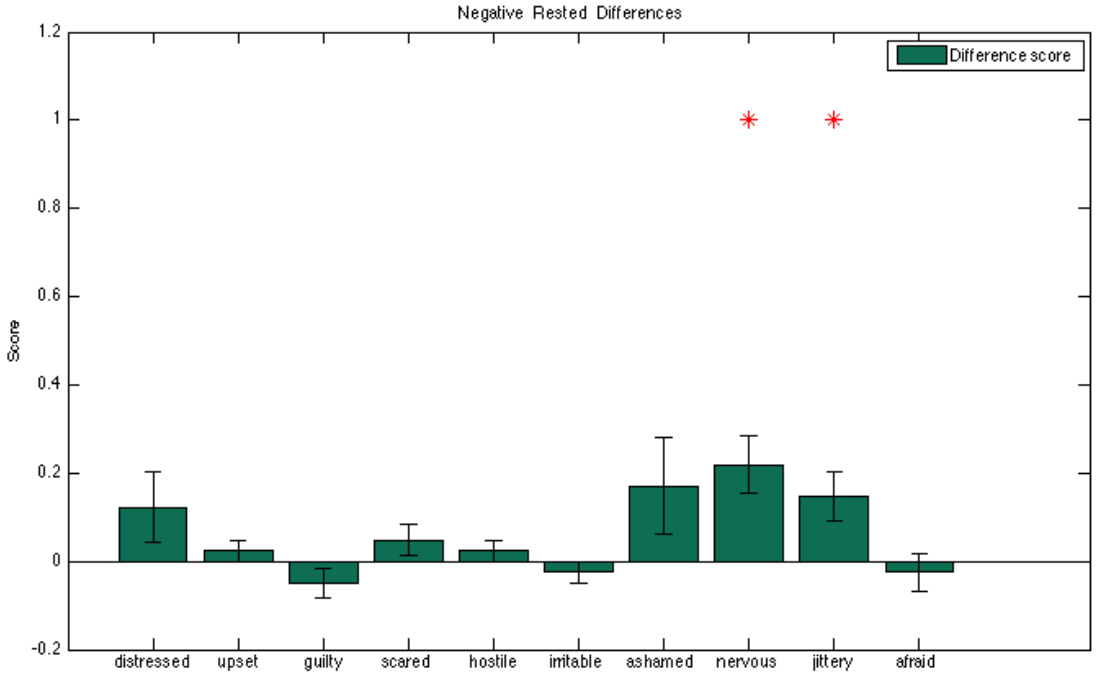

FIGURE 2.6: Bar graph showing the differences in negative mood ratings across the night after sleep (Morning *minus* Night 1), for each of the individual negative moods from the PANAS scale. Bars with asterisks indicate the negative moods that significantly increase after a night's sleep. Error bars show standard error. $*$: $p < 0.05$

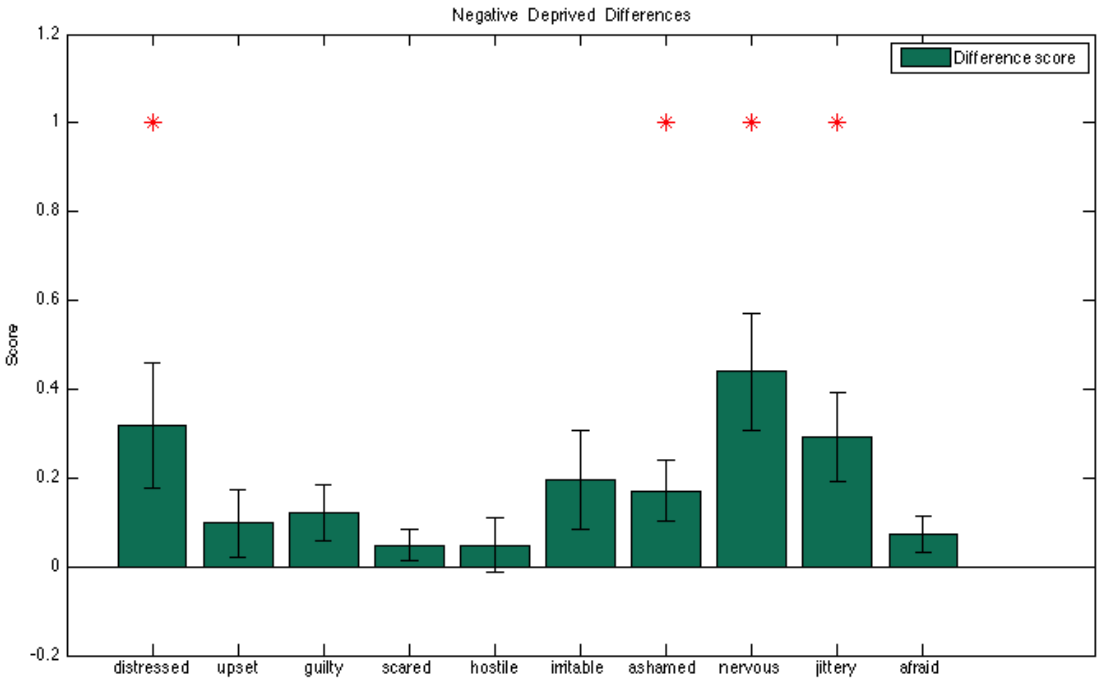

FIGURE 2.7: Bar graph showing the differences in negative mood ratings across the night after sleep-deprivation (Morning *minus* Night 1), for each of the individual negative moods from the PANAS scale. Bars with asterisks indicate the negative moods that significantly decrease after a full night's sleep-deprivation. Error bars show standard error. $*$: $p < 0.05$

2.5.1.5 Individual moods in PA and NA

To examine the components of change in positive and negative mood, change scores across a night of sleep as well as a night of deprivation were calculated for each of the ten individual moods within the PA and NA scale. Figures 2.4 – 2.7 show the change scores with all significantly different moods marked (all reported significant levels at $p < 0.05$).

For PA, the moods "excited", "alert", "determined", "attentive" were significantly higher following a night of sleep. Following a night of deprivation, however, the moods "interested", "strong", "enthusiastic", "proud", "alert", "inspired", "attentive" and "active" were significantly decreased.

For NA, the mood ratings for "nervous" and "jittery" were higher after sleep than compared to before. Following a night of deprivation, the negative moods "distressed", "ashamed", "nervous" and "jittery" were significantly increased.

2.5.2 Sleep-dependent mood changes

2.5.2.1 Correlation of sleep architecture with significantly different moods

Difference scores - the change in mood rating across a night - were correlated with properties of sleep architecture across subjects, which includes "Total sleep time" for each of the sleep stages "1", "2", "3", "4", "REM", as well as for "NREM" and "Slow wave" sleep. Specifically, the difference scores from only those individual moods within the PA and NA scale that changed significantly across a night's sleep, and the sum of those change scores within the PA and NA moods, were examined.

Within the NA moods, "jittery" and "nervous" ratings were found to increase significantly after sleep. The difference score for "jittery" (but not "nervous") positively correlated with total sleep time of Stage 4 sleep ($r = 0.327, p < 0.05$) (e.g. the longer the total sleep time, the greater the increase in jittery score in the morning). Additionally, the summed difference scores of "jittery" and "nervous" positively correlated with total sleep time of Stage 4 sleep ($r = 0.387, p < 0.05$).

No correlations were found with difference scores in the PA moods.

2.5.2.2 Correlation of sleep statistics and spectral power with significantly different moods

The difference scores from moods that changed significantly after a night's sleep, as well as the sum of these scores within the PA and NA scale, were used as regressors and fitted against the spectral density per sleep stage (Stage 1, Stage 2, Stage 3, Stage 4, slow wave sleep, NREM sleep, REM sleep) per frequency band ($Slow(0.7-1Hz)$, $Delta(1-4.6Hz)$, $Theta(4.6-8Hz)$, $Alpha(8-12Hz)$, $Sigma(12-15Hz)$, $Beta_A(15-20Hz)$, $Beta_B(20-25Hz)$, $Beta_C(25-30Hz)$, $Beta_D(30-35Hz)$, $Beta_E(35-40Hz)$, $Beta_{Wide}(14-35Hz)$, $Gamma(30-40Hz)$).

Positive moods

Across a night's sleep, the lower the theta power in occipital channels, the greater the combined increase in the positive moods "alert", "attentive", "determined", and "excited" that are reported in the morning after sleep.

Each of these four positive moods were also examined separately. The lower the frontal sigma power, parietal theta power, as well as occipital slow, delta and beta$_A$ power during Stage 4 and slow wave sleep, the more "attentive" subjects feel in the morning. Subjects felt more "determined" in the morning when there was less left parietal theta activity during NREM sleep stages. Finally, the less beta and gamma power present during Stage 4 sleep, the more "excited" subjects felt in the morning.

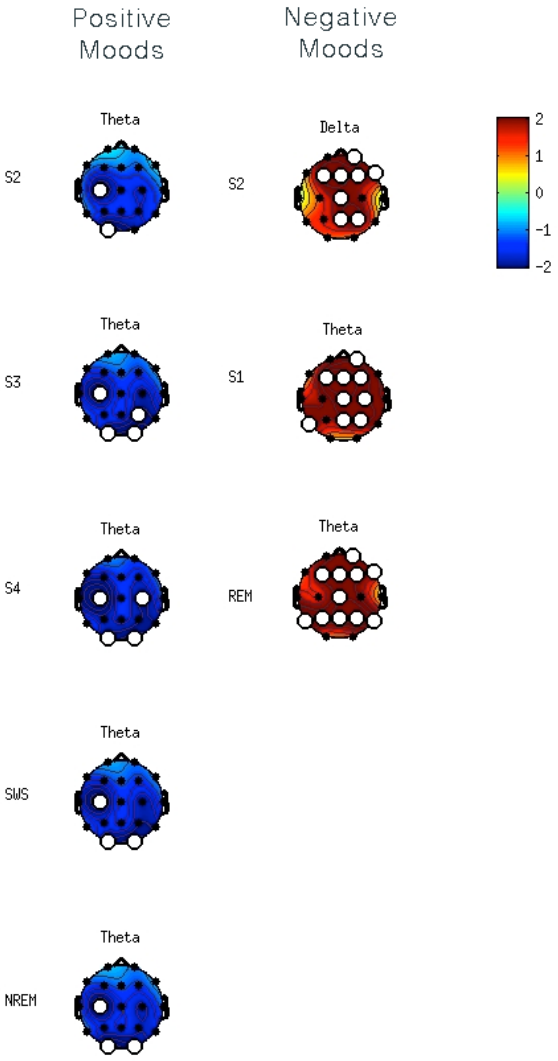

FIGURE 2.8: Topoplots showing the relationship between EEG frequency power during different sleep stages and the change in positive mood (PA) and negative mood (NA). The relationship between the *sum* of difference scores belonging to individual moods within the PA or NA scale that change significant across a night of sleep, and the frequency power of different spectral bands, are examined using a linear regression model. Color-bar represents the regression coefficient; blue indicates a negative relationship where lower spectral power predicts an increase in subjective mood rating after sleep; red indicates a positive relationship where greater spectral power predicts an increase in subjective mood rating after sleep. Topoplots here suggest that lower theta power in NREM sleep leads to an increase in positive moods, while greater delta in S2 sleep and greater theta in S1 and REM sleep leads to an increase in negative mood after sleep. Electrodes where significant relationships are observed are marked with a white dot ($p < 0.05$).

Negative moods

The same relationships were examined for negative moods. Across a night's sleep, the greater the whole-brain theta activity during Stage 1 and REM sleep, as well as greater whole-brain delta activity during S2 sleep, the higher the combined increase in "jittery" and "nervous" moods upon waking. "Jittery" mood increase upon waking was alone predicted by greater whole-brain theta activity during Stage 1 and REM sleep, as well lower frontal beta activity during Stage 1 sleep.

Topoplots in Figure 2.8 show significant correlations between difference scores and spectral power during sleep for the PA and NA moods. All results refer to absolute frequency power.

2.6 Discussion

The present study investigated the effects of sleep and sleep deprivation on subjective mood change, as well as the relationship between sleep physiology and subjective mood change. Results show that sleep deprivation increases negative mood and reduces positive mood, and that a post-deprivation nap does not return mood to pre-sleep baseline. Additionally, sleep physiology affect mood changes for PA and NA in opposite directions. Specifically, increase in positive mood is predicted by *low* theta power in NREM sleep EEG, but increase in negative mood is predicted by *high* theta power in REM sleep, as well as delta power in Stage 2 sleep. No significant difference in subjective mood was observed in the control subjects, for both PA and NA. Therefore, changes in mood are in deed attributed to the experimental manipulation (deprivation or recovery nap or sleep) rather than the passive passing of time.

2.6.1 Subjective mood changes across sleep and deprivation

The current findings that SD leads to significant decreases in positive mood and increases in negative mood is in line with the current literature (Franzen, Siegle, & Buysse, 2008). Of particular interest is that while PA decreases after SD and recovers after a nap, NA increases after SD but does not return to baseline after a nap. In other words, recovery of

normal subjective mood following SD applies only to positive moods but not to negative moods.

Previous studies have shown that a recovery night of sleep can reverse effects of dysfunctional emotional processing, such as restoring the ability to process facial expressions accurately (Gujar, McDonald, Nishida, & Walker, 2010). In fact, the emotional reactivity towards negative and aversive stimuli (e.g. angry and fearful faces) increases across a day, but even taking a mid-day nap can reverse this effect, where the same negative emotive stimuli induce a lower level of negative emotion. After napping, positive stimuli (e.g. happy faces) also evoke a higher level of subjective positive mood than compared to before. Sleep can restore the accurate interpretation and regulation of emotion signals, by resetting the appropriate limbic subcortical-cortical connectivity. A night of sleep depotentiates amygdala reactivity and re-establishes mPFC connectivity in response to prior emotional experiences (van der Helm et al., 2010), thereby reducing subjective emotionality.

However, the current study differs from the above evidence, such that subject's moods were measured in the absence of emotional stimuli. Therefore, while previous findings show that post-deprivation sleep can recover emotional recognition, for both NA and PA, the current study shows that sleep recovers subjective negative mood but not positive mood. The discrepency between the effect of SD on emotional *recognition* of stimuli, vs emotional *experience* as a baseline state, suggests that separate mechanisms are used for these different processes.

2.6.2 Sleep physiology and mood change

Previous studies have also suggested that the level of emotional regulation gained from sleep critically depends on the amount of REM sleep (van der Helm et al., 2011). Indeed, REM sleep provides an optimal environment in which affective homeostasis can take place. Its neuroanatomical, neurophysiological and neurochemical properties contribute to the consolidation of emotional memories while decreasing their emotional tone, and depotentiating the emotional "charge" accumulated from experiences across the waking day prior to sleep (van der Helm & Walker, 2012).

Such studies demonstrating the recovery effect of sleep have been conducted on subjects who were previously sleep-deprived. However, the current study measured the difference if subject mood across a night under normal circumstances, rather than after sleep deprivation. As such, the results from the current study reveal new findings of how sleep physiology changes subjective mood under normal circumstances.

The most prominent pattern in the relationship between mood change and sleep physiology is that the higher the theta oscillatory power during sleep the greater the increase in negative mood, and the greater the decrease in positive mood. Evidence exist to suggest that theta oscillations originating from the amygdala, even during sleep, is responsible for the reactivation and consolidation of fearful memories, triggering anxiety and increasing cortisol level, and is related to emotional arousal (Paré, Collins, & Pelletier, 2002). For example, rats with Chronic Immobilization Stress display abnormally long durations of REM sleep that is associated with synchronized theta oscillations in the amygdala (Hegde, Jayakrishnan, Chattarji, Kutty, & Laxmi, 2011). Results from the present study indicate that increases in emotions of "nervous" and "jittery" after sleeping are positively correlated with the magnitude of theta power during REM sleep, supporting the notion that theta oscillatory activity, which may be due to amygdala activity during REM sleep, is associated with stress.

2.7 Conclusion

By examining the detriments engendered by sleep loss, and the benefits resulting from sleep, the present study increases the understanding of sleep's role in regulating emotion. There exists theories describing the disconnectivity between the limbic areas and the prefrontal areas that may lead to this opposing behavioral effect, in which the amygdala, and other cortical mechanisms engaged in emotional arousal, are hyperactive due to a decreased inhibition from frontal regions. Actions are not expressed in accordance with the apparently heightened sense of emotion felt by a sleep deprived individual, because regions such the mPFC and the insula, responsible for high level integration of basic,

bodily sensations of emotion with more abstract cognitive constructs to guide action, are disconnected with the emotional circuitry.

While this theory does lend support to the findings that individuals show less emotionally intense physical responses after sleep deprivation, no study has thus far directly tested hypotheses of SD-dependent emotional dysfunction due to autonomic dysfunction. Future efforts should be directed at integrating the study of sleep deprivation and emotion on behavioural, neural and physiological levels. A further discussion is presented in Chapter 8.

Chapter 3

Recording simultaneous EEG-fMRI during sleep

Sleep stages are defined by changes in EEG oscillatory activity. To localize haemodynamic activity associated with each sleep stage, simultaneous EEG-fMRI is needed. This chapter presents the safety and technical issues that bimodal imaging with EEG-fMRI presents, including temperature rise at electrode sites, as well as artefacts in the BOLD signal related to gradient switching during fMRI acquisition, and movement and electrical signal generated from the subject's heartbeat. A preliminary test ($n = 3$) of temperature rise in the electrodes using a Fast Spin Echo sequence, with known high specific absorption rate, at 1.5T is conducted to establish the safety limits of this method using a specially designed recording hardware.

3.1 Technical challenges

Simultaneous EEG-fMRI recording is designed to capture the electrophysiological and haemodynamic manifestations of brain activity synchronously. This technique originated from epilepsy imaging, driven by the need for non-invasive imaging of the epileptic focus. In cognitive neuroscience, different sources of information have been used to understand the generation of oscillation patterns from the EEG signal, such as intracranial recordings, studies in lesion patients, animal studies and EEG source localisation.

EEG-fMRI represents an attractive alternative to these methods, which have their limitations, and is a strategy that uses EEG's high temporal resolution to specify the role of distinct oscillatory patterns in combination with reliable neuroanatomical information. However, a number of drawbacks in terms of basic physiology, study design, artifacts and analysis techniques must be considered to avoid noisy data acquisition or erroneous inference of EEG-fMRI results. The following section will outline the main technical considerations of EEG-fMRI recording, as well as its combination with sleep.

3.1.1 Safety

Recording EEG inside the MR environment leads to two major safety considerations. First, there is the hazard of introducing ferromagnetic materials into the scanner, and second, currents induced by the changing gradient fields in the electrodes and attached wires can produce eddy currents, leading to heating of electrode heads and possible burning of the subject's scalp. Currents induced in loops formed between the electrode leads, as well as currents induced along longer electrode leads such as the EMG and ECG channels also contribute to heating hazard. If the tissue forms part of the loop, the electromotive force will drive a current through this and lead to temperature increase. There is no safety standard specifically addressing combined EEG-fMRI, hence recommended safety limits are taken only from manufacturer recommendations.

3.1.2 Gradient artefacts

The term gradient artifact is used to describe the EEG contamination representing the electromotive force (emf) induced in the electrode lead loops by the changing magnetic fields applied during imaging. There are two distinct components that are attributed to the gradient and radio-frequency (RF) fields respectively. The former range in frequency from slice repetition interval (approximately 10-20 Hz) up to the kHz range, as seen in the right half of Figure 3.1. The RF fields have a fundamental component at the Larmour frequency of the scanner, dependent on field strength. A 1.5 T scanner will have a Larmour frequency of around 63 MHz. Additionally, lower frequency components

reflecting the RF pulse rate and pulse shape are also seen in the left half of Figure 3.1. Imaging artifact is significantly large and obscures the EEG waveforms completely.

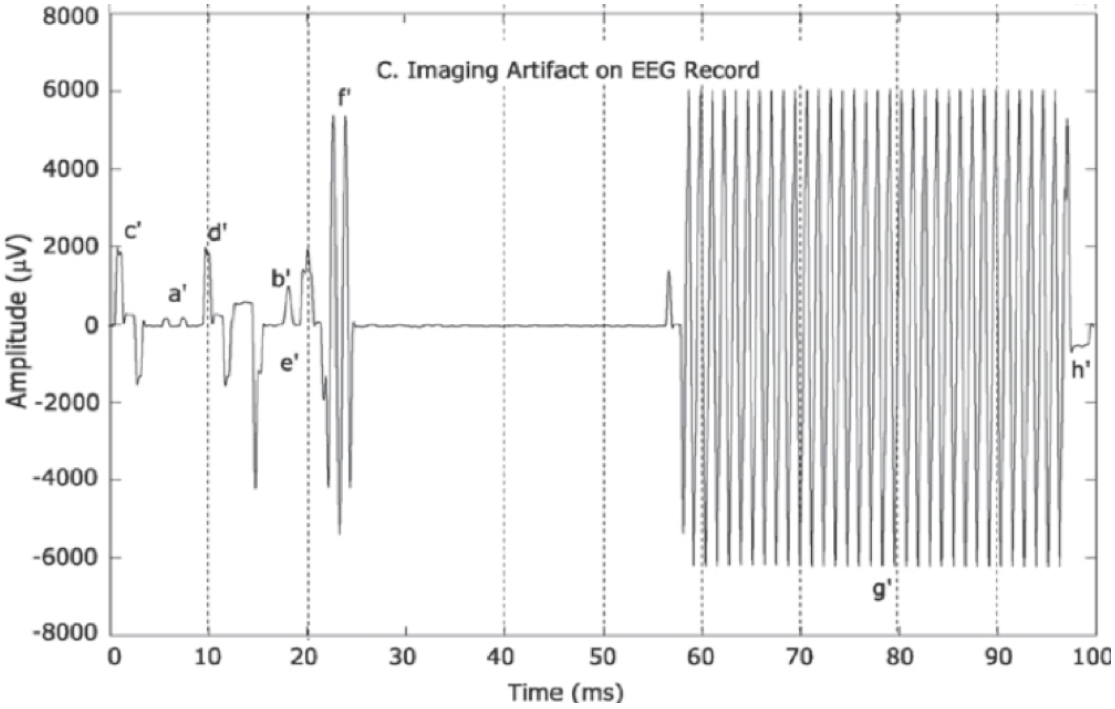

FIGURE 3.1: Example of a gradient artifact waveform in the EEG trace for a single slice, with peak amplitudes reaching 6000 uV during gradient switching.

Correct electrode lead arrangement when recording inside the scanner can reduce heating as well as scanner artifacts in the EEG trace. The *emf* induced in a conductive loop is proportional to the loop area and the rate of the change of magnetic flux cutting the loop. Minimising the area of any loop formed by the electrode leads can therefore reduce gradient artifacts by the fast switching of gradient fields during volume acquisition. The main method to achieve this is by bunching electrodes together at a single point on the head, then further minimizing the loop area by twisting the wires together as far as possible along the entire path, from the subjects head to the amplifier inputs. This keeps the leads in close proximity to each other, and results in the cancellation of induced *emfs* in adjacent twists. Some loop area is inevitable, since EEG is recorded between separate points on the head. Electrode caps with permanently fixed and flushed electrodes help to reduce this problem as well.

Variation in loop area also induces artifacts in the EEG, and so electrode lead movement must be minimized. Such variations can result from the movement of the electrode leads caused by a ballistocardiogram, small head movements and scanner vibration. Weighing down the electrodes that lead out of the scanner bore with sandbags, and placing padding under the leads and amplifier, fixing the subjects head and the use of electrode cap together help to minimize this effect.

Developments in artifact subtraction methods have now made simultaneous EEG-fMRI recording routine, with the requirement of a high sampling rate (5000 Hz) to capture the gradient switching and a large dynamic range in the amplifier to avoid saturation from the high amplitude gradient noise. Signal range should be of the order 20-30 mV, with a recommended minimum signal resolution of 0.5 μV. Low pass filtering alone cannot remove all the imaging artifact, and the artifact removal method most commonly used to date is based on the subtraction of an artifact template derived from averaging the artifact over a number of volume repetitions (Allen, Josephs, & Turner, 2000). Accurate calculation of the artifact template can be aided by obtaining slice markers for precise timing and aligning. Additionally, the EEG sampling must be synchronized to the MR scanner clock to avoid temporal jitter in the EEG.

3.1.3 Pulse artefacts

The EEG recorded inside the MR scanner is further contaminated by cardiac-related movement of the electrodes, or blood flow in the static field. These are referred to as pulse artifacts, and are typically 10-100 μV in amplitude, overlapping the EEG frequency range (Allen, Polizzi, Krakow, Fish, & Lemieux, 1998); Figure 3.2). Pulse artifacts are removed using a moving-average template subtraction method similar to that for gradient artifacts. The R-waves of the cardiac QRS complex represents the most prominent artifact peak and are open chosen as reference points in the artifact template.

3.1.4 Sleeping

Sleeping inside the MR scanner poses a range of difficulties:

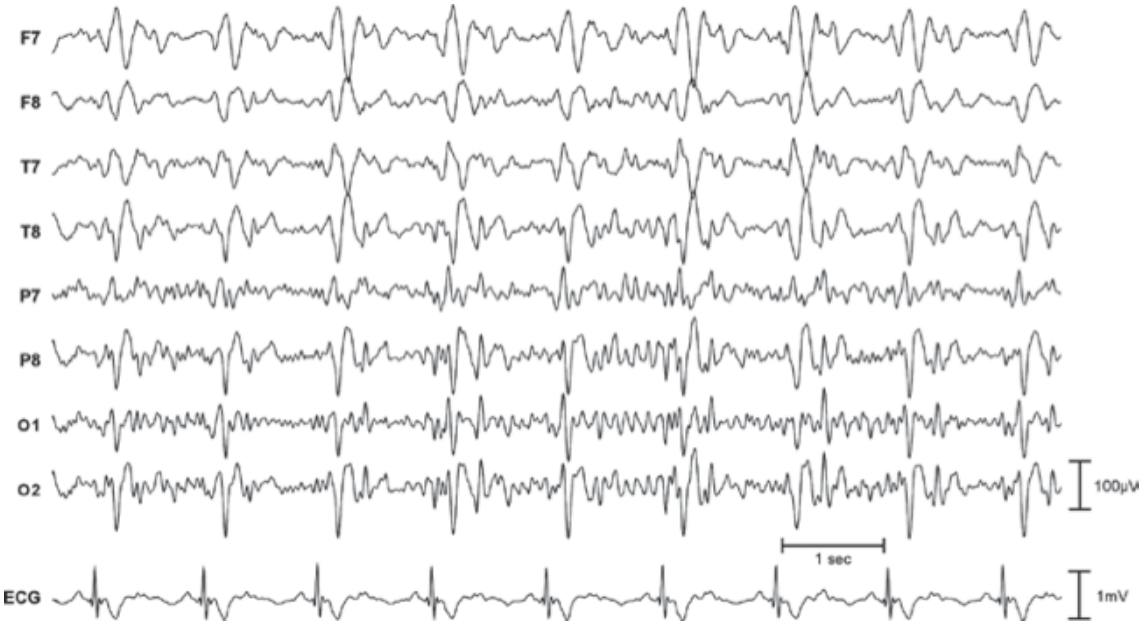

FIGURE 3.2: Example of ongoing EEG data contaminated by the pulse artifact. The artifact is most prominent at lateral sites over the left and right hemispheres. The temporal pattern corresponds to the cardiac cycle and is delayed in relation to the R-peak of the bottom ECG trace by around 200 ms.

1. Participant may not fall asleep or stay asleep due to discomfort, noisy environment, or general unease due to unfamiliar setting

2. Electrophysiological recordings may be contaminated by sweating over long durations and introduce slow drips into the signal

3. Extended fMRI recording time may introduce field inhomogeneity that degrades over time due to hardware instabilities or subject movements

4. The coils transmitting magnetic field gradients for long periods can lead to hardware temperature instability

5. Participants' movements increase during sleep, from body movements, heavy breathing and mycloni (jerking) in the descent to sleep

6. Drop-out rate in sleep studies are high due to the above issues

7. REM sleep is fragmented and reduced due to the loudness level of the scanner

8. There is no guarantee that all the subjects will cycle through all the sleep stages within the time constraint (2 hours maximum scan time)

As such, the study protocol of the main experiment is designed to tackle some of the main issues listed here, through partial sleep deprivation and experimental timing.

3.2 Preliminary technical study: heating safety

The purpose of this initial safety test was to determine whether conducting an EEG-fMRI study with a body transmitter coil would induce higher temperature rise in the electrodes, compared to the manufacturer-recommended use of a head transmitter coil. High powered sequences were used to specifically maximize the temperature increase, so as to derive a safety ceiling as a reference. A Fast Spin Echo (FSE) sequence was selected for this test, as it has a high specific absorption rate and has been previously shown to raise temperature at electrode sites faster than compared to Echo Planar Imaging (EPI) or Spoiled Gradient (SPGR) sequences (Boucousis et al., 2012).

3.2.1 Materials and methods

3.2.1.1 Participants

3 participants (mean age: 29 years; 1 female) of differing height and mass were specifically chosen for this safety test. All gave written informed consent and received financial compensation for their participation in this study, which was approved by the Ethics Committee of the University College London. No participants had any history of medical, traumatic, psychiatric disorders.

3.2.1.2 Design

A T2 FSE sequence with known high specific absorption rate (SAR) was used to test the ceiling temperature changes within a 6 minute scan sequence. This was conducted

inside a Seimens 1.5T MRI scanner, using a body transmitter coil and a 32 channel head receiver coil. EEG was recorded with a 14-channel MR-compatible electrode cap (see Figure 3.3) designed to specifically address safety and artifact issues addressed in the previous section while providing an adequate polysomnographic montage system to enable accurate sleep scoring in the subsequent main experiments. Temperature was recorded with fibre-optic cables inserted inside the electrolytic gel cavities of the following channels: Clavicle, FPz, FC5, Chin.

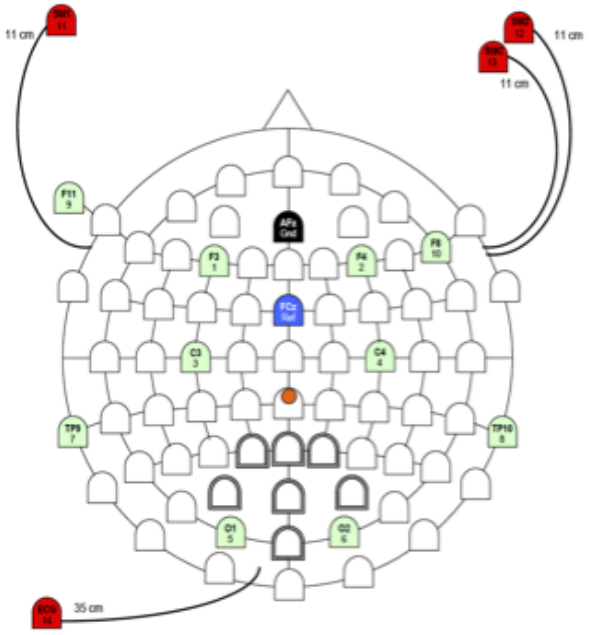

FIGURE 3.3: Montage of 14-channel MR-compatible cap used for sleep recordings in the MRI scanner. Recording reference at FCz; EOGs (F11, F8) integrated in the cap for better MR-quality; additional ECG electrode for pulse artifact removal computations; 3 EMG channels for sleep stage monitoring. (Red electrodes with drop-down cables are more susceptible to RF interference)

3.2.2 Results & Discussion

Figure 3.4 shows the temperature change plotted across time for each channel (N = 3). The largest temperature increases were observed in the channels with longer cables (clavicle and china electrodes). The highest SAR (relative to head weight) recorded was 3.1 W/kg, and the highest change in temperature was 4.4 degrees Celsius, which was

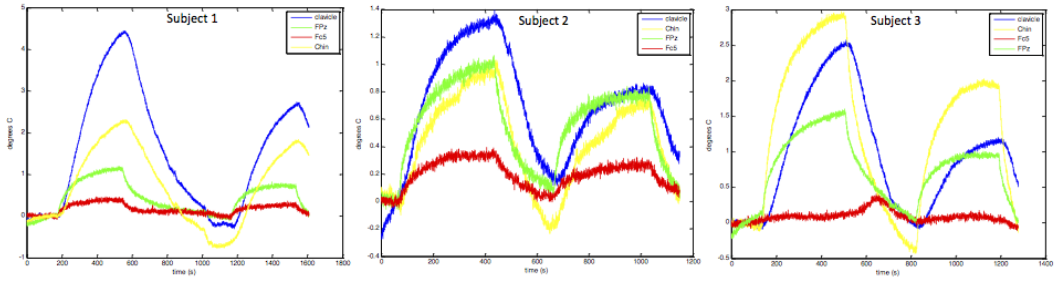

FIGURE 3.4: Temperatures for each channel are differentiated across time and plotted for each subject. Subject 1 shows the greatest temperature increase (4.4 C) within the 6 minute scan sequence.

Subject	*Max. delta T*	*Location*	*SAR*	*Mass*	*Height*
1	4.4	Clavicle	3.0 W/kg head av	85 kg	193 cm
2	1.3	Clavicle	3.1 W/kg head av	67 kg	162 cm
3	3.0	Chin	2.5 W/kg head av	52 kg	165 cm

TABLE 3.1: Summary of the maximum temperature change and corresponding channel detected in each subject

observed from the subject 1 who had the highest mass and height. Table 3.1 summarizes the main findings from this safety test.

The maximum temperature increase observed in 6 minutes with a high SAR sequence was 4.4 degrees Celcius, at 3.0 W/kg. As predicted, longer electrode wires running to the chin and clavicle are more prone to heating than standard cap electrodes. The EPI sequence used for the main EEG- fMRI sleep experiments presented in subsequent sections have 30 times less SAR (0.1 W/kg), and lie within a conservative safety region even at longer scan times (i.e. $>$ 100 min). Results from this safety test were relayed to the electrode cap manufacturer and were approved for use inside the 1.5T scanner for sleep recordings.

Chapter 4

BOLD signal changes from wake to non-rapid eye movement sleep

This chapter replicates a study by Kaufmann et al. (2006), which examines the BOLD signal changes in the transition from wakefulness to light and deep non-rapid eye movement sleep. EEG and fMRI data were acquired from subjects ($N = 11$) during the first cycle of nocturnal sleep following partial sleep deprivation (21 hours). Durations of continuous, artefact-free data (> 2 minutes) from Wake, Light NREM sleep (Stage 2) and slow wave sleep (SWS; Stage 3 and 4 collapsed) thorughout the sleep cycle were used to model sleep stage onset and duration in the general linear model. Compared to waking baseline, activity in the globus pallidus decreased during SWS, lending support to existing theories of the basal ganglia's role in sleep maintenance. Additionally, relative to light NREM sleep, activity in the brain stem region and the posterior cingulate cortex decreases during SWS, supporting the notion of decreasing consciousness in the descent to deep sleep.

4.1 Introduction

Sleep has been shown to play an important role in a wide range of information processing, such as memory consolidation (Stickgold & Walker, 2007), emotional regulation

(van der Helm et al., 2010), and creativity (Stickgold & Walker, 2004). The standard criteria for electrophysiological characterization of sleep relies on tracking changes in EEG frequency based on 30 second temporal resolution data, recorded from a sparse, whole-brain montage. However, sleep EEG dynamics show regional differences (Massimini, Huber, Ferrarelli, Hill, & Tononi, 2004), and these changes in activity may not be a global phenomenon, but rather involve local brain processes (Nir et al., 2011; Donner & Siegel, 2011). To understand these local processes, greater spatial accuracy is needed.

The current study aims to resolve the spatial distribution of neural activity during the onset of different sleep stages, using concurrent EEG-fMRI. This method allows a spatial characterization of cortical regions involved in driving the stage transitions (i.e. if higher BOLD signal is present in a deeper sleep stage than compared to its preceding stage), as well as those that are inhibited during stage changes (i.e. if lower BOLD signal is present in a deeper stage than compared to wakefulness, or to its preceding stage).

4.2 Materials and methods

4.2.1 Experimental design

4.2.1.1 Subjects

Eleven young healthy paid volunteers (6 females; age range, 18-26 years; mean age, 23.9 years) gave written informed consent according to the institutional guidelines before participating in this study, which was approved by the local Ethical Committee. Subjects were screened using the Beck Anxiety Inventory and Depression Inventory I for anxiety-related disorders, and the Epworth Sleepiness Scale, Pittsburgh Sleep Quality Index and the Munich Chronotype Questionnaire for sleep-related disorders (see Appendix B). No subjects reported excessive daytime sleepiness or sleep disturbances. The subjects had no history of neurological and psychiatric disorders, or substance abuse, and had no sleep disturbances or recent time zone ships.

4.2.1.2 Sleep deprivation procedure and instructions

Subjects followed a 2-day constant sleep-schedule before the experiment, during which they were instructed to sleep at 10.30pm for no more than 7.5 hours and to refrain from all caffeine and alcohol-containing substances and intense physical activity during this period. Compliance to the schedule was assessed with sleep diaries and wrist actigraphy (Somnowatch). The experiments were performed between 3.00 and 6.00 am, such that subjects were partially sleep deprived (21 hours) to increase sleep pressure without significantly altering their sleep architecture.

Subjects' heads were fitted with ear-muffs and foam pads for sound insulation, and were immobilized to minimize movement artifacts. The scanning room was completely darkened during the experiment. Subjects were asked stay awake for 5-10 minutes with their eyes closed aper the scan initiated, after which they were allowed to fall asleep. The session was stopped when the subject was either completely awake or indicated discomfort with a pneumatic squeeze ball, or when a full sleep cycle was completed. A typical session lasted 100 minutes.

4.2.2 Data acquisition

4.2.2.1 MRI acquisition

Functional MRI time-series were acquired using a 1.5T MR scanner (Avanto; Siemens, Erlangen, Germany). Multislice T2*-weighted fMRI images were obtained with a gradient echo-planar sequence, using axial slice orientation (35 slices; voxel size, 3 3 3 mm3; matrix size, 64 64 35; repetition time (TR) = 2975 ms; echo time (TE) = 40 ms; flip angle = 90; field of view = 192 mm; delay = 0). The total volumes acquired ranged from 1654-2106 across subjects, excluding the first 8 volumes discarded to allow for T1 equilibration effects. A structural T1-weighted 3D MP- RAGE sequence (TR = 1960 ms; TE = 5.6 ms; inversion time, 1100 ms; field of view, 256 224 mm2; matrix size, 256 224 160; voxel size 1 1 1 mm) was also acquired in all subjects.

4.2.2.2 EEG and physiologic recordings

Simultaneous polysomnography recordings were made using an MR-compatible electrode cap comprising 14 sintered silver-silver chloride pin electrodes (see Figure 6 from previous section): six EEG channels placed in a subset of locations of the 10-20 International System, two electrooculograms, three submental electromyographies, and an electrocardiogram (modified for sleep; VisionRecorder version 1.03, Brain Products), using a MR-compatible 32 channel amplifier (BrainAmp MR plus; Brain Products GmbH). The reference electrode was located between Fz and Cz and the ground electrode below Oz, all on the brain midline. Electrode impedance was kept <5 kOhms in addition to the 5 kOhm resistor built into the electrodes. The data acquisition rate was 5 kHz, with an analog band-pass filter set to 0.016250 Hz. Data were collected in a continuous fashion. EEG was monitored online with real-time gradient and pulse artifacts correction with a 10-second sliding-window template subtraction method using in-house algorithms.

4.3 Data analysis

4.3.1 EEG preprocessing, analysis and sleep staging

Artifacts related to gradient switching and cardio-ballistic effects were removed using standard routines available in Analyze software (Brain Products; see Appendix B for details). The artifact-free EEG data was then band-pass filtered between 0.5 and 30 Hz. Sleep-staging was performed in accordance with standardized techniques, using C3,C4,O1,O2, right and left EOG and EMG channels. Sleep was visually scored in 30-second epochs according to standard criteria (Rechtschaffen & Kales, 1968b). (For detailed statistical sleep data, see Appendix A.)

The hypnograms were then screened for intervals corresponding to continuous periods of Wake, Stage 2, 3 or 4 (stage 1 sleep, and rapid-eye- movement (REM) sleep were excluded), devoid of any arousals or movement times in either EEG or fMRI and lasting more than 2 minutes.

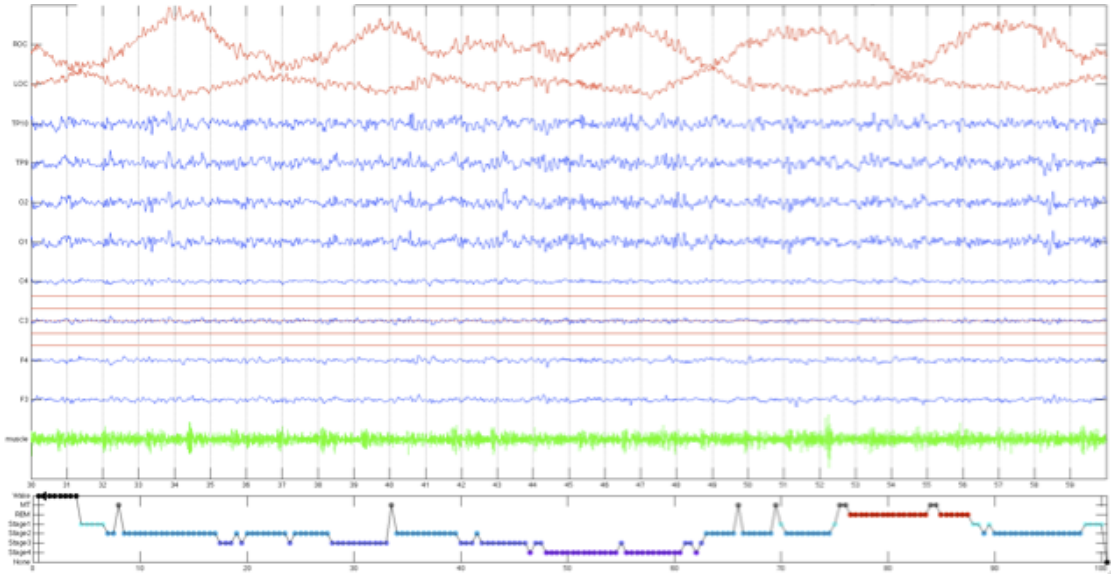

FIGURE 4.1: An epoch in the Wake stage. EOG traces (red) show slow eye-rolling, and the EEG (blue) is dominated by alpha activity. EMG (green) is relatively high. Red horizontal lines indicate 100 uV scale; negative is plotted upwards. Bottom panel indicates the hypnogram of the subject's sleep duration, from which the epoch is taken.

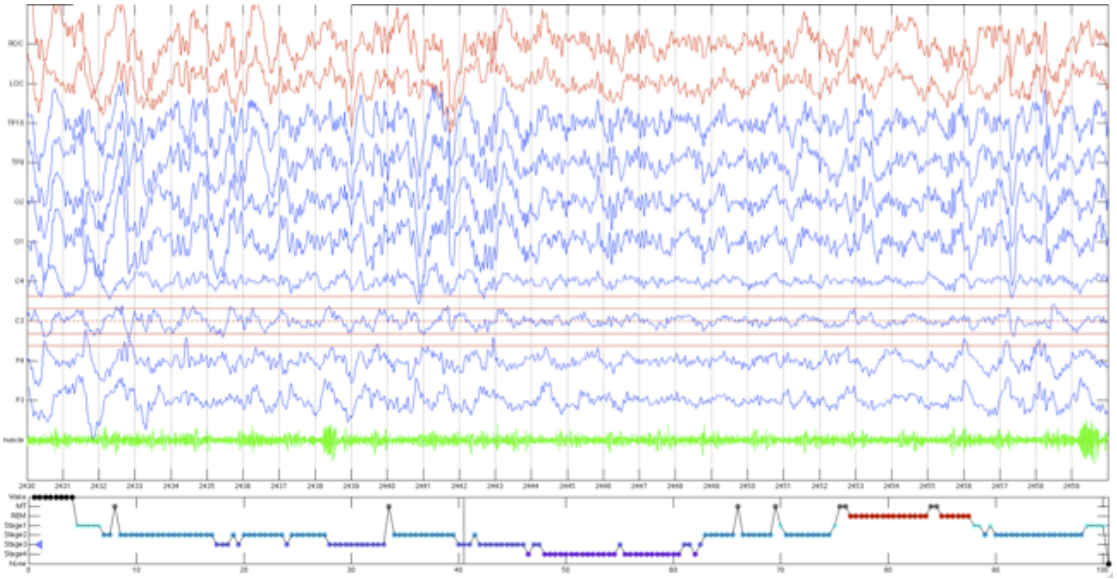

FIGURE 4.2: This epoch shows a typical Stage 3 trace, in which the left half (¡50 %) contains high-amplitude slow waves (¿1 Hz) and delta waves (1-4 Hz).

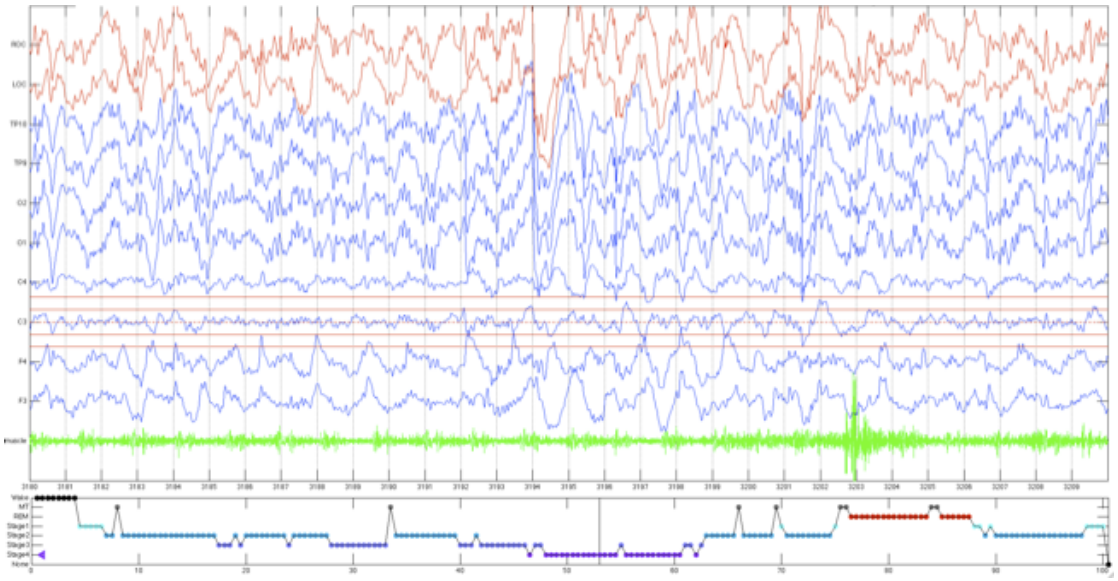

FIGURE 4.3: An epoch of Stage 4 sleep, in which the entire epoch is dominated by delta and slow waves. The EMG here is lowest compared to all other NREM stages.

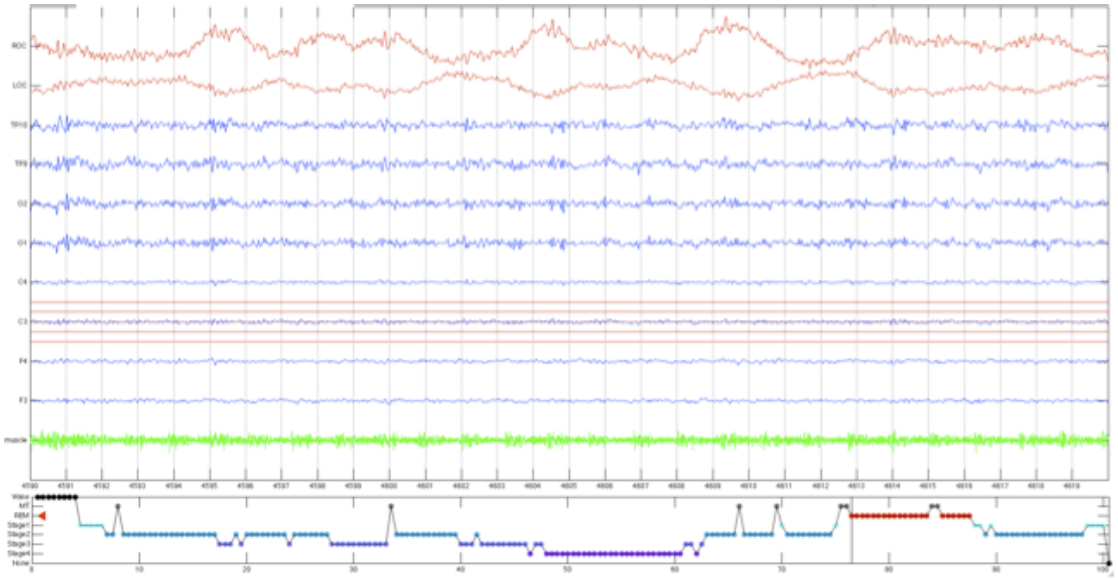

FIGURE 4.4: An epoch of phasic REM sleep, in which the EOG traces (top red) show periodic rapid eye movements. The EEG is of a low-amplitude, mixed frequency similar to that during wakefulness with eyes open, and the EMG here is at its lowest within the entire recording.

Figures 4.1 to 4.4 show 30 second traces of the EOG, EEG and EMG time series, scored as Wake, Stage 2, Stage 3, Stage 4 and REM respectively. Clear differences in the amplitude and frequency density between the 30 second traces of each sleep stage is evident. The bottom trace in each Figure shows the stage scoring for the entire sleep recording. The series of consecutive fMRI volumes corresponding to a chosen sleep period were selected from the complete fMRI time series and constituted a "session" for further analysis. fMRI and EEG data corresponding to stages 3 and 4 were collapsed as a single stage representing SWS in all subsequent analyses.

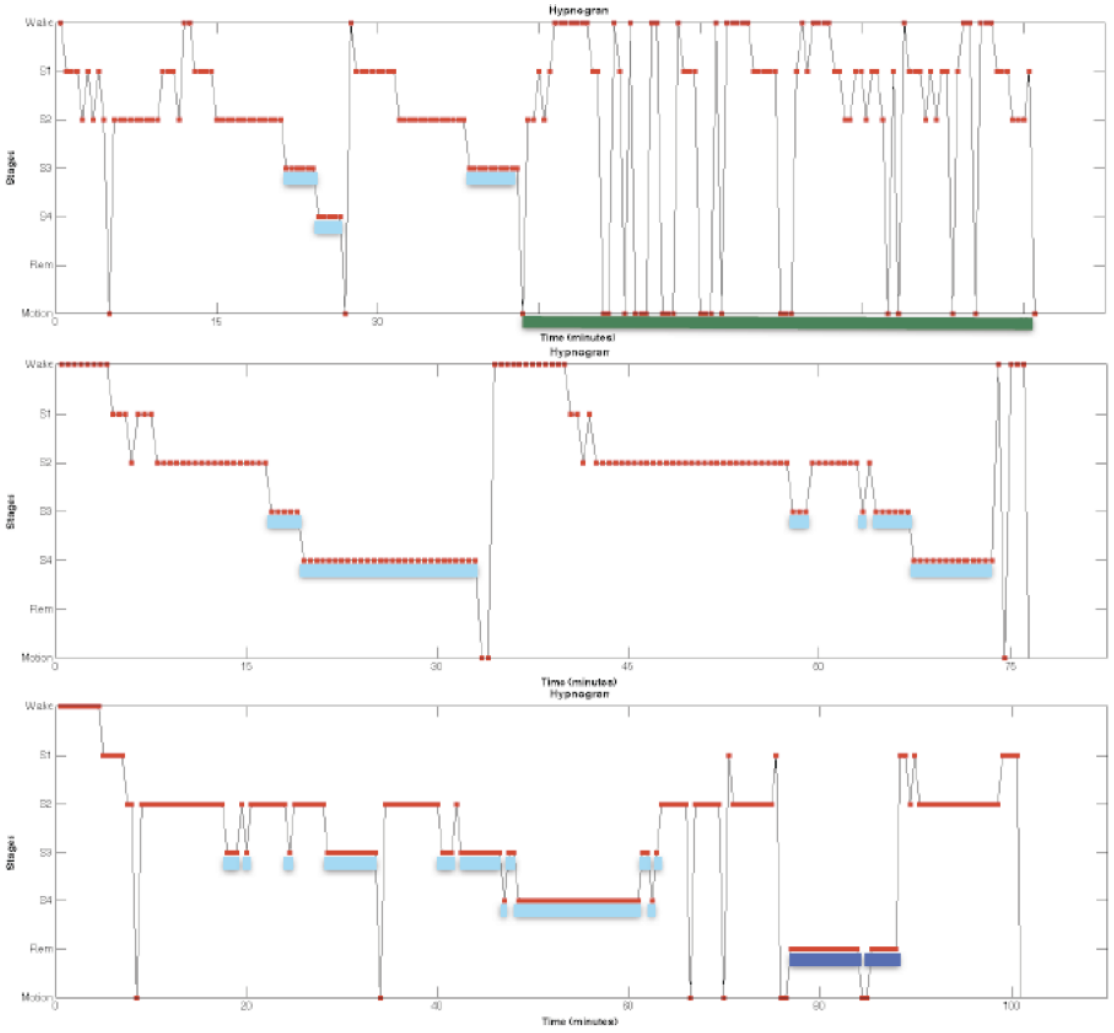

FIGURE 4.5: Example hypnograms of three subjects. Vertical axis indicates sleep stage, with Motion on the bottom. Horizontal axis indicates time in minutes. Green bar highlights increase in motion in the second half of the night in that subject. Light blue highlights slow wave sleep. Dark blue highlights REM sleep, present in only 3 of 11 subjects in the data sample.

4.3.2 fMRI preprocessing

Functional volumes were preprocessed with Statistical Parametric Mapping 8 (SPM8; www.fil.ion.ucl.ac.uk/spm/sopware/spm8) implemented in MATLAB (version 7.11, Mathworks). The fMRI time series was realigned using rigid body transformation of all images to the first image to correct for head motion (data with head movements >2 mm were excluded). Global effects from the images were estimated using a voxel-level linear model of the global signal (Macey, Macey, Kumar, & Harper, 2004) to remove effects of signal drift unrelated to the conditions. Effects that match the global signal were removed from the voxel's time course by means of regression.

For each individual subject, the mean functional image (built on the basis of all realigned volumes) was coregistered with the subject's structural image, and the fMRI time series was then spatially normalized (two-dimensional spline; voxel size 2 2 2 mm) to an echo planar imaging template conforming to the Montreal Neurological Institute (MNI) space and spatially smoothed with a Gaussian kernel of 8 mm full width half maximum (FWHM).

4.3.3 fMRI artifact signal removal

fMRI data were residualized by multiple regression analysis in the GLM framework against the following regressors: (1-6) six parameters derived from the realignment step, (7-12) their respective first order derivatives (13, 14) global signals from white matter (WM) and CSF, and (15, 16) their respective first-order derivatives. The resulting residual images represent the error term of the model and therefore only contain signal fluctuations unexplained by motion, WM or CSF regressors.

4.3.4 fMRI data analysis

Data analysis was performed using SPM by modeling the sleep stages, as determined by scoring the EEG, as stimulus functions with the movement parameters as regressors of no interest within the general linear model. Intra-subject variance was assessed in

a fixed-effects analysis, and between-subject variance was assessed in a random-effects analysis. A less conservative threshold of uncorrected 0.001 ($k = 25$) was chosen for an alpha level because only six subjects were able to be included in the the second-level analysis.

4.4 Results

Eleven healthy young adult subjects (18-26, 6 female) took part in this study. As Figure 4.5 indicates, there was large variation between and within subjects in terms of sleep stage stability, movement frequency, and the depth of sleep. Data from a total of five subjects were discarded because they were unable to enter deep sleep (SWS) in the MR environment (n=3), because of movement artifacts (n=1), and because they immediately fell asleep without providing baseline data for the awake state (n=1). Data from 6 subjects were finally included in the analysis. This attrition rate is typical of sleep imaging studies (see (Kaufmann et al., 2006; Horovitz et al., 2009a) etc). Stages 3 and 4 were collapsed as SWS because the two sleep stages are, by definition, qualitatively similar according to their EEG reflecting high delta activity.

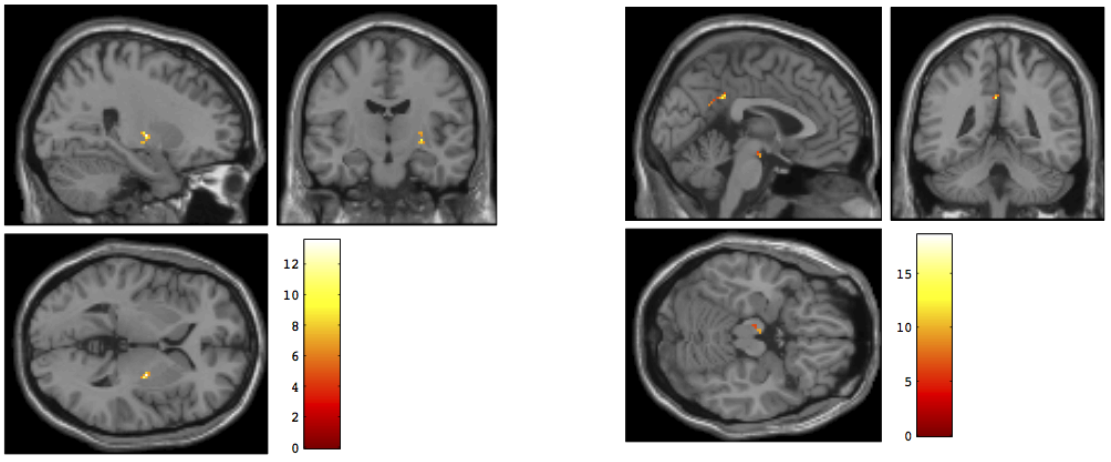

FIGURE 4.6: Results from the whole brain GLM analysis: Contrast images are thresholded at $p < 0.001$ uncorr, $k = 25$, colourbars denote T-value. The posterior cingulate cortex and the brain stem region are more active during light NREM sleep than in slow wave sleep (right image), and that the globus pallidus is more active during wake than in slow wave sleep (left image).

Contrast	*Anatomical region*	*Hemisphere*	*x*	*y*	*z*	*Cluster size (voxels)*	*z-value*	*T-value*
W > SWS	Globus Pallidus	Right	26	-10	2	25	4.11	13.52
2 > SWS	Posterior cingulate	Left	-2	-44	32	26	4.09	13.33
2 > SWS	Midbrain tegmentum	Left	-12	-14	-14	25	4.45	18.50

TABLE 4.1: Location of statistically significant voxels (see Figure 4.6) in stereotactic space (MNI coordinates: x y z) for the comparison of W > SWS and 2 > SWS contrasts.

BOLD activity during light NREM sleep and SWS was contrasted against the wake baseline, and against each other. Relative to the wake baseline, the right globus pallidus decreased activation during SWS, $T(5) = 13.52$, $p < 0.001$ (Figure 4.6, left).

Relative to light NREM sleep, during SWS there was also a decrease in activation in the PCC, $T(5) = 13.33$, $p < 0.001$, and in the tegmentum of the brainstem, $T(5) = 18.50$, $p < 0.001$ (Figure 4.6, right; Table 4.1). No clusters survived Family-wise error correction for any of the NREM-NREM and the NREM-Wake contrasts.

4.5 Discussion and conclusion

Human sleep stages are differentiated by distinct electrophysiological patterns generated by local neuronal populations. There is no literature consensus on the macroscopic spatial distribution of these signal generators contributing to the transition from wake into successive sleep stages. The current study compared the BOLD signal strength of different NREM sleep stages against each other and against a waking baseline. We found that during SWS, the globus pallidus decreases in activity relative to during wake. Additionally, the posterior cingulate cortex (PCC) and the region corresponding to the substantia nigra of the midbrain tegmentum decrease activity in the descent from light NREM sleep to SWS.

That PCC deactivates during SWS agrees with the general consensus that consciousness decreases as sleep deepens. The PCC is implicated as a neural substrate important for

awareness and forms the central node of the default mode network. Previous work has also demonstrated a decrease in functional connectivity between the PCC and frontal regions (Horovitz et al., 2009a)during deep sleep. The result from this study suggests that the decrease in functional connectivity in the default mode network in the descent into SWS may be attributed to decreased activity in the PCC itself.

The substantia nigra belongs to the basal ganglia, and plays an important role in controlling movement. Parkinson disease patients with lesions to the substantia nigra pars compacta (SNc) have been shown to experience sleep disturbances (Poewe & Högl, 2000), implicating its role in sleep-wake regulation. The deactivation of the globus pallidus during SWS, relative to the waking baseline, futher highlights the role of the dopaminergic basal ganglia system in sleep. Its importance in sleep regulation will be addressed and explored in further detail in the next chapter.

Compared to the study by Kaufmann et al. (2006) that used a similar analysis method and alpha value threshold, the current findings of three clusters is relatively small. This may be due to the use of a smaller sample size (compared to N=9 in Kaufmann et al., 2006); however, when the same analysis was conducted with eight subjects, all of whom underwent stage 2 sleep, similarly low numbers of significant clusters survived (these additional two subjects were discarded from the main group analysis as they did not reach deep sleep). Therefore sample size was an unlikely determining factor of the low number of significant clusters from this analysis.

Falling asleep in the scanner exacerbates the variable waxing and waning of vigilance. This increases sleep stage fluctuation and increases the number of stage transitions, which may provide more "trial onsets" that lead to greater statistical power. However, the durations of these sleep stages are in fact unstable and brief. The current study applied a two-minute threshold so as to capture stable stretches of sleep, which increased data attrition and decreased sample size.

Directly modeling stage transition onsets as condition regressors may not be the optimal method of revealing the spatial distribution of BOLD activity during different sleep stages. Indeed, majority of EEG-fMRI studies investigating the BOLD correlates of sleep have chosen to either examine activation associated with specific EEG events,

such as slow oscillations (Dang-Vu et al., 2008) or spindles (Schabus et al., 2007), or the sleep-dependent changes in functional connectivity in different neural networks (Larson-Prior et al., 2009; Horovitz et al., 2009a).

Given the importance of oscillations in information processing in neural circuits (Bullmore & Sporns, 2009; Sejnowski, 2006), examining changes in functional connectivity within the brain may be a more sensitive method for identifying sleep-related network dynamics. While the influence of different sleep stages on activity in the PCC and within the default mode network has been well characterized in the literature, less in known about the basal ganglia network. The following chapter investigates the way in which the neural activity within the basal ganglia network changes during sleep.

Chapter 5

Experiment 2: Basal ganglia networks in human non-rapid eye movement sleep

A growing number of studies show that the basal ganglia play an important role in sleep regulation and maintenance. In particular, the striatum and the globus pallidus have been suggested to promote wake and sleep respectively. This study examines the functional connectivity of the basal ganglia with the whole brain during different stages of non-rapid eye movemet (NREM) sleep. Electroencephalography (EEG) and functional magnetic resonance imaging (fMRI) measures were taken from eleven subjects while they slept following partial sleep deprivation. One cycle of sleep was recorded and functional connectivity for Wake, Light NREM sleep (Stage 2) and Slow Wave Sleep (SWS; Stages 3 and 4) were calculated using the bilateral putamen, bilateral caudate nuclei and bilateral globus pallidus as seeds. Results show that sleep leads to an increase in functional connectivity between the basal ganglia and nodes within the motor network, and exhibits a distribution pattern in line with the tripartite division model of basal ganglia connectivity. Results are discussed in terms of motor learning and memory consolidation.

5.1 Introduction

The basal ganglia (BG) are subcortical brain structures known to play an important role in motor, cognitive and affective behaviors that operate during wakefulness (Mink, 1996; Nambu, 2008). In addition, a growing number of studies have recently implicated the BG in the control of sleep-wake (S-W) behavior. Basal ganglia discharge rates have been shown to decrease along the transition from wakefulness to deep non-rapid eye movement (NREM) sleep (Urbain et al., 2000), as well as display cyclic brisk firing correlated with slow-wave membrane potentials (Mahon et al., 2006). Additionally, patients with basal ganglia-related neurodegenerative disorders, such as Parkinson's and Huntington's disease, often experience sleep-related issues that include sleep-maintenance insomnia, nighttime arousal and daytime sleepiness (Factor, McAlarney, Sanchez-Ramos, & Weiner, 1990).

It is proposed that the key S-W control circuit of the BG is confined to the striato-pallidocortical loop (Vetrivelan, Qiu, Chang, & Lu, 2010), as extensive lesions to the thalamus, subthalamic nuclei and the substantia nigra do not alter S-W behavior significantly (Qiu, Vetrivelan, Fuller, & Lu, 2010; Vanderwolf & Stewart, 1988). In general, a pattern emerges in the reported findings suggesting that the striatum - comprised of the caudate nucleus and putamen - is wake promoting, while the globus pallidus is sleep promoting.

In rodents, lesions to the striatum lead to abnormal sleep architecture and significant increase in sleep (Qiu et al., 2010). In humans, functional imaging has also shown that activity in the striatum decreases in the transition from wakefulness to different NREM sleep stages. For example, decreases in regional cerebral blood flow (rCBF) were reported in the caudate nucleus during NREM sleep (Maquet et al., 1997), and blood oxygenation level dependent (BOLD) signal in both the caudate and putamen were also found to decrease during NREM sleep (Kaufmann et al., 2006).

On the other hand, lesions to the globus pallidus in rodents can lead to profound insomnia, increase in total wake time, as well as fragmented S-W cycles (Vetrivelan et al., 2010). The globus pallidus may also play an important role during sleep oscillations via thalamocortical drive (Ushimaru, Ueta, & Kawaguchi, 2012). In humans, functional

connectivity between the globus pallidus and both frontocentral and parietooccipital cortical sites show sleep-specific coherence patterns (Salih et al., 2009). In light NREM sleep, the globus pallidus was coupled with the parietooccipital cortex at 14 Hz, corresponding to the frequency band of slow sleep spindles. In deep NREM sleep, coherence was highest between the globus pallidus and the frontocentral cortex in the slow wave frequency range (0.5-1.5 Hz).

Natural progression from wakefulness to deep NREM sleep is characterized by the gradual slowing of the ongoing EEG oscillation. Spontaneous fluctuations in resting state BOLD signal show phase correlation in widely distributed functional networks, and can track changes related to modulations in EEG synchrony. Correlations in BOLD signal between brain regions have been observed during human sleep, within the default mode, attentional and executive networks (Horovitz et al., 2009a; Koike et al., 2011; Larson-Prior et al., 2009), in co-occurrence with sleep spindles (Andrade et al., 2011), examination of small-world network properties of the whole brain (Spoormaker et al., 2010, 2011), as well as after sleep deprivation (De Havas, Parimal, Soon, & Chee, 2012).

The current study investigated the hypothesis that the globus pallidus and striatum in humans exert bidirectional influence on the cortex in the descent from wake to deep NREM sleep. fMRI was used to examine functional connectivity between the whole-brain and: 1) the bilateral pallidum, 2) bilateral caudate nuclei and 3) bilateral putamen during NREM sleep, by using the time courses of these subregions as seed regressors. We analyzed their functional connectivity correlates during wakefulness (W), light NREM sleep (stage 2 sleep) and slow wave sleep (stages 3 and 4).

5.2 Methods

5.2.1 Participants

Eleven young healthy paid volunteers (6 females; age range, 18-26 years; mean age, 23.9 years) gave written informed consent according to the institutional guidelines before participating in this study, which was approved by the local Ethical Committee. Subjects

were screened using the Beck Anxiety Inventory and Depression Inventory I for anxiety-related disorders, and the Epworth Sleepiness Scale, Pittsburgh Sleep Quality Index and the Munich Chronotype Questionnaire for sleep-related disorders (see Appendix B). No subjects reported excessive daytime sleepiness or sleep disturbances. The subjects had no history of neurological and psychiatric disorders, or substance abuse, and had no sleep disturbances or recent time zone shifts.

5.2.2 Design

Subjects followed a 2-day constant sleep-schedule before the experiment, during which they were instructed to sleep at 10.30pm for no more than 7.5 hours and to refrain from all caffeine and alcohol-containing substances and intense physical activity during this period. Compliance to the schedule was assessed with sleep diaries and wrist actigraphy (Somnowatch). The experiments were performed between 3.00 and 6.00 am, such that subjects were partially sleep deprived to increase sleep pressure without significantly altering their sleep architecture. Subjects' heads were fitted with ear-muffs and foam pads for sound insulation, and were immobilized to minimize movement artifacts. The scanning room was completely darkened during the experiment. Subjects were asked stay awake for 5-10 minutes with their eyes closed after the scan initiated, after which they were allowed to fall asleep. The session was stopped when the subject was either completely awake or indicated discomfort with a pneumatic squeeze ball, or when a full sleep cycle was completed. A typical session lasted approx. 100 minutes.

5.2.3 EEG acquisition

Simultaneous polysomnography recordings were made using an MR-compatible electrode cap comprising 14 sintered silver-silver chloride pin electrodes: six EEG channels placed in a subset of locations of the 10-20 International System, two electrooculograms, three submental electromyographies, and an electrocardiogram (modified for sleep; VisionRecorder version 1.03, Brain Products), using a MR-compatible 32 channel amplifier (BrainAmp MR plus; Brain Products GmbH). The reference electrode was located between Fz and Cz and the ground electrode below Oz, all on the brain midline. Electrode

impedance was kept <5 kOhms in addition to the 5 kOhm resistor built into the electrodes. The data acquisition rate was 5 kHz, with an analog band-pass filter set to 0.016-250 Hz. Data were collected in a continuous fashion. EEG was monitored online with gradient and pulse artifacts corrected with a 10-second sliding-window template subtraction method using in-house algorithms.

5.2.4 fMRI acquisition

Functional MRI time-series were acquired using a 1.5T MR scanner (Avanto; Siemens, Erlangen, Germany). Multislice T2∗-weighted fMRI images were obtained with a gradient echo-planar sequence, using axial slice orientation (35 slices; voxel size, 3×3×3 mm; matrix size, 64×64×35; repetition time (TR) = 2975 ms; echo time (TE) = 40 ms; flip angle = 90°; field of view = 192 mm; delay = 0). The total volumes acquired ranged from 1654-2106 across subjects, excluding the first 8 volumes discarded to allow for T1 equilibration effects. A structural T1-weighted 3D MP-RAGE sequence (TR = 1960 ms; TE = 5.6 ms; inversion time, 1100 ms; field of view, 256×224 mm^2; matrix size, 256×224×160; voxel size 1 mm^3) was also acquired in all subjects.

5.2.5 EEG analysis

Artifacts related to gradient switching and cardio-ballistic effects were removed using standard routines available in Analyze software (Brain Products). The data was band-pass filtered between 0.5 and 30 Hz, and manual sleep stage scoring following Rechtschaffen and Kales (1968a) criteria was performed in 30 sec window epochs. The hypnograms were then screened for intervals corresponding to continuous periods of Wake, Stage 2, 3 or 4 (stage 1 sleep, and rapid-eye-movement (REM) sleep were excluded), devoid of any arousals or movement times in either EEG or fMRI, and lasting more than 2 minutes.

The series of consecutive fMRI volumes corresponding to a chosen sleep period were selected from the complete fMRI time series and constituted a "session" for further

analysis. fMRI and EEG data corresponding to stages 3 and 4 were collapsed as a single stage representing SWS in all subsequent analyses.

5.2.6 fMRI preprocessing

Functional volumes were preprocessed with SPM8 (www.fil.ion.ucl.ac.uk/spm/software/spm8) implemented in MATLAB (version 7.11, Mathworks). The fMRI time series was realigned using rigid body transformation of all images to the first image to correct for head motion (data with head movements >2 mm were excluded). Global effects from the images were estimated using a voxel-level linear model of the global signal (Macey et al., 2004) to remove effects of signal drift unrelated to the conditions. Effects that match the global signal were removed from the voxel's time course by means of regression. For each individual subject, the mean functional image (built on the basis of all realigned volumes) was co-registered with the subject's structural image, and the fMRI time series was then spatially normalized (two-dimensional spline; voxel size 2×2×2 mm) to an echo planar imaging template conforming to the Montreal Neurological Institute (MNI) space and spatially smoothed with a Gaussian kernel of 8mm full-width half maximum (FWHM).

5.2.7 fMRI artificial signal removal

fMRI data were residualized by multiple regression analysis in the GLM framework against the following regressors: (1-6) six parameters derived from the realignment step, (7-12) their respective first order derivatives (13, 14) globals signals from white matter (WM) and cerebral spinal fluid (CSF), and (15, 16) their respective first-order derivatives. The resulting residual images represent the error term of the model and therefore only contain signal fluctuations unexplained by motion, WM or CSF regressors.

5.2.8 fMRI correlation analysis

Data from a total of five subjects had to be discarded because they were not able to fall into deep (SWS) sleep in the noisy and uncomfortable laboratory environment ($n = 3$),

because of movement artifacts ($n = 1$), or because they immediately fell asleep without providing baseline data for the awake state ($n = 1$). Data from 6 out of 11 subjects were finally included in the analysis.

Automated subcortical segmentation was performed with FreeSurfer using cytoarchitechtonic probability maps to define the bilateral caudate nuclei, bilateral putamen and bilateral globus pallidus in each subject's T1 scan. Each subject's automated segmentation results were normalized into MNI space, and for each BG subregion the intersection (logical "AND") of all subjects' extracted volume was used as a seed region. For each subject and sleep stage, a seed time-course was computed as the mean value of the time courses of all voxels inside each bilateral subregion.

For each subject and sleep stage, these time courses were correlated with each voxel in the brain. Second-level beta values are Fisher transformed correlation coefficient values - or Z-values, which directly relate to the correlation coefficient units (r values) from the first level analysis. For analyzing sleep stage influences, second level random-effects analysis was performed using a two-factorial design (subregion: three subregions; and sleep: wakefulness, Stage 2, SWS). Effects of sleep and subregion were tested using ANOVA. In addition, independent sample t-tests in both directions were performed (W vs. S2, W vs. SWS, and S2 vs. SWS).

The composite maps collected during wakefulness, Stage 2 and SWS were thresholded at $p_{FDR} < 0.05$, extent $k > 25$ voxels, and show positive correlations with seed regions. For the main effects of sleep and subregion, interaction between them, and for the bidirectional sleep stage comparisons, a cluster collection threshold was defined at $p < 0.0005$, extent $k > 25$ voxels. All activation maps are shown on the group-mean 3D T1-weighted image. All figures are displayed using the neurological convention.

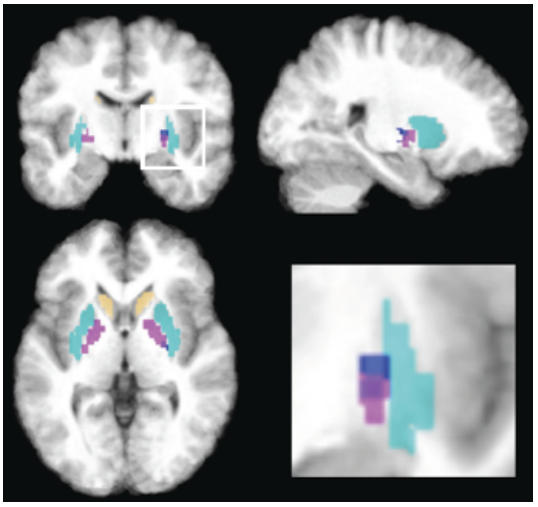

FIGURE 5.1: Bilateral caudate (beige), putamen (turquoise) and globus pallidus (pink) regions extracted from the T1 anatomical structural scans of all subjects who showed sufficient epochs of slow wave sleep (logical AND; N=6), and overlaid on the mean anatomical image. The bilateral caudate, putamen and globus pallidus are used as seed ROIs for functional connectivity analysis. The cluster from the Wake ¿ SWS contrast (dark blue, bottom right panel) from Chapter 4 corresponds to the right dorsal posterior pallidum.

5.3 Results

5.3.1 Basal ganglia connectivity during wake

Functional connectivity was examined using regional seed-to-voxel bivariate correlation; beta values in group level analyses represent Fisher-transformed correlation coefficient values, or Z-values.

During wake, bilateral globus pallidus connectivity did not extend beyond the seed region (Figure 5.2 A, red clusters). The distribution of the caudate nucleus network connectivity extended to the left thalamus (Figure 5.2 B, red clusters), which partially replicates existing studies examining functional connectivity using multiple regression or seed regions parcellated differently from the current study (Barnes et al., 2010; Di Martino et al., 2008). The bilateral putamen connectivity network during wake included the caudate, anterior cingulate cortex, thalamus and insula (Figure 5.2 C, red clusters)(see Figure 5.3 for all clusters).

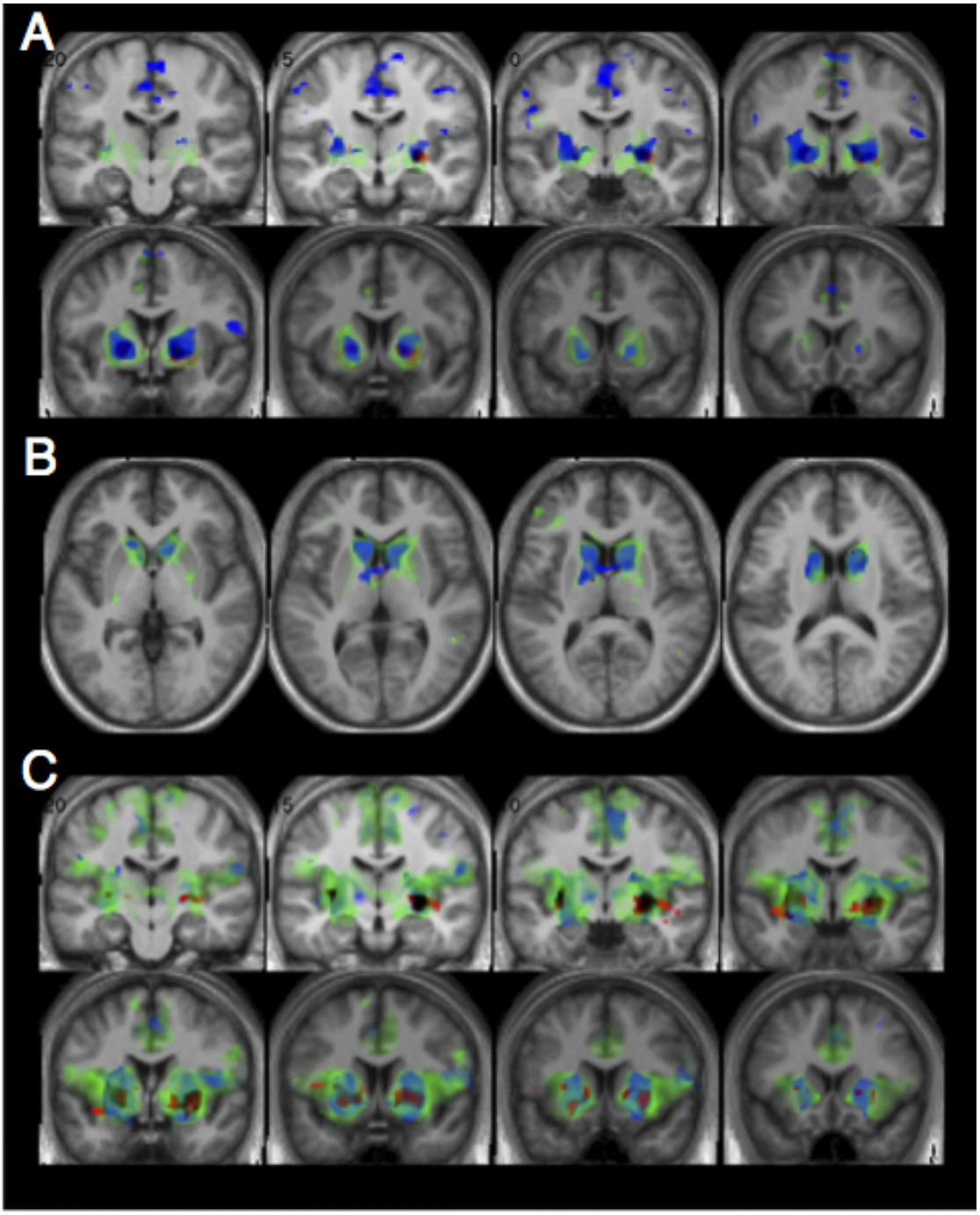

FIGURE 5.2: Composite maps show functional connectivity of the bilateral globus pallidus (A), bilateral caudate (B) and bilateral putamen (C). Functional connectivity maps for each seed region during wake (red clusters), light NREM sleep (green clusters) and deep NREM sleep (blue clusters) are overlaid on top of each other.All clusters are thresholded at $p < 0.05$, FDR corrected, $k = 25$ voxels; all beta values represent Fisher-transformed correlation coefficients i.e. Z-value.

Condition, Seed	Region	x	y	z	Cluster size (voxels)	Cluster p-FDR	Peak p-FDR
Wake, Bilateral Pallidum	R Pallidum	28	-14	-2	681	0.000	0.986
	L Pallidum	-20	2	0	320	0.000	0.986
S2, Bilateral Pallidum	R Pallidum	16	-2	0	6405	0.000	0.065
	L ACC	-8	0	42	601	0.000	0.984
	L Postcentral gyrus	-48	-10	24	95	0.063	0.984
	R Precentral gyrus	52	2	14	75	0.105	0.984
	L ACC	-10	34	14	60	0.159	0.984
	R Lingual gyrus	16	-48	-12	45	0.267	0.984
SWS, Bilateral Pallidum	R Pallidum	18	0	0	1234	0.000	0.963
	L Pallidum	-28	-6	10	1128	0.000	0.963
	R Medial precentral gyrus	6	-20	60	944	0.000	0.963
	R Lateral precentral gyrus	54	0	16	134	0.001	0.963
	L Precentral gyrus	-50	-10	30	94	0.003	0.963
	L Precentral gyrus	-56	-10	40	89	0.004	0.963
	R Precentral gyrus	42	-14	44	72	0.008	0.963
	L IPL	-60	-32	22	64	0.012	0.963
	L ACC	-2	14	42	60	0.014	0.963
	R Postcentral gyrus,	18	-38	52	37	0.061	0.963
	R Precentral gyrus	54	-6	38	27	0.123	0.963
Wake, Bilateral Caudate	R Caudate	10	12	14	136	0.000	0.958
	L Thalamus (dorsomedial nucleus)	-10	-6	10	40	0.000	0.958
S2, Bilateral Caudate	R Caudate	18	10	16	4203	0.000	0.299
	R Cerebellum	16	-36	-18	153	0.003	0.991
	L IFG	-34	34	10	122	0.006	0.991
	L Cerebellum	-16	-38	-22	60	0.069	0.991
	R MTG	58	-38	-2	39	0.177	0.991
	R ITG (temporoccipital)	50	-48	6	36	0.177	0.875
	R ITG (posterior)	50	-28	-32	33	0.183	0.991
SWS, Bilateral Caudate	L Caudate	-2	2	10	1800	0.000	0.497
Wake, Bilateral Putamen	R Putamen	28	-4	-4	1251	0.000	1.000
	L Caudate	-14	12	2	844	0.000	1.000
	L ACC	-2	42	4	50	0.012	1.000
	L Thalamus (ventral lateral nucleus)	-14	-24	2	35	0.039	1.000
	L Insula	-40	6	6	29	0.059	1.000
S2, Bilateral Putamen	L Putamen	-26	0	8	20030	0.000	0.048
	L Premotor Cortex	-10	4	64	9539	0.000	0.430
	R Cerebellum	22	-46	-26	782	0.000	0.915
	R Posterior supramarginal gyrus	60	-42	42	187	0.071	0.736
	R Precentral gyrus	38	-16	42	28	0.874	0.981
SWS, Bilateral Putamen	R Insula	44	2	12	4379	0.000	0.311
	L Putamen	-30	-2	-10	3766	0.000	0.697
	R Premotor cortex	6	-8	60	2063	0.000	0.963
	L Precentral gyrus	-18	-30	56	139	0.026	0.963
	L IPL	-50	-22	28	55	0.307	0.813
	R MFG	32	16	48	39	0.436	0.963
	R ACC	4	34	14	37	0.436	0.963
	R Precentral gyrus	44	-16	42	35	0.436	0.963
	L ACC	-4	28	-6	27	0.562	0.963

FIGURE 5.3: Table showing the center of mass for voxel-by-voxel correlations with bilateral pallidum, bilateral caudate, and bilateral putamen seeds respectively, during wake, light NREM sleep (S2), and deep NREM sleep (SWS). All reported clusters are thresholded at $p < 0.05$, $FDR - corr$, $k = 25$ voxels. The first column indicates the sleep condition (Wake vs. S2 vs. SWS) under which the seed region's functional connectivity is calculated. The second column indicates the cortical region that the significant cluster corresponds to. The third, fourth and fifth columns indicate the MNI coordinates for the x, y and z axes respectively. The sixth colum indicates the cluster size (k value). The seventh column shows the cluster-level significance level with FDR correction. The last column shows the significance level of the peak voxel within that cluster, with FDR correction.

5.3.2 Basal ganglia connectivity during NREM sleep

During NREM sleep, BOLD signal time-course in the bilateral globus pallidus showed positive correlation with signal in the putamen, primary and supplementary motor areas, the anterior cingulate cortex (ACC) , and the left inferior parietal lobule (IPL) (Figure 5.2 A, green and blue clusters).

Putamen functional connectivity pattern during NREM sleep was similar to that of the pallidum, with additional coactivation seen in the posterior cingulate cortex (PCC), cerebellum, ventral anterior and ventral lateral (VA/VL) nuclei of the thalamus and somatosensory areas (Figure 5.2 C, green and blue clusters).

In both light and deep NREM sleep, the bilateral caudate showed network activity limited to the VA of the thalamus, putamen, cerebellum, left inferior frontal gyrus (IFG) and right posterior middle temporal gyrus (MTG) during light NREM sleep (Figure 5.2 B, green and blue clusters).

To examine the effects of different sleep stages on connectivity strength, a 2-way ANOVA with factors *seed region* (pallidum, caudate, putamen) and *sleep stage* (wake, light NREM, deep NREM) was conducted. A seed-region by sleep-state interaction was found in the PCC (Figure 5.4 A) and the supramarginal gyrus of the IPL (Figure 5.4 B), and a significant main effect of sleep state was found in the left IFG (Figure 5.4 C). A main effect of BG subregion covering parietal sensorimotor and mid-cingulate areas, the insular cortices, IFG and posterior temporooccipital regions was also observed. All clusters were thresholded at $p < 0.0005$, uncorr., $k = 25$.

To further examine the sleep stage-dependent changes in BG functional connectivity, paired t-tests comparing correlation strengths between the three sleep states were conducted separately for each subregion.

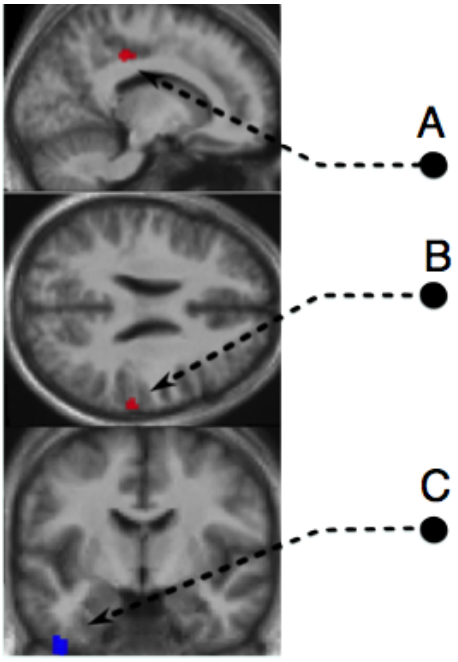

FIGURE 5.4: A 3-by-3 repeated-measures ANOVA (Sleep state: wake, light NREM sleep (S2), deep NREM sleep (SWS); Seed region: bilateral caudate, bilateral pallidum, bilateral putamen) was performed on functional connectivity strength. Beta values are Fisher-transformed correlation coefficiants from the first-level analysis. There was an interaction between sleep state and seed region, which modulated functional connectivity strength in the posterior cingulate cortex (A, red cluster) and the supramarginal gyrus / inferior parietal lobule (B, red cluster). There was also a main effect of sleep state on functional connectivity strength of the inferior frontal gyrus (C, blue cluster).

5.3.3 Decreases in coactivation during NREM sleep

All t-tests clusters were thresholded at $p < 0.0005$, uncorr., $k = 25$. There was significant decrease in functional connectivity between the globus pallidus and the bilateral posterior insula (Figure 5.5 C), anterior parahippocampal gyrus (PHG; Figure 5.5 B), pons (W>S2/SWS), and cerebellum (W>SWS).

Putamen coactivation with the posterior MTG (W>S2/SWS), middle frontal gyrus (MFG; W>S2) and the anterior inferior temporal gyrus (ITG; S2>SWS) also decreased. No significant decreases in caudate functional connectivity were found during NREM sleep.

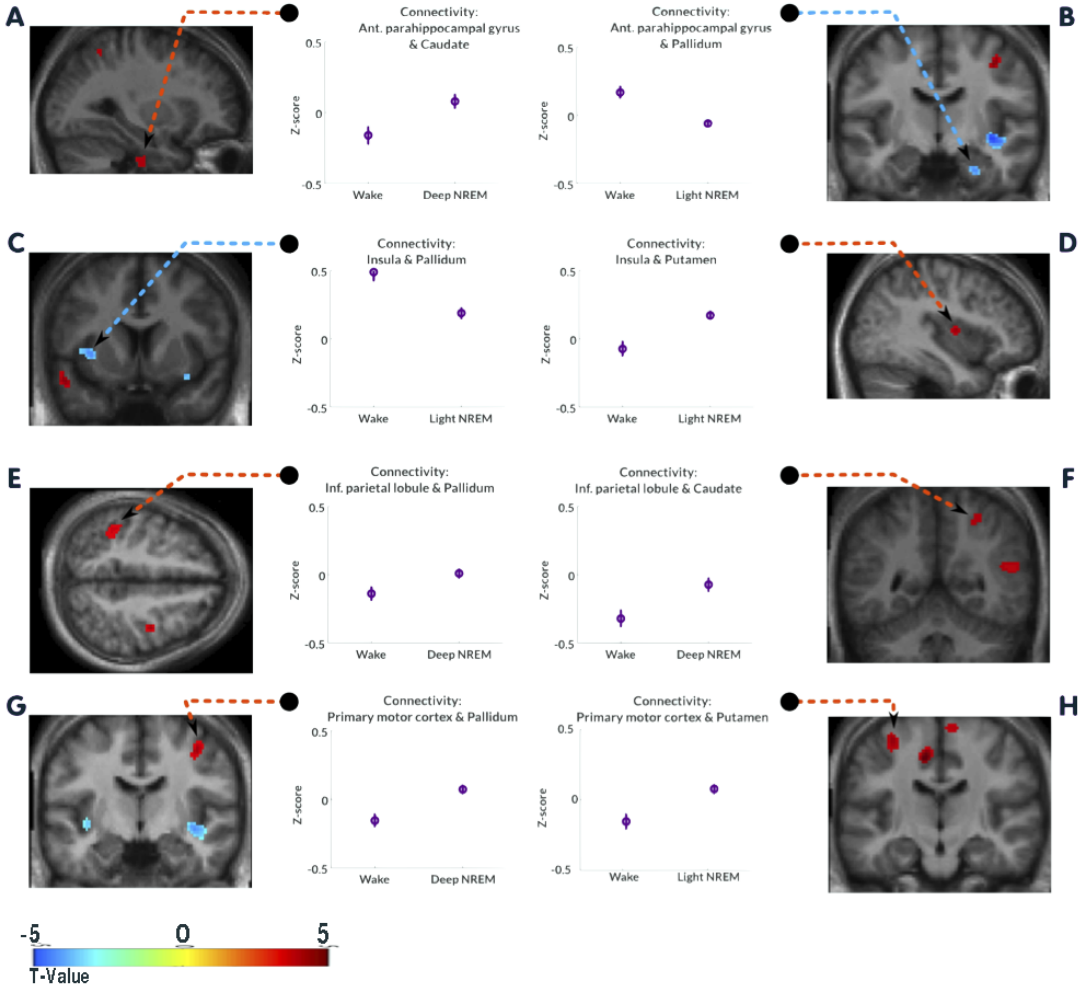

FIGURE 5.5: Statistical parametric maps and graphs show results from t-tests comparing the functional connectivity strength of the basal ganglia seed regions across sleep states. Specifically, connectivity between the Wake state vs. light NREM or deep NREM is compared. Beta values used for the t-contrast calculation are Fisher-transformed correlation coefficients from the first level analysis (Z-value). Statistical t-maps presented indicate clusters that significantly increase or decrease in coactivation with the seed region, depending on sleep state. Each graph shows the functional connectivity strength between a seed region and the indicated cluster (arrow) in the Wake and either the Deep or Light NREM sleep. Increases in coactivation during sleep (red clusters) are seen between the bilateral globus pallidus with the primary motor cortex (G) and with the inferior parietal lobule (E), between the bilateral caudate with the anterior parahippocampal gyrus (A) and with the inferior parietal lobule (F), and between the bilateral putamen with primary motor cortex (H) and with the insula (D). Decreases in coactivation during sleep (blue clusters) are seen between the bilateral globus pallidus with the anterior hippocampal gyrus (B) and with the insula (C). All clusters are thresholded at $p < 0.0005$, *uncorr.*, $k = 25$.

5.3.4 Increases in coactivation during NREM sleep

During NREM sleep, there was increased coactivation between the globus pallidus and the primary motor cortex (S2/SWS>W; Figure 5.5 G), left IPL (SWS>W; Figure 3E) and left IFG (SWS>S2). The putamen also increased functional connectivity with the primary motor cortex (Figure 5.5 H) in light NREM sleep, and with the supplementary motor areas in both light and deep NREM sleep. In contrast to the pallidum, the putamen increased coactivation with the bilateral posterior insular cortices during light NREM sleep (Figure 5.5 D). The caudate increased coactivation with the angular gyrus of the IPL in both light and deep NREM sleep (Figure 5.5 F), and with the anterior PHG in deep sleep (Figure 5.5 A), again in contrast to the pallidum.

5.4 Discussion

Correlations in BOLD signal between brain regions have been observed during human sleep, within a range of brain networks and during different sleep stages. Functional connectivity of basal ganglia subregions have also been explored during NREM sleep with electrophysiological recordings (Salih et al., 2009), and during wake with fMRI (Barnes et al., 2010; Di Martino et al., 2008). The present study tested the hypothesis that the caudate nucleus, putamen and globus pallidus would exhibit different coactivation patterns in a sleep stage-dependent manner, based on previous findings suggesting their involvement in sleep-wake regulation.

5.4.1 Globus pallidus and putamen increase connectivity with primary motor cortex during sleep

The putamen is considered the main relay structure of the basal ganglia, and shows positive functional connectivity with primary and supplementary motor areas, as well as the ACC and precuneus (Di Martino et al., 2008) and insula (Postuma and Dagher, 2006) during waking resting state. Increase in connectivity between the putamen and the primary and supplementary motor areas during sleep as found in the current study

suggests that a strengthening of this network dynamic in the absence of other non-motor nodes, such as the ACC and precuneus involved in executive function, that are usually coupled in activity with the putamen in the waking state.

Previous intracortical sleep recordings show coherence between the globus pallidus and the sensorimotor areas at spindle frequencies in light NREM sleep, and between the globus pallidus and frontal regions at slow-wave frequencies in deep NREM sleep (Salih et al., 2009). This corroborates the current finding that the globus pallidus and primary motor cortex increase coactivation during NREM sleep. Although many studies have shown that motor learning can occur during sleep (Walker et al., 2005; Walker, Brakefield, Morgan, Hobson, & Stickgold, 2002; Gais et al., 2008), and that disruption of the primary motor cortex can disrupt motor skill learning (Robertson, 2005), no study has so far examined how plasticity *within* the primary motor cortex itself occurs during sleep. The fundamental function of the primary motor cortex is voluntary movement control. Recent studies have shown that this function relies on distributed networks rather than discrete representations, and that these networks are capable of modification (Sanes & Donoghue, 2000). The increased coactivation between the globus pallidus and the primary motor cortex observed in the current findings during sleep, compared to wake, may play a role in the sleep-dependent strengthening of the primary motor cortex network.

While increased pallidal coactivation with frontal regions was also found in the current study, this was constrained to the IFG and frontal pole in the transition from light to deep NREM sleep - in agreement with a deep sleep-specific pallidal-frontal involvement (Salih et al., 2009). The globus pallidus is the main output nucleus of the basal ganglia in humans, and plays an important role in voluntary control of movement upstream to the primary motor cortex. In particular, pallidal-frontal loops have been implicated in behavioral goal-determination and action-specification (). The frontal cortex has been shown to decrease in functional connectivity with the PCC within the default mode network during deep sleep (Horovitz et al., 2009b) to suggest diminished conscious awareness, as well as desynchronize with the limbic circuit and the hippocampus during REM sleep (Johnson, 2006). The strengthening of connectivity between the frontal

regions with the globus pallidus , however, has been suggested to reflect the specific nature of the motor system in NREM sleep, and further supports the notion of sleep-dependent motor circuit integration.

5.4.2 Globus pallidus and caudate increase connectivity with inferior parietal lobule during sleep

The inferior parietal lobule (IPL) of the posterior parietal cortex (PPC) is associated with sensorimotor integration and forms the path of the motor commands (from IPL to premotor to primary motor cortex) (Chersi, Ferrari, & Fogassi, 2011; Geyer, Luppino, Ekamp, & Zilles, 2005; Mesulam, 2009). Of interest is the finding that lesions to the IPL are often found in patients showing signs of spatial neglect, which occurs more frequently when the basal ganglia are also damaged (R. T. Watson, Valenstein, & Heilman, 1981). For both the globus pallidus and caudate, functional connectivity with the IPL increases only during deep NREM sleep, which may suggest a special role for deep sleep in strengthening this connection in the absence of external interfering information.

5.4.3 Globus pallidus vs. putamen connectivity with posterior insula

The posterior insular cortex (PIC) forms part of the lamina I spinothalamocortical pathway, and during wake, is responsible for providing an objective interoceptive representation of the body's physiological condition (for review, see (Craig, 2009)). Functional connectivity of the insula in the waking resting brain shows an anterior/posterior division in network activity, with the PIC linked to premotor, sensorimotor, supplementary motor and middle posterior cingulate cortices, as well as to the basal ganglia, and the ventroanterior/ventrolateral nuclei of the thalamus, highlighting its role in sensorimotor integration (Cauda et al., 2011). Additionally, a meta-analysis of basal ganglia functional connectivity reported caudate and putamen coactivation with the anterior and posterior insula respectively during waking resting state (Postuma, 2005), consistent with the somatotopic anatomical connections previously described between these structures (Chikama, McFarland, Amaral, & Haber, 1997).

In the current findings, the globus pallidus exhibited functional connectivity with the PIC that decreased during light NREM sleep. In contrast, the putamen increased its functional connectivity with the PIC during both light and deep sleep. Specifically, the globus pallidus decreased coactivation with the ventral posterior and the putamen increased coactivation with the dorsal PIC in the current study. This inverse relationship supports the notion that the globus pallidus and striatum play opposing roles in sleep-wake behavior.

5.4.4 Globus pallidus vs. caudate connectivity with anterior parahippocampal gyrus

Similarly, the globus pallidus and the caudate show opposite changes in connectivity strength with the parahippocampal gyrus (PHG) during sleep. In deep NREM sleep, the globus pallidus decreases coactivation with the region of the anterior PHG corresponding to the uncus, while the caudate increases coactivation with the same region during deep sleep. The anterior PHG forms part of the perirhinal cortex of the limbic circuit and forms the anterior connection of the temporal lobe to the area of the basal ganglia. The involvement of this limbic area, together with the insula, suggest that NREM sleep may serve a special function not only in motor functions, but also in emotional regulatory functions. Importantly, this pattern of findings also further supports the hypothesis that the globus pallidus and striatum share an inverse relationship in their influence on sleep wake behavior.

5.4.5 Tripartite division model

Of interest are the four brain regions that show consistent change in connectivity to different basal ganglia subregions during sleep, namely the insula, anterior parahippocampal gyrus, motor cortex and the inferior parietal lobule. These correspond with limbic, sensorimotor and associative regions respectively, a pattern that lends support to the tripartite division model of striatum connectivity (Parent & Hazrati, 1995). These divisions have been shown in functional connectivity patterns obtained during wake, with

a rostral/caudal and dorsal/ventral division of the striatum (Postuma, 2005). Although the striatum could not be segmented according to the same subregions, our findings indicate that the tripartite division network is maintained during NREM sleep, with its network dynamics strengthened at different stages of NREM sleep.

5.5 Conclusion

Existing studies of resting state functional connectivity during NREM sleep have identified discordant results, with some arguing that functional connectivity is preserved across levels of arousal as spontaneous BOLD signal fluctuations exhibit quasi-structural properties (Horovitz et al., 2008; Larson-Prior et al., 2009), while others find a decrease in connectivity with sleep (Horovitz et al., 2009a; Massimini, 2005).

The present findings show that functional connectivity between basal ganglia subregions and the rest of the cortex increase and decrease connectivity strength to cortical regions depending on basal ganglia subregion, as well as sleep stage. In general, the striatum increases connectivity to the insula, anterior parahippocampal gyrus, motor cortex and inferior parietal lobule during NREM sleep, while the globus pallidus decreases connectivity to the insula and anterior parahippocampal gyrus only during NREM sleep. Additionally, the pattern of brain regions that change coactivation strength with the basal ganglia are in line with the tripartite division model of basal ganglia connectivity.

Furthermore, there is strong evidence in the current results suggesting that NREM sleep plays an important role in the integration of the motor network, in which functional connectivity between the basal ganglia and motor areas increase coactiviation. Plasticity of motor networks that are related to motor memory consolidation may occur as a result of sleep-dependent coactivation increases. Future studies of sleep and motor learning can benefit from taking the basal ganglia activity and connectivity changes into consideration.

Chapter 6

Investigating BOLD correlates of induced oscillations

The way in which EEG frequency power changes affect the BOLD signal can be better understood by manipulating the dominant oscillatory electrical activity in the brain. This chapter introduces oscillatory cortical stimulation, with a focus on transcranial alternating current stimulation (tACS), and its concurrent use with fMRI, as a means of understanding the BOLD correlates of oscillations in the brain. First, the different methods of artifically entraining oscillations is reviewed, followed by the physiological mechanisms of tACS, and concludes with the methodological concerns when combined with fMRI.

6.1 Oscillatory cortical stimulation

A large body of evidence suggests that oscillatory activity of different frequencies have important roles in information processing inside the brain, and are considered evolutionarily relevant, rather than by-products of neuronal signal transduction. Network oscillations may bias information input selection, group neurons into assemblies in a function-specific manner, and facilitate synaptic plasticity. Moreover, different frequencies of neuronal oscillations are hypothesized to play specific functional roles, such as

memory and encoding, local and global cortical signal processing, temporal representation of information, and many other cognitive processes. Whether such oscillations arise as a result of an individual's intention, or whether their pre-existence is responsible for guiding decision making processes that result in the illusion of free will, has fueled a chicken-and-egg debate pertaining to the role of oscillations in human existence and consciousness, but is not within the scope of the current review.

The role of oscillatory activity in the brain has been widely studied using EEG, MEG, ECoG, LFPs and other intra-cranial methods. fMRI has also been used to examine BOLD activity related to processes with distinctly characteristic oscillatory signatures. In addition to observational studies of neural synchrony, oscillatory entrainment is also possible using periodically delivered stimuli (e.g. flashing visual percepts or periodic sound signals) to induce frequency-specific electrophysiological signals.

The last decade has witnessed a growth in studies that seek to directly induce or alter neuronal oscillations using non-invasive stimulation techniques, such as transcranial magnetic stimulation (TMS) or transcranial electrical stimulation. For example, repetitive TMS (rTMS) can cause periodic firing in neuronal populations when electrical pulses are delivered in regular intervals (Thut et al., 2011; Thut & Miniussi, 2009), in a manner of high spatial precision to ensure a localized neuronal population is directly excited by each TMS pulse. However, rTMS is usually delivered in brief pulses of about $100\mu s$ duration, repeated at the frequency of interest - this results in a wide range of frequencies induced in addition to the frequency of interest, which may lead to ambiguous effects. Nonetheless, several studies have demonstrated frequency-specific effects on behavior using rTMS (Romei, Driver, Schyns, & Thut, 2011), suggesting that the entrained oscillatory activity is dominated by the stimulated frequency and overrides the broad-band responses of the single pulses.

Transcranial electrical stimulation methods, including transcranial direct current stimulation (tDCS), transcranial random noise stimulation (tRNS), oscillatory transcranial direct current stimulation (otDCS) and most of all transcranial alternating current stimulation (tACS), have also demonstrated the ability to modulate physiollogically relevant brain activity, sometimes at a frequency-specific manner. These methods all operate by

Table 6.1: Types of transcranial electrical stimulation

tDCS	Direct, flat, and continuous signal, typically applied over a few minutes
tRNS	Oscillating signal with a random-noise frequency spectrum
tACS	Alternating signal, in a sinusoidal or rectangular shape
otDCS	Alternating current superimposed onto a direct current (e.g. tACS and tDCS combined)

passing an electrical signal from one electrode to another, where an individual's brain is used to complete the circuit. In this way, an electrical signal can be passed through the cortex (via the skull) to induced artificial neuronal synchrony. tRNS, tDCS, otDCS and tACS differ in the shape of the electrical signal passed through the circuit, as described in the table 6.1. These signals can be negative or positive (anodal or cathodal), and the beginning and end of the signals can be ramped up and down respectively over time. The phase parameters of the stimulation signal can also be manipulated.

Of these stimulation methods, tACS represents the artificial signal that most closely resembles the recorded electrical signals resulting from synchronous firing of neuronal populations - e.g. the sinusoidal signal adheres most to the alternating 'ON' and 'OFF' behavior of population firing. Therefore, tACS is considered the best method electrical stimulation method for entraining oscillations. Although there is ongoing debate as to whether tACS truly modulates brain oscillations (Brignani, Ruzzoli, Mauri, & Miniussi, 2013), several of studies have shown that, using tACS, both behavior and EEG recorded in humans are affected (Zaehle, 2009; Wach et al., 2013; Angelakis et al., 2013; Kanai, Chaieb, Antal, Walsh, & Paulus, 2008; Chaieb, Paulus, & Antal, 2011; Fedorov et al., 2010, 2011).

6.2 Physiological mechanism of tACS

tACS is defined by the alternating direction of the applied current, and aims to interfere with ongoing oscillations in the brain (Antal et al., 2008). The neurophysiological mechanisms that underpin the effects seen during tACS remain unknown and speculative. Since the direction of current is constantly changing in tACS, this decreases the

possibility of extramembrane potential polarization (e.g. the proposed mechanism for tDCS) as the underlying cause (Zaghi, Acar, Hultgren, Boggio, & Fregni, 2010).

Although tACS has been proposed to function by inducing synchronous changes in brain activity (Schroeder & Barr, 2001), some studies have reported no change in EEG activity before or after the stimulation (Antal et al., 2008), suggesting that any effect on oscillatory activity is likely to be limited to the stimulation period. One theory propose that stimulating with a constantly varying electrical force induces noise that interferes with oscillations in the brain. Another theory suggests that some effects associated with transcranial electrical stimulation (i.e. analgesic) may simply be secondary responses to peripheral nerve stimulation (Nekhendzy et al., 2006). Others also posit that the changes seen in neuronal activity during stimulation are the result of altered neurotransmitter and endorphin release (Limoge et al., 1999, Kirsch D, 2004), although a causal relationship between stimulation and endorphin/neurotransmitter release remains elusive.

The literature to date is unable to conclusively determine an underlying mechanism for the effects seen during stimulation with tACS. However, there exists sufficient evidence to show that tACS does indeed alter brain activity, and illustrates electrphysiological phenomena that give a better understanding of the mechanisms of tACS.

6.2.1 Animal studies

High frequency sinusoidal stimulation applied to a rat hippocampus at 50-200 Hz led to activity suppression of cell bodies and axons (Jensen & Durand, 2007), supporting findings that AC electrical stimulation or tDCS delivered in an intermittent manner may interfere with ongoing cortical processes (Yamamoto et al., 2006, Marshall et al., 2005).

Multi-unit activity (MUA) recordings in animals show that spike activity is synchronized to different electrical stimulation frequencies (Fröhlich & McCormick, 2010). The steeper the voltage change in the electrical stimulation signal, the stronger the neural firing, compared to slower transient voltage changes that reach the same voltage maximum. This demonstrates that in addition to the absolute voltage levels, the temporal dynamics of voltage changes - e.g. the stimulation frequency - determines neural firing.

The same effects can be achieved with weaker currents that penetrate the skull, as shown with intracranial recordings made in rats while being stimulated with surface electrodes (Ozen et al., 2010). A low intracranial electric field of $1V/m$ is sufficient to cause phase-locking between the extracranially applied sinusoidal current and neural firing. Variables like skull thickness and electrode placement, however, also affect the size of the current that must be applied extracranially to induce such an electric field.

6.2.2 Human studies

tACS has been shown to entrain alpha activity in humans, where the spectral density of alpha EEG recorded during simultaneous tACS, applied at the individual's specific ongoing alpha frequency, was found to increase (Zaehle, 2009). This study provided the first human evidence that tACS effectively interacts with physiological oscillations. In humans, there exists a non-linear relationship between cortical excitation changes and the intensity of tACS. This was demonstrated in a study that measured motor evoked potentials (MEPs) in response to single TMS pulses - as an index of excitation threshold, while tACS was simultaneously applied to the primary motor cortex at 140 Hz (Moliadze, Atalay, Antal, & Paulus, 2012). High stimulation intensities of 1 mA led to lowered motor threshold, suggesting excitation, whereas low stimulation intensities of 0.2 mA resulted in an increased motor threshold, indicating inhibition. Interestingly, intermediate intensities of 0.6 and 0.8 mA did not effect motor threshold. These results suggest that while inhibitory neurons are more sensitive to electrical stimulation and fire even at lower intensities of stimulation, excitatory neurons are less susceptible to stimulation, and require a stronger current, but their activity dominates inhibitory neurons and thus leads to net excitatory effect. Lastly, no changes in neuron firing threshold are detected at intermediate stimulation levels because the inhibitory and excitatory effects cancel each other out.

6.3 Stimulation parameters

The efficacy of tACS depends on current density and electrode size, the shape and location of the electrode, strength of current, number of trials, duration and phase of the stimulus, which together determine the effect of induced electrical field on cortical activity (Nitsche, Antal, Liebetanz, & Lang, 2008).

Electrode size determines how focal the electrical stimulation is, with larger electrodes stimulating with less anatomical specificity (Nitsche, Cohen, et al., 2008; Nitsche et al., 2007). While unfavorable, it may be of little importance for tACS stimulation, which is believed to affect the cortex in a global manner. The reference electrode can be made functionally inert by increasing its size, enabling the desired excitability shift by the stimulation electrode without necessarily shifting excitability of another brain area in the other direction (Nitsche, Cohen, et al., 2008).

Current density is not equally distributed over the surface of an electrode, with significantly higher current densities forming at the electrodes edges. Additionally, depending on the position of the electrode, current can be shunted across the scalp and will not stimulate the brain (Rush & Driscoll, 1968; Miranda, Lomarev, & Hallett, 2006; Bikson, Datta, & Elwassif, 2009).

To maximise the probability of stimulating the desired neuronal population and producing the intended stimulation effects, accurate positioning of the electrodes is crucial. Different electrode montages result in varying amounts of shunting, thereby altering the amount of current delivered to the brain tissue (Nitsche, Cohen, et al., 2008).

6.4 Combining tACS with fMRI

6.4.1 Imaging artefacts induced by electrical stimulation during fMRI

Combining tACS with concurrent fMRI can provide insight into how electrical stimulation modulates neural activity, by examining BOLD response in the whole brain or specific regions of interest. The precise translation from an applied electrical stimulation

on the scalp to a detected BOLD signal remains unclear, and presumably reflects the following relationsips:

- A combination of affective and functional connectivity,
- The complex, non-linear response of a neuron in response to electrical stimulation, and
- The non-monotonic re tifying transformation to BOLD or arterial spin labelling (ASL) signal.

MRI imaging sequences rely on carefully controlled magnetic field distributions, which may be disrupted by the magnetic fields generated by applied currents. BOLD signal is sensitive to local magnetic fields, and may therefore be distorted when electrical signals are simultaneously applied during acquisition.

Real physioloigcal BOLD changes induced by tDCS, versus possible concurrent signal artifacts resulting from the current flow in the tissue, are not easily differentiated. To test this, a conventional echo-planar imaging sequence was used to image post-mortem brains, which normally do not show any functional hemodynamic changes in brain activity during fMRI recording. Transcranial electrical stimulation was applied, concurrently during fMRI acquisition, to either the primary motor cortex or the temporo-parietal junction (TPJ) (with the reference electrode at the contralateral orbit), and three different conditions were applied: anodal and cathodal tDCS, and 40 Hz sinusoidal tACS(Antal et al., 2012). Any detected EPI signal results only from artifacts induced by the currents. This was found to be the largest between the electrodes during tDCS to both M1 and the TPJ, with the maximum intensities found in the cerebralspinal fluid (CSF) and scalp, and a similar spatial profile for both anodal and cathodal montages. Conversely, stimulation with sinusoidal tACS, which had net-zero charge, no EPI signal was detected.

The voltage distribution in a volume during constant current flow in a resistive medium is determined by the Laplace equation. Finite element method (FEM) modelling of the current flow was therefore used to compute current density, which revealed local maxima in both superficial CSF and ventricles during tDCS (Antal et al., 2012), coinciding with

large EPI signals. The distributions were also montage specific, with different profiles for M1 and TPJ stimulation. In addition, the change in EPI signal roughly corresponded to the polarity change in the vertical B_Z magnetic field in the post-mortem brains, caused by the applied currents. Specifically, upwards pointing B_Z fields coincide with increase in EPI signal, and downward pointing fields with decreased EPI signal. Overall, the locations of highest intensity of EPI signal coincide with computational estimates of electric current distribution and the resulting vertical B_Z magnetic field.

MRI signal is sensitive to local variations in static magnetic field generated by current flow in the brain. While static DC currents cause current-flow imaging, confirming that inhomogeneous magnetic fields resulting from current flow can produce distortions in the MRI signal, this effect was absent when applying tACS. This suggests that the opposing polarities induced by sinusoidal AC stimulation causes the EPI signal to reverse with equal strength, resulting in net-zero activity. The fMRI signal artifact from current flow is therefore a lesser concern for concurrent use with tACS as compared to DC stimulation.

6.5 Conclusion

Given the importance of oscillatory activity in sleep, and its effect on sleep-related cognitive functions such as learning and memory consolidation, as well as emotional regulation, several studies have attempted to enhance such effects by inducing artificial oscillatory activity during sleep (Marshall, Helgadóttir, Mölle, & Born, 2006; Marshall, 2004). Indeed, these studies report that by 'boosting' the power of oscillations with transcranial electrical stimulation in the sleeping brain, especially of slow waves, thereby increasing the size of neuronal populations firing in synchrony, leads to increase in long term memory consolidation. However, the mechanism of oscillation entrainment with transcranial electrical stimulation remains unclear in terms of the way it affects neural network communication. The following experiment seeks to map the spatial distribution of cortical activation that is related to transcranial alternating current stimulation at

specific frequencies. This method serves to demonstrate that the cortical activity related to tACS is indeed frequency dependent.

Chapter 7

Experiment 3: V1 tACS induces frequency-dependent BOLD activation in the visual system

Transcranial alternating current stimulation (tACS) offers a way to artificially induce ongoing oscillations in the human brain. However, it remains unclear whether tACS leads to activation of different cortical nodes to facilitate network communication, as is the proposed function of naturally occuring oscillations. The current study uses tACS with functional magnetic resonance imaging (fMRI) to test the hypothesis that different neural networks can be activated by different oscillation frequencies. tACS was applied to the primary visual cortex while fMRI was recorded (n = 20), under an Eyes Open and Eyes Closed condition, which have previously been shown to alter behavioural outcome of tACS in a frequency dependent manner (Kanai, Paulus, & Walsh, 2010). tACS was applied at the theta, beta, alpha and gamma frequencies. Results indicate that different areas of the visual cortex are activated differently depending on the frequecy of the stimulation. In particular, V4 activity was dependent on both the stimulation frequency, as well as the Eyes open vs. closed conditions. Implications for tACS as a means of driving oscillations is discussed.

7.1 Introduction

Recent years have seen an advancement in the methodology and application of transcranial electrical stimulation. The most widely studied technique, transcranial direct current stimulation (tDCS), has been shown to alter neuronal excitability by polarization of the extra-membrane potential, and can alter motor thresholds (Moliadze et al., 2012), visual perception (Kar & Krekelberg, 2012) and even cognition such attention and encoding (Laczó, Antal, Niebergall, Treue, & Paulus, 2013).

On the other hand, transcranial alternating current stimulation (tACS) has been less well understood with regards to its mechanism and ability to alter cognition. tACS provides an important tool for the study of neural oscillations, which occur in a wide range of processes, from visual attention and memory encoding to motor control and language processing, as well as during altered states of consciousness, including naturally occuring light and deep sleep, dream states and meditative states, artificially induced states from hallucinogens, out-of-body or near death experiences, and disease states such as coma, minimally conscious or vegetative states. Therefore, understanding the way in which tACS alters oscillatory activity is crucial for establishing accurate cognitive alteration.

7.2 Phosphenes and their origin

To date, the most reliable evidence of frequency-dependent modulation of brain activity using tACS has been the ability to induce phosphenes at frequency-specific conditions, although other studies have also provided evidence of oscillatory modulation by studying cognitive processes with know oscillatory signatures.

The term "phosphene" is used to describe the visual phenomena experienced during electrical stimulation of the visual cortex, originating from the greek words *phos* (light) and *phainein* (show). In 1755 Chalres Le Roy generated phosphenes by electrically stimulating the occipital cortex of a blind man, in an attempt to restore sight (Antal, Paulus, & Nitsche, 2011). Technological advancements have enabled non-invasive brain

stimulation by placing electrodes on the scalp. For example, stimulation over the visual cortex at high voltages but with short periods of discharge yielded phosphenes (Merton & Morton, 1980), but electrical stimulation was painful and caused the scalp muscles to contract. Transcranial magnetic stimulation (TMS) is advantageous in its ability to induce phosphenes at a stable intensity both across subjects and over time (Meyer, Diehl, Steinmetz, Britton, & Benecke, 1991; Boroojerdi, Prager, Muellbacher, & Cohen, 2000), but is known to affect frequencies outside of the stimulation frequency, thus reducing

tACS has been shown to induce phosphenes in a frequency-dependent manner, when applied to the primary visual cortex (Kanai et al., 2008). Specifically, phosphenes were induced only during stimulation at the alpha frequency (8-12 Hz) when individual's had their eyes closed, or were in a dark environment (Figure 7.1 bottom row). Conversely, when individuals had their eyes open, phosphenes were seen only during stimulation at the beta (14-22Hz) frequency (Figure 7.2 top row). This evidence is in agreement with the finding that alpha frequency oscillations in early visual areas predominate during eyes closed or dark resting conditions (H. Berger, 1929). Alpha activity becomes suppressed during the eyes-opened or light conditions, and higher frequencies (i.e. beta) predominate. The strong correlation between oscillatory function and stimulation frequency in this study strengthens the idea that tACS provides a novel method for interfering with cortical oscillations in a frequency dependent manner.

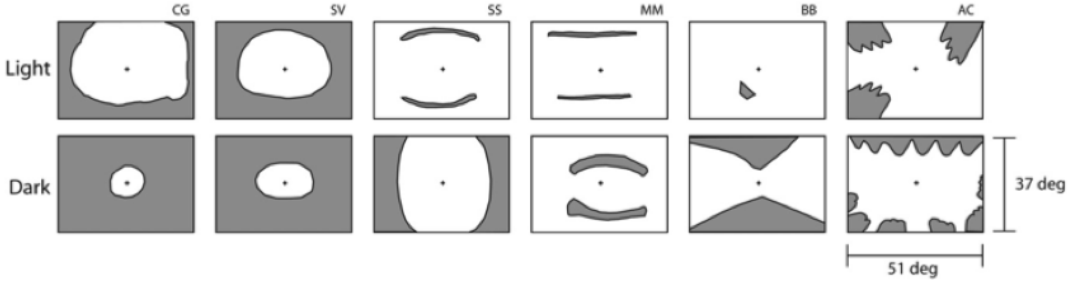

FIGURE 7.1: Drawings representing subjects' perceptions of phosphenes, when the visual cortex is stimulated using tACS at positions Oz and Cz of the 10-20 International System. Grey regions represent phosphenes. During the dark condition (bottom panel) subjects were stimulated with 10Hz (alpha). In the light condition (upper panel) stimulation was performed at 20Hz (beta). Each column represents a single subject (Kanai et al., 2008).

The origin of phosphenes observed during tACS has been a topic of debate. Rather than caused by neuronal excitation from the oscillatory electrical signal of tACS, an alternative proposal suggests that the tACS current passes over the scalp and through cerebrospinal fluid (CSF) to the retina, directly stimulating the retinal ganglion cells, thereby creating retinal phosphenes which are misinterpreted as cortically induced. Strengthening this view is the finding that when electrodes are placed closer to the orbit, phosphenes are perceived as being stronger (Schutter & Hortensius, 2010). Furthermore, when AC stimulation is directly applied to the retina, a peak in retinal excitability is seen at around 20Hz (Motokawa & Ebe, 1952), consistent with the frequency associated with phosphenes previously reported in the 'light' condition (Kanai et al., 2008). The change in frequency required for phosphene induction may be in response to an alteration in retinal sensitivity, resulting from dark adaptation (Schwarz, 1947).

In an attempt to rectify the ambiguity surrounding the source of phosphenes, a subsequent study illustrated that tACS affects the cortex in a frequency dependent manner (Kanai et al., 2010). Whilst measuring cortical excitability with TMS, tACS was applied at different frequencies. TMS acts directly on the visual cortex and yields phosphenes at a particular intensity, known as the phosphene threshold (PT). Changes in PT were only seen during stimulation at situation-appropriate frequencies (i.e. beta stimulation with eyes open). The study demonstrates that tACS is an effective method by which to stimulate the visual cortex in a frequency dependent manner, but unable to resolve whether phosphenes are of cortical or retinal origin. Another study calculated the theoretical amount of current that could reach the retina (Paulus, 2010), with the electrodes in the Oz-Cz montage. Results revealed that only a small amount of current would reach the orbit and was insufficient to induce retinal phosphenes (Motokawa & Ebe, 1952).

7.3 BOLD correlates of oscillations

The current study aims to lend validity to tACS by demonstrating that it can indeed modulate neural activity in a frequency-specific manner, by not only using phosphene

induction as a behavioural index, but more importantly, by demonstrating that stimulation at different frequencies leads to different spatial dynamics of cortical activiation. There exists in the literature a limited number of studies investigating the haemodynamic correlates of endogenous oscillations (in particular sleep; see Chapter 1), as well as BOLD correlates of tDCS (Baudewig, Nitsche, & Paulus, 2001). However, no study so far has examined the spatial profiles of BOLD signal in the brain that are directly related to different frequency stimulation applied with tACS. By measuring BOLD signal with fMRI while simultaneously applying tACS at different frequencies to the visual cortex, we hypothesise that 1) phosphene induction is frequency dependent, and 2) the spatial distribution of cortical regions activated as a result of tACS is also frequency dependent.

7.4 Methods

7.4.1 Subjects

Simultaneous fMRI-tACS was applied to 20 subjects (10 Females and 10 males; age range 20-31 years, mean age 22.3 years old 2.65SD). fMRI was acquired at 1.5T (SIEMENS Avanto) with use of the standard 32 channel head coil and gradients (25 mT m -1). Written informed consent was obtained in all cases before any stimulation and the study was approved by the UCL Ethics Committee.

7.4.2 Experimental design

In order to ensure each subject had a clear subjective perceptual definition of phosphenes, each subject was tested for susceptibility to stimulation-induced phosphenes outside of the scanner; the equipment was not altered in any way. The current intensity was monotonically increased until subjects reported clear phosphenes.

fMRI data was then acquired from each subject across four sessions, each consisting of 8 trials of stimulation. Four different stimulation frequencies were tested, chosen to correspond to the median frequency within the theta, alpha, beta and low gamma

band. Each stimulation frequency was repeated twice within each session. The orders of frequencies were pseudo-randomised across sessions.

The initial resting baseline lasted for 47 seconds, and each subsequent period of stimulation lasted for 30 seconds (the first stimulation starting at approximately 47 seconds of scanning), interleaved with a 20 second rest period between stimulation trials. The subjects were instructed to keep their eyes open for the first and third sessions (Eyes Open condition), and to keep their eyes closed for the second and fourth sessions (Eyes Closed condition). During the Eyes open sessions, subjects were asked to fixate on a black cross, which was located on an opaque screen and could be viewed by the subject through a mirror arrangement atop the headcoil.

For all sessions, subjects were to respond via a button press on the right hand when they saw phosphenes at any time, and to respond via a left hand button press when they felt any physical tingling-sensation during the stimulation. The latter served as a task to engage subjects awareness of their physical sensations and to discourage mind-wandering, but did not form part of the experimental data. There was a period of rest between sessions, during which we allowed the subject to report any sensations or visions they had experienced.

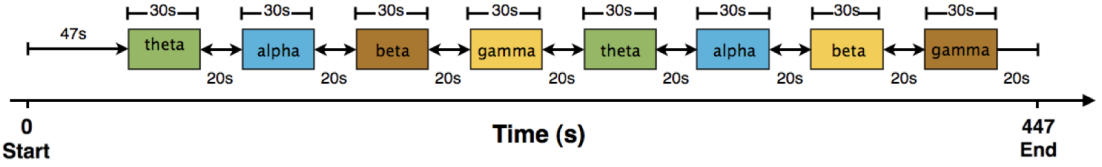

FIGURE 7.2: Example of a session. First stimulation frequency administered after 47s and last for 30s (colored boxes). Stimulation is broken up with 20s rest periods. Each frequency stimulated twice per session theta (green), alpha (blue), beta (brown) and gamma (yellow).

7.4.3 Transcranial alternating current stimulation

tACS was administered using a pair of conductive rubber electrodes connected to a battery driven constant-current stimulator (neuroConn, UK) which was located outside

of the magnet room. The round stimulation electrode was of 1cm radius and the square reference electrode pad measured 9cm by 6cm. The stimulation electrode was placed at Oz and the reference electrode placed over the vertex Cz as governed by the international 10-20 system; using conventional electrode gel and a swim cap (100% silicone) to immobilize the electrode positions. Conductive adhesive electrolytic paste was used to eradicate the need for constant saline administration, as is commonly required in non-fMRI tACS studies. The impedance between the two electrodes was always kept below 10 kOhms. The waveform of the stimulation was sinusoidal, with zero DC offset and starting at zero-degree phase. Stimulation at four frequencies were used: 5 Hz, 10 Hz, 20 Hz and 40 Hz, with the stimulation intensity held constant at 1000A peak to peak. Maximum current densities were 318 uAcm-2 for the stimulation electrode, and 18.5 uAcm-2 for the reference electrode.

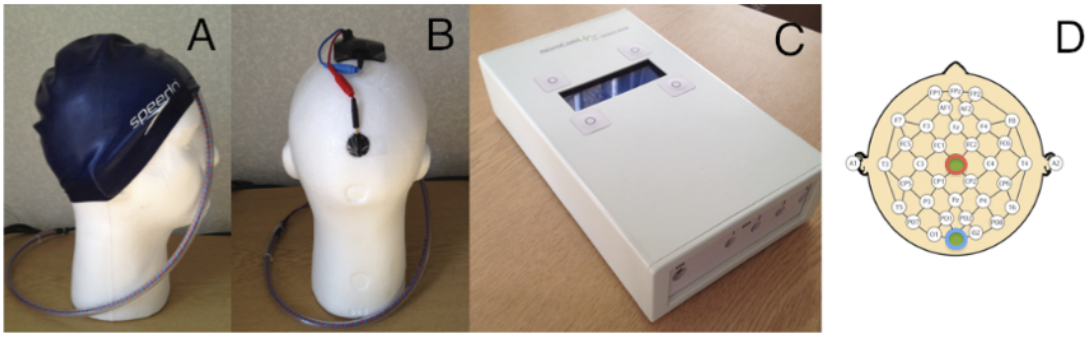

FIGURE 7.3: Experimental setup. A) 100% silicone swim cap was used to keep the electrodes in position during scanning, B) (rear view of head) electrode positioning, stimulation electrode (red) at Oz, reference electrode (blue) placed at Cz, C) NeuroConn constant-current stimulator (methods), D) electrode montage used Oz (red circle) and Cz (blue circle).

7.4.4 MRI room setup

The battery powered stimulation console was kept in the console room at all times, and connected to an input radio-frequency filter containing Lossy-ferrite chokes via two separate electrodes (anode and cathode). This input filter was then connected to another output filter located in the scanner room placed just behind the body-coil of the MR scanner via a long electric cable that passed from the console room, through a waveguide

into the scanner room guided around the periphery and kept at least 1 meter from the scanner itself. The stimulation electrodes connected the subjects scalp to the output filter and were fed between the headcoil and projection mirror, elevated at the bores isocenter level.

7.4.5 fMRI acquisition

A 1.5 T Siemens Avanto MRI scanner was used for acquisition of T2*-weighted echo-planar images sensitive to BOLD contrast (64 x 64; 3 x 3 mm pixels; TR = 2.975 s; TE: 40 ms; flip angle 90 degrees). The brain was covered by volumes that comprised 35 axial slices (3 mm thick, oriented to the AC-PC plane), A total of 160 volumes per session were acquired excluding the first 4 volumes discarded to allow for T1 equilibration effects. Additionally, T1-weighted structural images were acquired (256 x 224; 1 x 1 x 1mm cubic voxels; 160 slices; TR: 12 ms; TE: 5.6 ms; flip angle 19 degrees).

7.4.6 fMRI data analysis

Preprocessing and data analysis were performed using Statistical Parametric Mapping software (SPM8; Wellcome Department of Cognitive Neurology, London, UK) implemented in Matlab 2010b (MathWorks). Images were motion corrected, and realigned to the first image of the first session. For each subject, the mean image of the realigned timeseries was co-registered with the individuals structural image. This produced a unique set of warps for each subject, used for spatial normalization of the functional images to the Montreal Neurological institute template. Images were then smoothed with an 8 mm full-width half-max Gaussian kernel.

For each subject, stimulation related activity was assessed by convolving a vector of stimulation onsets with a canonical haemodynamic response function, the six motion parameters determined from the realignment preprocessing step (three rigid body translations, three rotations) were used as nuisance regressors in the fixed-effects design matrix for modeling movement related artifact in the timeseries. A general linear model (GLM) (Penny et al., 2005) was specified for each subject to investigate the effects of interest.

TABLE 7.1: Table representing number of subjects who saw phosphenes at each frequency across the eyes open and closed condition total subjects ($n = 19$)

Condition	Theta	Alpha	Beta	Gamma
Eyes open	9	13	14	3
Eyes closed	7	10	8	3

The subsequently generated SPM maps from first level T-contrasts were taken through to a second-level random-effects analysis to assess group-level differences. All subsequent activations reported refer to significant clusters of T- contrasts (thresholded at $p < 0.001$ uncorrected, $k < 20$) unless otherwise stated.

7.5 Results

7.5.1 Behavioural report of phosphene induction

Of the twenty subjects tested, one subject's data was contaminated by radio-frequency noise and therefore discarded from subsequent analysis. The table below summarizes the total number of subjects who reported seeing phosphenes in each of the eight stimulation conditions.

For each section, fMRI results from analysis performed on all subjects ($n = 19$), regardless of whether they reported phosphenes, is first described. This is followed by the results from analysis limited to subjects who reported phosphenes for each corresponding stimulation condition.

7.5.2 fMRI during stimulation with Eyes Closed

In the eyes closed condition, activity from all the Eyes Closed non-stimulation periods were used as a baseline. Activation and suppression reported during stimulation is relative to baseline activity.

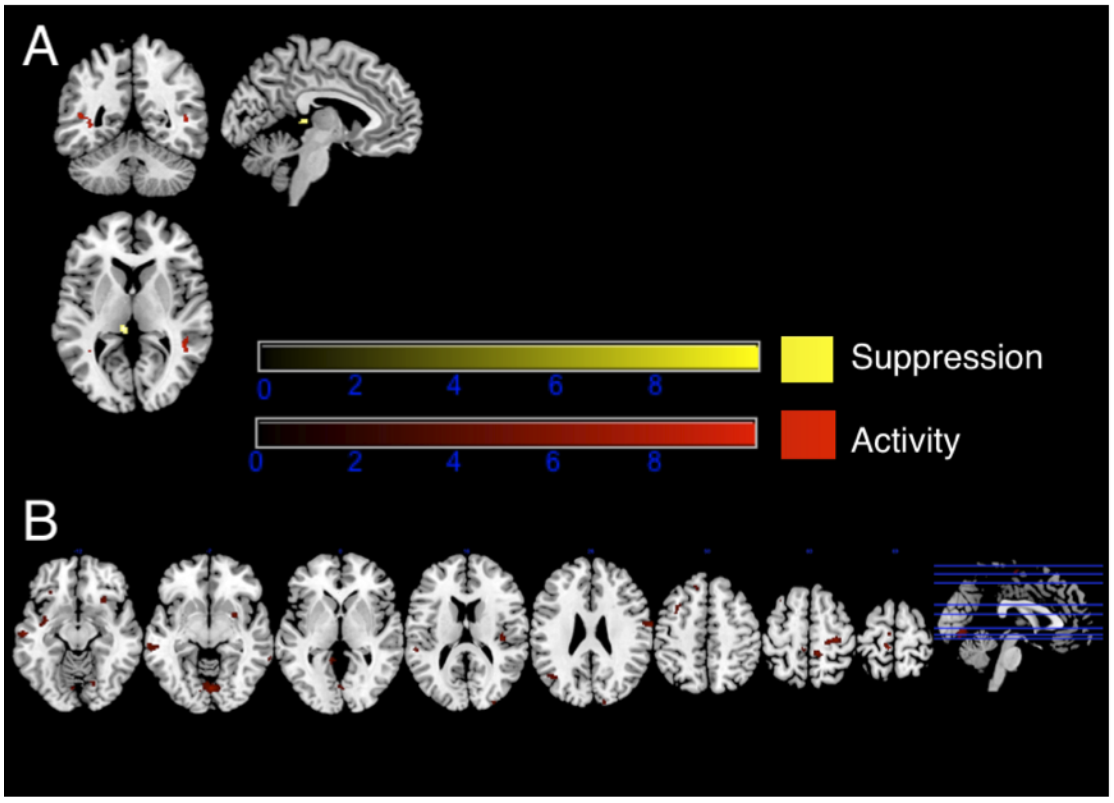

FIGURE 7.4: fMRI group level contrasts; T-maps indicate activity (red) and suppression (yellow) in stimulation conditions relative to baseline (all non-stimulation periods). A) BOLD signal changes related to theta stimulation in the Eyes Closed (EC) condition. B) BOLD changes related to beta stimulation in EC condition. All clusters thresholded at $p < 0.001$ and $k < 20$

7.5.2.1 Theta

Stimulation at theta frequency in the Eyes Closed condition across all subjects ($n = 19$) induced activity in the right middle temporal gyrus ($t(18) = 5.20$) and left supramarginal gyrus ($t(18) = 4.59$) (Figure 7.4A). Additionally, theta stimulation displays some sub-threshold suppressed activity in the left thalamus ($t(18) = 4.32$, $k = 19$). No significant clusters were found when analysis was confined to phosphene-seers only ($n = 7$).

7.5.2.2 Alpha

No significant clusters survived the statistical test, when stimulating at alpha in the eyes closed condition for all subjects ($n = 19$), as well as for those who reported phosphenes ($n = 10$).

7.5.2.3 Beta

In the beta stimulation, Eyes Closed condition, no significant clusters survived statistical test when examining across all subjects ($n = 19$). However, analysis of beta stimulation restricted to only phosphene reporters ($n = 8$) reveals activity in the right ($t(7) = 7.37$) and left ($t(7) = 6.16$) V2, left lateral occipital cortex ($t(7) = 8.24$), left frontal orbital cortex ($t(7) = 6.63$), left superior frontal ($t(7) = 14.58$) and left middle frontal gyri ($t(7)$ = 9.14 and 6.99), left ($t(7)$ = 9.97 and 7.66) and right middle temporal gyri ($t(7)$ = 6.78), right lingual gyrus ($t(7) = 10.59$), right putamen ($t(7) = 9.05$), left ($t(7) = 8.08$) and right insular cortex ($t(7) = 6.56$), left premotor cortex ($t(7) = 6.93$), precentral gyri bilaterally ($t(7)$ = 11.38 and 10.67), right primary ($t(7)$ = 10.06 and 9.64) and secondary somatosensory cortexes ($t(7) = 17.02$) and left planum temporale ($t(7) = 7.63$) (Figure 7.4B).

7.5.2.4 Gamma

In the eyes closed condition during gamma stimulation, no significant clusters survived statistical test ($n = 19$ and $n = 3$).

7.5.3 fMRI during stimulation with Eyes Open

Activity from all the Eyes Open, non-stimulation periods was used as a baseline and subtracted from activity during stimulation periods.

7.5.3.1 Theta

Stimulation with theta across all subjects ($n = 19$) reveals activity in the left callosal body ($t(18) = 5.55$).

Analyzing eyes open theta stimulation in only those subjects who saw phosphenes ($n = 8$) reveals activity in the left thalamus ($t(7) = 11.98$) (Figure 7.5C).

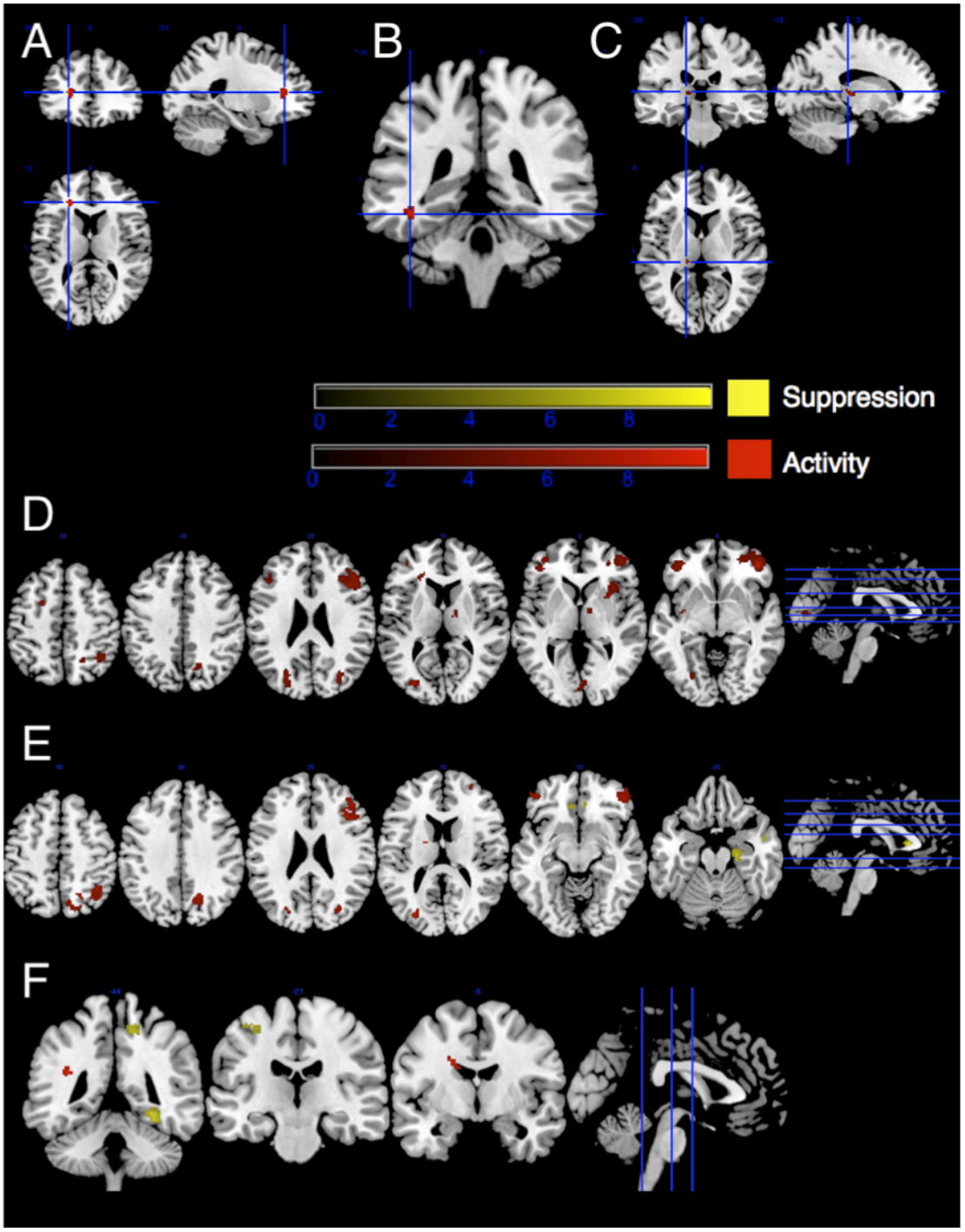

FIGURE 7.5: fMRI group level contrasts; t-maps indicate BOLD activity (red) and suppression (yellow) in stimulation conditions relative to baseline (all non-stimulation periods). All clusters shown are thresholded at $p < 0.001$, uncorrected, $k < 20$. *A*) Activity during theta stimulation in Eyes Open (EO) condition. *B*) Activity with beta stimulation in EO condition. *C*) Activity during theta stimulation in EO condition (phosphene reporters only; $n = 8$). *D, E*) Activity and suppression during alpha stimulation in the EO condition (phosphene reporters only, $n = 12$). *F*) Activity during beta stimulation in EO condition (phosphene reporters only, $n = 13$).

7.5.3.2 Alpha

Alpha stimulation in the Eyes Open condition ($n = 19$) compared to baseline reveals activity in the right V1 calcarine sulcus ($t(18) = 4.38$), left V4 occipito-fusiform gyrus ($t(18) = 4.29$), left ($t(18) = 8.26$) and right ($t(18) = 5.00$) lateral occipital cortex, left inferior occipito-frontal fascicle ($t(18) = 4.48$), right thalamus ($t(18) = 5.20$), right ($t(18) = 5.77$) and left ($t(18) = 4.08$) middle frontal gyri, the right ($t(18) = 6.82$ and 5.77) and left ($t(18) = 5.40$) frontal poles, left superior frontal gyrus ($t(18) = 4.89$), right putamen ($t(18) = 4.76$), right precuneus cortex ($t(18) = 6.19$), right superior parietal lobule ($t(18) = 4.55$) and left callosal body ($t(18) = 4.66$).

When analysis is restricted to only those subjects who reported phosphenes ($n = 13$), activity is seen in the left ($t(12) = 6.09$) and right ($t(12) = 5.38$) lateral occipital cortices, left ($t(12) = 4.95$) and right ($t(12) = 8.16$) frontal poles, left thalamus ($t(12) = 5.07$), right angular gyrus ($t(12) = 4.63$), right precuneus cortex ($t(12) = 6.80$) and the right middle frontal gyrus ($t(12) = 6.05$).

Furthermore, negative BOLD signal representing activity suppression is seen in the left paracingulate gyrus ($t(12) = 4.95$), right hippocampus ($t(12) = 5.84$), right callosal body ($t(12) = 8.00$) and the right middle temporal gyrus ($t(12) = 5.57$).

7.5.3.3 Beta

In the eyes open condition, stimulating with beta across all subjects ($n = 19$) activity was revealed in the left optic radiation ($t(18) = 5.99$). When limiting analysis to phosphene reporters (n = 14) activity is found in the left optic raditation ($t(13) = 6.04$) and left superior occipital frontal fascicle ($t(13) = 4.88$). Suppression is seen in the right precuneus cortex ($t(13) = 7.67$), right temporal occipital fusiform cortex ($t(13) = 6.33$) and left precentral gyrus ($t(13) = 6.04$).

7.5.3.4 Gamma

No significant clusters survived statistical test when stimulating with eyes open at gamma frequency, across all subjects ($n = 19$ and $n = 3$).

7.5.4 Interaction of frequency x eyes OC and Main effect of Eyes Open vs. Closed

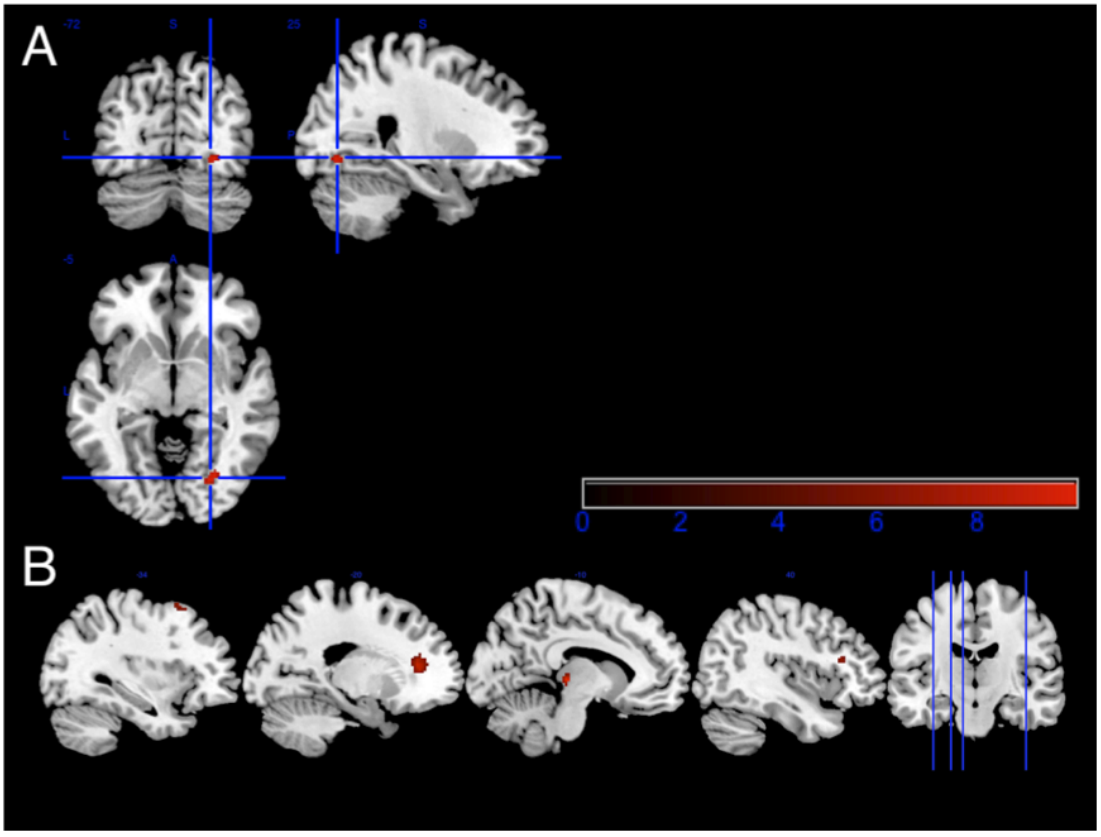

FIGURE 7.6: fMRI group level ANOVA; all clusters significant at$p < 0.001$ uncorrected and $k < 20$ A) F-maps showing interaction of Frequency × Eyes OC condition. B) Main effect of Eyes OC condition.

A 4×2 (theta, alpha, beta, gamma frequencies × Eyes Open, Eyes Closed) within-subject ANOVA was performed ($n = 19$). A significant Frequency × Eyes-OC interaction was found in V4 ($F(3,144) = 7.30$, p<0.001 uncorrected, k =20) (Figure 7.6 A). There was no significant main effect of frequency.

Main effect of Eyes OC is seen in the left thalamus ($F(1,144) = 25.32$), left callosal body ($F(1,144) = 21.40$), the right inferior frontal ($F(1,144) = 16.13$) and left middle frontal gyri ($F(1,144) = 16.05$) all significant at $p < 0.001$ uncorrected, $k < 20$ (Figure 7.6 B).

7.5.5 Eyes Open > Eyes Closed

Brain areas that are more active during the Eyes Open condition, compared to Eyes Closed condition, can be found by subtracting the results of one condition from the other. First, Eyes Open baseline activity is subtracted from Eyes Open stimulation activity ($EO_s - EO_b$), and similarly Eyes Closed baseline activity is subtracted from Eyes Closed stimulation activity ($EC_s - EC_b$). The residuals from each subtraction can then be compared against one another (e.g. $(EO_s - EO_b) - (EC_s - EC_b)$). This calculation is performed for each individual and results across all subjects are compared to determine the areas of shared activation.

7.5.5.1 Theta: Open > Closed activity

No significant clusters survive statistical testing when all subjects ($n = 19$) are examined. More activity is seen in the right insular cortex ($t(6) = 9.95$) during eyes open theta stimulation, compared to the eyes closed condition, when limited to subjects who reported phosphenes ($n = 7$) (Figure 7.8 A).

7.5.5.2 Alpha: Open > Closed activity

During alpha stimulation in the eyes open condition ($n = 19$), increased activity is found in the left superior frontal gyrus ($t(18) = 5.38$), left ($t(18) = 4.66$) and right ($t(18) = 5.28$) middle frontal gyri, the left ($t(18) = 5.02$) and right ($t(18) = 4.54$) frontal poles, right inferior frontal gyrus ($t(18) = 4.89$) and the left putamen ($t(18) = 4.37$), when compared to the eyes closed condition across all subjects ($n = 19$) (Figure 7.8 B).

When analysis is restricted to only those that report phosphenes ($n = 10$) more activity is seen in the right lateral occipital cortex ($t(9) = 4.99$), right ($t(9) = 8.68$) and left middle

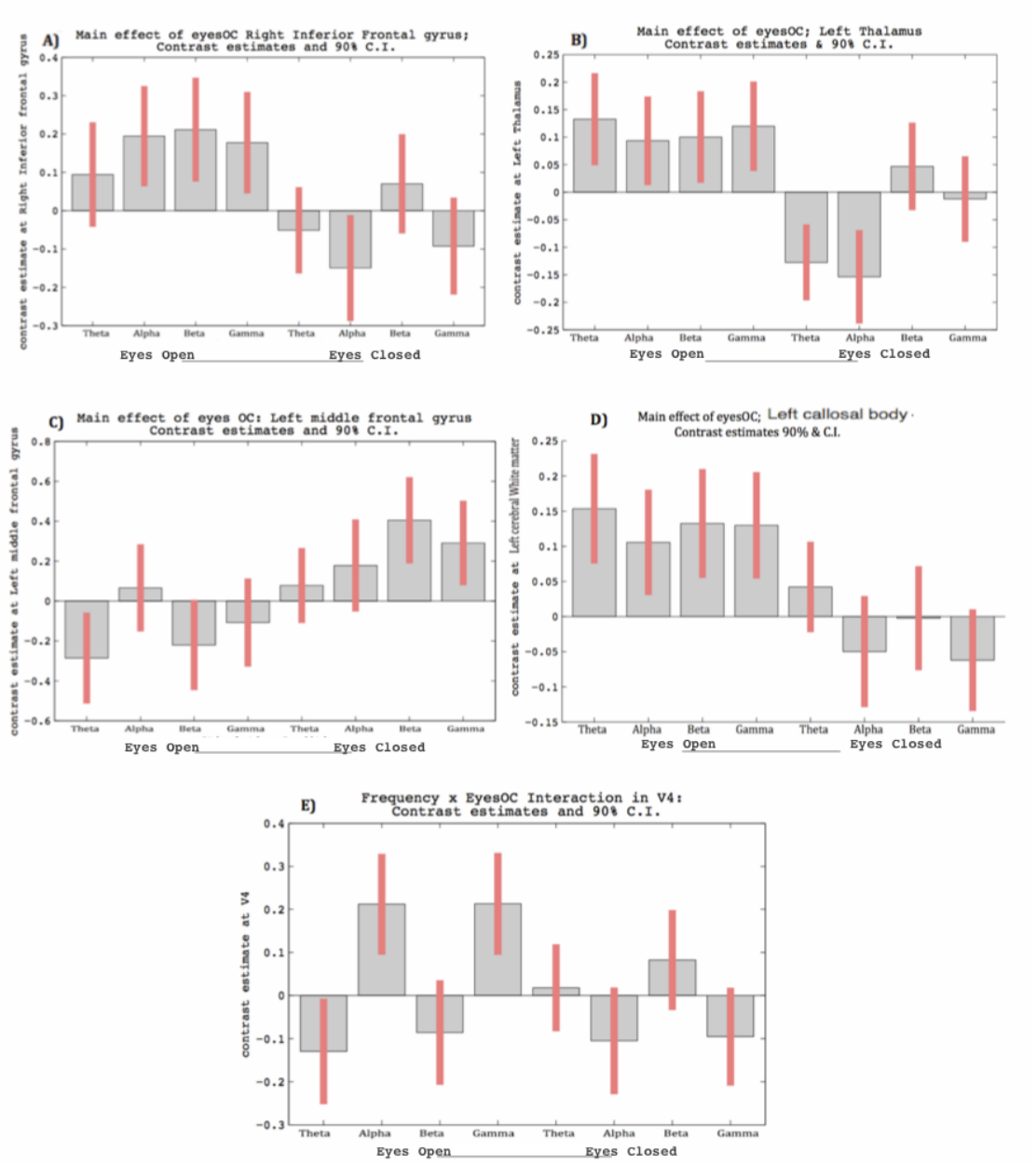

FIGURE 7.7: A to D: Parameter estimates of BOLD signal change in significant clusters from a 2×3 ANOVA analysis. First four columns on the left represent stimulation in the Eyes Open condition. Last four columns on the right represent stimulation in the Eyes Closed condition. The (A) right Inferior frontal gyrus, (B) left thalamus, (C) left middle frontal gyrus and (D) left callosal body show activation depending on whether eyes are open or closed, but independent of stimulation frequency. The change in BOLD signal in V4 (E) demonstrates an interaction between Frequency and Eyes OC condition. During alpha and gamma stimulation, V4 BOLD signal increases when eyes are Opened, but decreases when eyes are closed. In contrast, during theta and beta stimulation, V4 BOLD signal decreases when eyes are opened but increases when eyes are closed. All bars represent 90% confidence intervals.

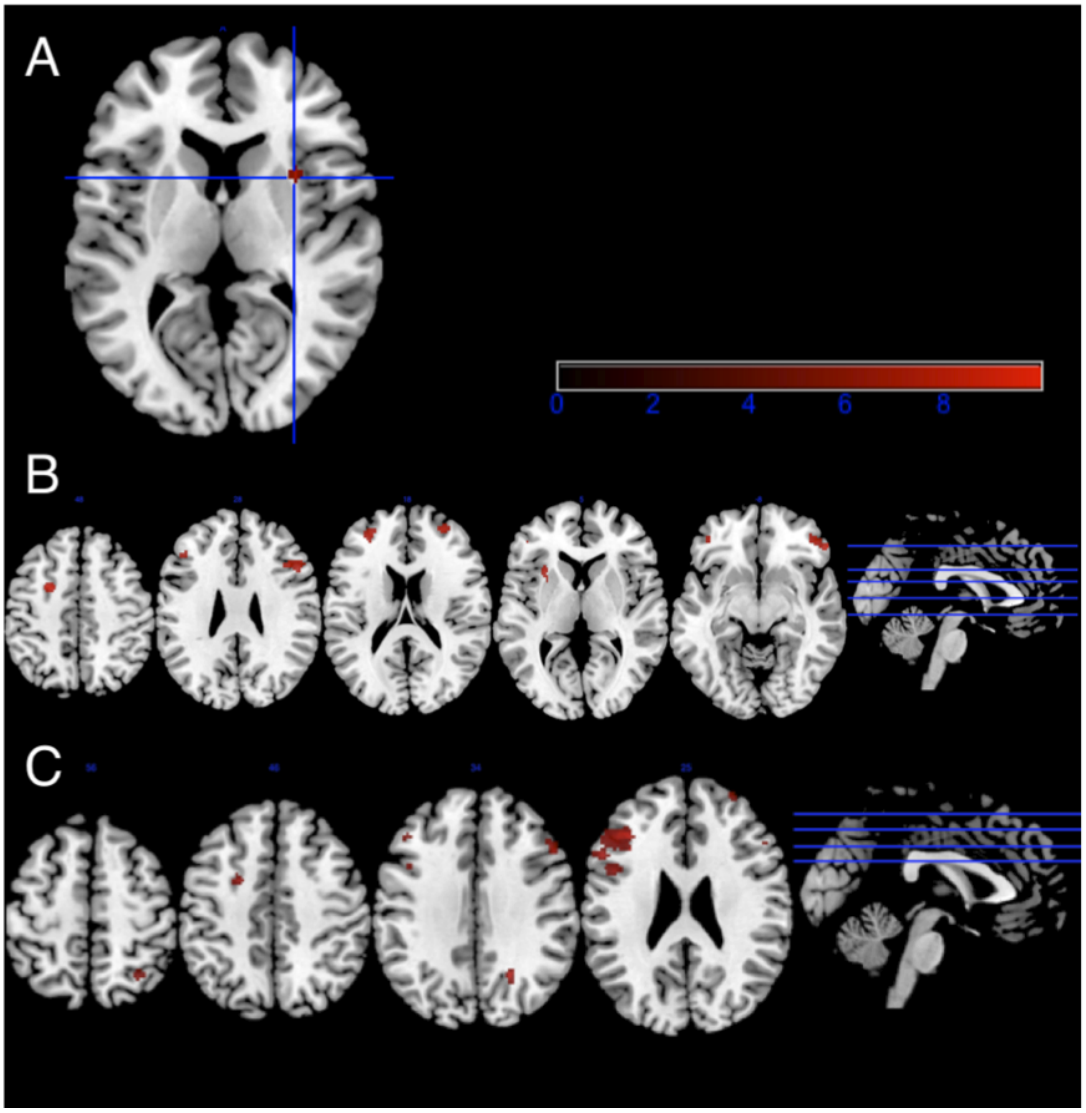

FIGURE 7.8: fMRI group level contrasts; t-maps showing activity greater during Eyes Open compared to Eyes Closed condition. A) Theta stimulation (only phosphene reporters) B) Alpha stimulation C) Alpha stimulation (phosphene reporters only). All clusters thresholded at p<0.001 uncorrected, k =20.

($t(9) = 7.96$) frontal gyri, left superior frontal gyrus ($t(9) = 6.09$), right precuneus cortex ($t(9) = 8.28$) and right frontal pole ($t(9) = 5.35$) in the alpha eyes open condition, than in the eyes closed condition (Figure 7.8 C).

7.5.5.3 Beta and Gamma: Open > Closed activity

No significant clusters survived the statistical test for beta and gamma stimulation when examining all subjects as well as only phosphene-seers.

7.5.6 Eyes Closed > Eyes Opened

To illuminate brain areas that are more active during the Eyes Closed condition compared to the Eyes Open condition, a similar calculation method as above was applied (e.g. $(EC_s - EC_b) - (EO_s - EO_b)$) for each individual subject, then examined on a group level.

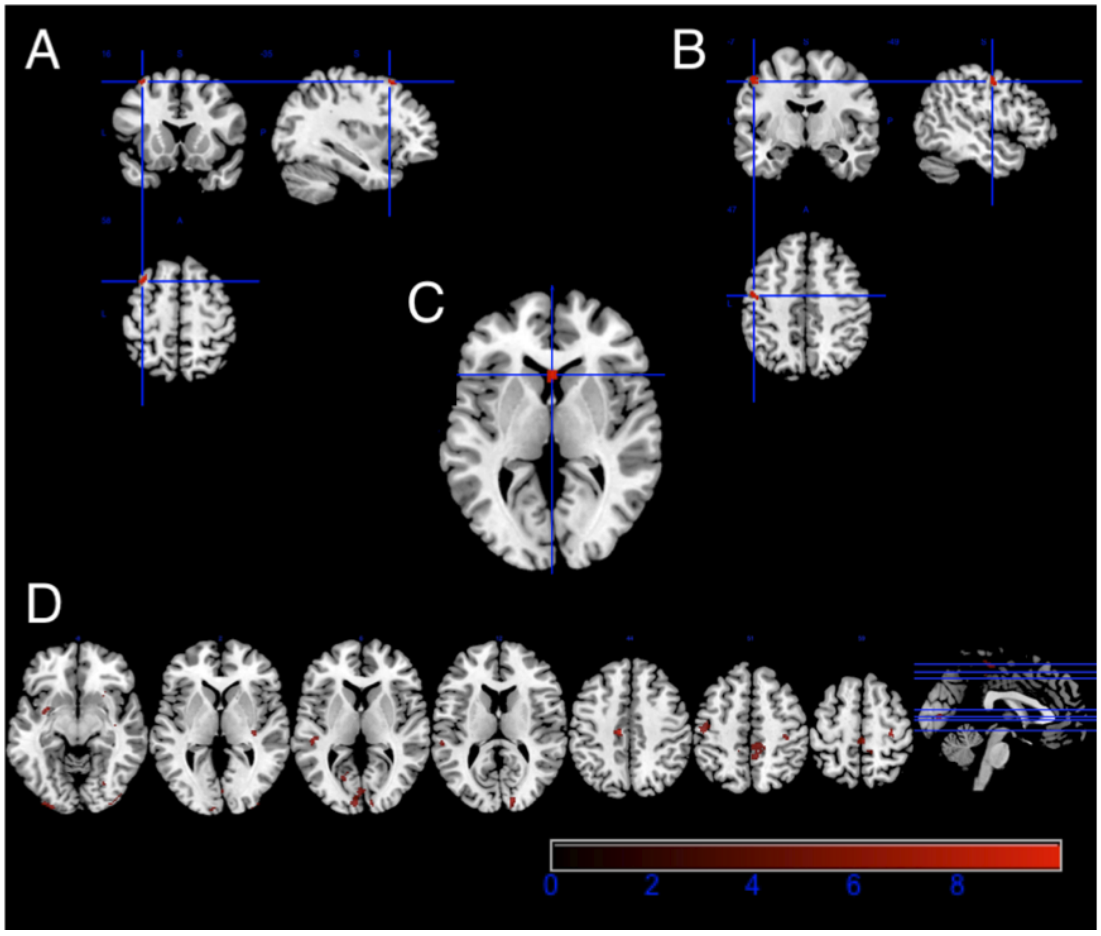

FIGURE 7.9: fMRI group level contrasts; t-maps showing activity greater during Eyes Closed vs. Eyes Open condition. A) Beta stimulation B) Theta stimulation C) Alpha stimulation (phosphene reporters only) D) Beta stimulation (phosphene reporters only). All clusters thresholded at p>0.001 uncorrected, $k = 20$

7.5.6.1 Theta: Closed > Open activity

Greater activation was found in the left premotor cortex ($t(18) = 4.26$) during theta stimulation with Eyes Closed when compared to the Eyes Open condition across all subjects ($n = 19$) (Figure 7.9 B). No significant clusters survived statistical test when examining phosphene-seers only.

7.5.6.2 Alpha: Closed > Open activity

No significant clusters survived statistical test when all subjects were examined. Analyzing only those subjects who reported phosphenes during alpha stimulation ($n = 10$), greater activity was found in the right callosal body ($t(9) = 5.23$) during the Eyes Closed condition. Subthreshold activity ($k = 17$) in the right hippocampus ($t(9) = 7.76$) was also observed. (Figure 7.9 C)

7.5.6.3 Beta: Closed > Open activity

More activity is found in the left middle frontal gyrus ($t(18) = 4.52$) during eyes closed beta stimulation when compared to the eyes open condition across all subjects ($n = 19$) (Figure 7.9 A).

Restricting analysis to those subjects who reported seeing phosphenes ($n = 8$), increased activity in the Eyes Closed condition can be seen in the left ($t(7) = 6.86$ and 6.35) and right primary visual cortex ($t(7) = 8.65$), right V2 ($t(7) = 7.21$), left ($t(7) = 7.47$) and right ($t(7) = 7.14$) V4, right cingulate gyrus ($t(7) = 7.34$), right frontal orbital cortex ($t(7) = 7.13$), left inferior occipito-frontal fascicle ($t(7) = 7.49$), left ($t(7) = 10.15$) and right ($t(7) = 8.03$ and 7.23) precentral gyri, left primary ($t(7) = 9.90$ and 7.95) and left secondary ($t(7) = 7.55$ and 7.47) somatosensory cortices and right insula ($t(7) = 9.91$), when compared to the eyes open condition (Figure 7.9 D).

7.5.6.4 Gamma: Closed > Open activity

No significant clusters survived statistical test, when determining increased activity in the eyes closed condition across all subjects as well as across phosphene seers only ($n = 19$ and $n = 3$), during gamma stimulation.

7.6 Discussion

The aim of this experiment was to monitor changes in whole-brain activity while tACS was applied to the primary visual cortex. BOLD signal was measured in response to stimulation at the theta (5Hz), alpha (10Hz), beta (20Hz) and gamma (40Hz) frequencies, and behavioral reports of phosphene induction were collected. tACS was found to modulate BOLD signal in a frequency-dependent manner, as well as a phosphene-dependent manner.

7.6.1 Frequency by Eyes Open/Close interaction

Mutual activation was discovered within V4 when comparing across all subjects and frequencies. Furthermore, V4 is differentially activated according to frequency and condition.In an alpha-dominant environment (e.g. eyes closed), stimulation in the alpha frequency decreases V4 activity, while beta stimulation increases V4 activity. In contrast, in a beta-dominant environment (e.g. eyes open), beta stimulation decreases V4 activity, while alpha stimulation increases V4 activity. This opposing effect, especially observed in the alpha and beta stimulation frequencies when considering past tACS literature, indicates that V4 activity is frequency-dependent in opposite directions depending on the dominant ongoing EEG frequency.

V4 is an extrastriate area involved heavily in modulating attention (Moran & Desimone, 1985). Activity in V4 may represent the subject's tactile attention to the phosphene site during stimulation, as stimulation with tACS is accompanied with a tickling sensation, subjects' attention may become selectively heightened during stimulation periods. Alternatively this activity might reflect the subject attending to the phosphenes, but this is unlikely as not all subjects reported seeing phosphenes.

Relative to previous findings, where one would expect beta to predominate in the light condition (i.e. eyes open) and alpha in the dark (i.e. eyes closed) (Kanai et al., 2008, Kanai et al., 2010), it is interesting to note that beta and alpha frequencies appear to work in opposition to one another, depending on the condition. This finding might represent different cortical oscillations working against one another, to activate or suppress

a neural area. Neural oscillations may thereby provide an effective means by which to regulate neural activity in a metabolically efficient manner.

7.6.2 Main effect of eyes open vs. closed

Stimulation to V1 with the eyes open reveal that the right inferior frontal gyrus, left thalamus and left callosal body are activated across all frequencies. When the eyes are closed, however these areas show suppressed activity. The similarities seen between these areas during stimulation suggests their connectivity and may share similar functions. The right middle frontal gyrus demonstrates the opposite trend, and may act as a gating mechanism.

7.6.3 Consistencies and differences in the current literature

Stimulating at alpha, in the eyes closed condition is known to yield phosphenes (Kanai et al., 2008), however analysis of alpha stimulation eyes closed across all subjects revealed no significant clusters. Conversely beta stimulation (limited to phosphene reporters) with eyes closed revealed widespread activity, including visual and frontal areas bilaterally. Stimulating at beta with eyes open revealed activity concurrent with the literature, but activation was dominant in the optic radiation with less activity in the visual cortex. These findings may be the result of shunted stimulation (Rush & Driscoll, 1968), or might suggest that tACS interacts with the brain in a more global manner, not limited to the site of stimulation. When restricting analysis across all frequencies to only those who report phosphenes, despite similar behavioral findings, we found different anatomical interactions. This suggests further that tACS affects the cortex differently according to the frequency used (Antal et al., 2008).

The source of phosphenes is the subject of ongoing debate. The thalamus is well established as a relay point within the visual system. In this study thalamic activity is recurrent across different frequencies and conditions. However experimental design prevents us from determining the direction of activity. It may reflect feedback activity from

the thalamus, resulting from cortical phosphene induction; similarly if the phosphenes were of retinal origin we would expect to see feedforward activity in the thalamus.

7.6.4 Eyes closed vs. Eyes open activity

By isolating activity unique to the eyes closed condition relative to the eyes open condition, and limiting subject inclusion to phosphene reporters, widespread activity is seen during beta and alpha stimulation. Of particular interest is activity observed in the middle frontal gyrus during beta stimulation. As previously mentioned, this area shows greater activation in the eyes closed condition regardless of the stimulation frequency. The middle frontal gyrus activity seen during beta stimulation with eyes closed in phosphene reporters may therefore be due to the light condition and not the frequency used. The middle frontal gyrus has a role in executive function, particularly during what, where, when tasks (Talati & Hirsch, 2005). One would expect activity in this area to decrease in the eyes closed condition due to a reduction in visual stimuli; however our results indicate that during stimulation in the eyes closed condition activity in this area increases, presumably due to the presence of phosphenes.

In accordance with our main effect of eyes open vs. closed findings alpha stimulation shows activity in the middle frontal gyrus. As mentioned above this may be reflective of the condition and not the frequency used.

7.6.5 Future studies

In certain contrasts motor and somatosensory activity is apparent. The sensory findings may easily be explained by the slight tickling sensation that accompanies tACS. Additionally, the subjects indicate sensations and phosphenes through a button press, the finger movement required to do so is likely to correspond with increased motor processing activity. For future studies we could model button press and sensation report onsets as a regressor of no interest in an event related design, therefore accounting for confounds induced within the motor and somatosensory areas.

Phosphene thresholds are known to differ amongst individuals (Kanai et al., 2008). However, the amplitude of the current used in this experiment was held constant at 1000μA peak to peak, this current may potentially be below that required by some individuals to perceive phosphene perception, accounting for some of the absent phosphene reports. However the aim of this study was to display neural activity in response to changes in frequency, not current. Future studies might aim to alter stimulation according to an individuals threshold and subsequently compare neural activity in response to changes in current.

7.7 Conclusion

This study reveals BOLD correlates in response to tACS over the visual cortex. The results show different areas of activation in response to different stimulation frequencies, reiterating that tACS affects the brain in a frequency dependent manner. It also emerged that the middle frontal gyrus, the right inferior frontal gyrus, left thalamus and left callosal body react according to the condition and not the frequency used during stimulation, these areas might represent generalized activity or suppression in response to stimulation. The activity found in V4 when comparing across all frequencies and conditions is of particular interest. Activation in this area demonstrates what appears to be activity or suppression depending upon the frequency used. This might suggest that within V4 and potentially other areas, cortical oscillations act in opposing fashions, thereby forming through the endogenous rhythmic activity of the brain a gating mechanism for neuronal activity.

This study lays the anatomical groundwork for understanding the neural correlates to tACS, but further investigation is required to determine the role of these areas in phosphene production and why these areas are selectively activated during frequency specific stimulation.

Chapter 8

General discussion

This thesis examined the role of sleep oscillations in behavior and neurophysiology. The first experiment (Chapter 2) investigated the way in which sleep deprivation (SD) affected subjective emotional experience, as well as how dominant frequency bands during different sleep stages affected the change in subjective emotional experience across sleep. Results showed that SD increases negative mood and reduces positive mood, and that a post-deprivation nap returns the positive mood to pre-deprivation baseline, but *not* for negative mood. Additionally, the magnitude of mood change across a night of sleep was determined by the magnitude of frequency power of sleep oscillations. Increase in positive mood was predicted by *low* theta power in NREM sleep EEG, but increase in negative mood was predicted by *high* theta power in REM sleep, as well as delta power in Stage 2 sleep. Greater theta power in sleep was therefore shown to increase negative mood, and decrease positive mood.

The second experiment (Chapter 5) examined the functional connectivity dynamics of the basal ganglia network during different stages of NREM sleep. Seed-based functional connectivity was conducted by correlating the averaged BOLD signal time-series from the i) bilateral globus pallidus, ii) bilateral caudate nucleus, and iii) bilateral putamen. Results show that compared to network connectivity strength during wake, sleep leads to an increase in functional connectivity between the basal ganglia and nodes within the motor network. Results also indicate that the pallidum acts in opposition to the caudate and putamen in terms of connectivity strength during NREM sleep, where the pallidum

decreases connectivity with the posterior insula and the parahippocampal gyrus during sleep, while the putamen and the caudate increase connectivity with these structures respectively during NREM sleep.

The connectivity pattern also exhibits a distribution pattern in line with the tripartite division model (Parent & Hazrati, 1995), where the insula, anterior parahippocampal gyrus, motor cortex and the inferior parietal lobule are the main nodes that change connectivity strength with different basala ganglia regions during different sleep stages. These correspond with limbic, sensorimotor and associative regions respectively, and such divisions have been shown in previous studies of functional connectivity patterns obtained during wake, with a rostral/caudal and dorsal/ventral division of the striatum (Postuma, 2005). The current findings therefore indicate that while the tripartite division network is maintained during NREM sleep, its network dynamics are in fact strengthened at different stages of NREM sleep.

The third experiment (Chapter 7) investigated the way in which different frequencies of neural oscillations affect the distribution of cortical activity throughout a cortical network. Different stages of sleep are mainly characterized by the dominant frequency of cortical EEG, and Experiment 2 investigated the way in which different frequency bands altered the BOLD signal and functional relationship between cortical areas. Additionally, different studies have shown that applying an electrical signal to the brain can 'boost' ongoing oscillations, thereby leading to enahnced behavoural effects like learning and consolidation associated with sleep oscillations m(Marshall et al., 2006)(Marshall, 2004). Given this, the main purpose in this experiment was to determine whether externally applied electrical signals can influence the ongoing oscillatory EEG in such a way that the BOLD signal reflects this functional modulation. To do so, artificial oscillations were induced by applying tACS at different frequencies to the primary visual cortex, following a paradigm that has been shown to induce frequency-dependent behavioral effects in visual perception (Kanai et al., 2008). Different dominant baseline EEG frequencies were also behaviorally induced by using an Eyes Open (beta dominant) and an Eyes Closed (alpha dominant) condition. The results indicate that the BOLD

signal patterns in different nodes of the visual system changed in a frequency-dependent manner.

Results showed that the extrastriate area V4, involved in attentional modulation, displays BOLD signal changes that are frequency-dependent in either an increasing or decreasing fashion, depending on the dominant ongoing EEG frequency. It was also noted that beta and alpha stimulation altered BOLD activation depending on whether the dominant ongoing EEG power was alpha (eyes closed) or beta (eyes opened) frequency, suggesting an antagonistic relationship between alpha and beta oscillations that may work to activate or suppress a neural area. These results also indirectly show that different oscillatory frequencies, characteristic of different sleep stages, can indeed drive activity in different spatial nodes within a neural network, thereby influencing the communication dynamics between different cortical regions.

Altogether, these experiments reveal directly and indirectly that sleep, a non-quiescent process of neural synchrony, contains different levels of information processing that, beyond the electrophysiological level, can be detected in the dynamics of a neural network's BOLD functional connectivity, as well as the behavioral change experienced by the individual after sleep. Technical and theoretical implications of each experiment, as well as suggested future directions, are discussed below.

8.1 Experiment 1: Sleep and emotion

The relationship between sleep and emotion has been well documented (Walker, 2010; Walker & van der Helm, 2009; van der Helm et al., 2010, 2011; Gujar et al., 2010, 2011; Yoo et al., 2007). While most experiments in the literature have focused on individuals' responses towards stimuli that evoke emotional responses, the behavioural findings from experiment 1 suggest that even in the absence of specific stimulus, individuals' baseline subjective mood is altered by sleep, as well as by lack of sleep. The main finding is that lack of sleep decreases positive mood and increases negative mood significantly, and that sleep increases positive mood, and can even increase particular negative moods depending on the quality of sleep, but does not decrease negative mood signficantly.

In particular, theta power that putatively originates from amygdala activity, leading to reactivation of memories and information associated with fearful and anxious emotions, can predict how much more negative individuals feel, as well as how much less postive indivuals feel upon waking.

These observations are in support of the existing literature, which suggests that sleep regulates affective processing by re-establishing the functional connectivity between the medial and orbital prefrontal cortices and the amygdala, especially through REM sleep. A night of sleep deprivation (SD) will lead to lowered connectivity between these regions in the daytime, while a night of sleep returns the connectivity strength to baseline. The main hypothesis associated with these findings is that emotional regulation occurs after sleep because it leads to optimal functioning of this circuitry. The current findings in experiment 1 suggest that amygdala activity, as characterised by theta EEG power, may also be inhibited by prefrontal activity during sleep in healthy individuals. Therefore the less inhibition the amygdala receives during sleep, the higher the recorded EEG theta power, the higher the increase in negative mood, and the lower the increase in positive mood. The "re-established" connectivity between the amygdala and mPFC regions documented in previous studies may reflect the synaptic plasticity induced by coactivation between the same regions during sleep,

Prominent theories of emotion that include the central as well as the peripheral nervous system as mechanisms of emotional processing have not been taken into account in the literature of sleep and emotion. The following section offers an integration of the crucial component of the autonomic system into the effects of sleep on emotional regulation.

8.1.1 The autonomic nervous system and emotional experience

According to leading theories of emotion, the autonomic nervous system is central to the perception of emotion, whereby subjective feeling states result from representations of bodily responses elicited by emotional events (Damasio, 2003; Damasio et al., 2000). For example, the James-Lange theory argues that changes in bodily responses and the perception of them are necessary for emotional experience (James, 1894). According to this theory, different emotive events generate autonomic responses of different patterns,

even without awareness, and the intensity of the emotion experienced by the individual is determined by the sensitivity to these specific internal bodily changes. Indeed, even within the sympathetic axis, commonly adhered to as a unitary phenomenon in previous literature, exists discrete patterns where such responses accompanying defensive behavior, sensory, metabolic and thermal changes can be differentially induced and distinguished (Saper, 2002). To bridge the physiological phenomena with social and emotional behavior, other theories have proposed that peripheral arousal can only engender emotionality and determine its intensity when these signals are combined with cognitive context (Schacter & Singer, 1962; Damasio, 2003; Craig, 2009; Critchley, 2009).

The autonomic nervous system regulates internal bodily functions by providing neural input into every major bodily system, via the sympathetic and parasympathetic axes (Brading, 1999). The sympathetic nervous system is constantly active to maintain homeostasis, and mobilizes the body's neuronal and hormonal "fight or flight" stress response, or the "sympatho-adrenal response". This response acts primarily on the cardiovascular system to mediate pupil dilation, increased gut motility, and increased cardiac output. The brainstem nuclei drives peripheral sympathetic output, and terminal synapses are typically noradrenergic, responding to tonic levels of noradrenaline (NAd) and adrenaline (Ad). Parasympathetic activity, on the other hand, promotes recuperative functions that reduces heart rate, lowers blood pressure, and slows gut motility. As such, it is also referred to as the "feed and breed" or "rest and digest" system, facilitating activities such as sexual arousal, urination, digestion, defecation and salivation. Most peripheral bodily organs receive parasympathetic innervation via the vagus nerve, and are mediated by the neurotransmitter acetylcholine (ACh). Autonomic arousal responses have developed into potent social cues that reflect an individuals motivational state (Ekman, Levenson, & Friesen, 1983), and simultaneously act as indicators of emotional processing.

The intimate relationship between self-awareness of autonomic - and particularly sympathetic - response and the subjective experience of emotional intensity has been well established. This ability, referred to as interoception, links internal visceral processes to emotional feelings. A classic demonstration reveals that interoceptive awareness of one's

own heartbeats is positively correlated with day to day experiences of anxiety, and is reflected in greater BOLD response and gray matter volume of the right anterior insula (Critchley, Wiens, Rotshtein, Öhman, & Dolan, 2004). Critically this interoception-related area is also engaged when individuals are consciously monitoring (and reporting) the intensity of emotions they feel, moment to moment (Zaki, Davis, & Ochsner, 2012). Individuals skilled at recognizing emotional facial expressions also possess greater interoceptive awareness, and specifically employ greater insula and amygdala activity, while suppressing mPFC activity (Thom et al., 2012).

In humans, cardiac response is controlled via brainstem reflexes, which modulates the autonomic outflow of heart rate. Afferent signaling of the circulation state feedbacks into the solitary tract nucleus of the thalamus, which projects back to the brainstem to adjust cardiac output. Depolarization of the heart's sinoatrial (SA) node is controlled by neurotransmitters released at post-ganglionic terminals. Parasympathetic / vagal modulation depends on ACh release, which slows SA node discharge, while sympathetic modulation depends on NAd release to speed SA node discharge. Whereas vagal activity changes cardiac response rapidly with negligible time delay, sympathetic activity changes cardiac response slowly, with a 1-2 second pure time delay. The difference in time taken for heart rate to change depending on vagal vs. sympathetic modulation is captured by the heart rate variability (HRV). High frequencies (HF) of HRV ranging from 0.15 to 0.4 Hz, where heart rate changes quickly, reflects vagal-cardiac nerve traffic fluctuation. Low frequency (LF) HRV ranges from 0.05 to 0.15 Hz, and denotes sympathetic outflow to which cardiac response is slow. Other very low frequencies (VLF) and ultra low frequencies (ULF) of HRV are usually modulated by thermo-regulatory cycles and circadian rhythms respectively.

8.1.2 Autonomic nervous system and sleep

The relationship between autonomic activation systems and sleep has been well documented. Spectral analysis of HRV in overnight polysomnographic recording broadly describes a pattern of parasympathetic activity in NREM sleep, and a sympathovagal shift to sympathetic dominance occurring at the onset of and during REM sleep (Busek,

Vanková, Opavský, Salinger, & Nevsímalová, 2005). For example, the VLF component of HRV decreases during Stage 2 and SWS, but increases in REM sleep, indicating that thermo-regulatory processes are more active during REM sleep. The LF component of HRV in the supine position is mediated by both the sympathetic and parasympathetic activity, and is also highest in REM sleep, decreasing to a minimal value in SWS. On the other hand, HF components originating from respiration-related vagal activity are lowest in REM sleep, but elevated in NREM sleep. The LF/HF ratio, a measure of sympathovagal balance, also changes in different sleep stages, with the lowest value in SWS and conversely higher values in pre-REM Stage 2 sleep, and the highest value in REM sleep.

In the waking state, low-level information of physical sensations generated by the autonomic nervous system is combined with successively higher-level mental processes, which arise from the individual's environmental, motivational, cognitive and social conditions (Critchley, 2009). This cumulative re-mapping process integrates bottom-up homeostatic signals with higher-order feedback signals, resulting in a global emotional percept. This globally-mapped affective state then guides the response most optimal for the organism, such as verbal and facial expressions.

Taken together, these findings suggest that sympathetic activity is increased and parasympathetic activity reduced in REM-onset and during REM sleep, and *vice versa* for NREM sleep - an effect more prominent in males than females (Elsenbruch, Harnish, & Orr, 1999). The occurrence of elevated LF/HF ratio in pre-REM Stage 2 sleep gradually disappears in the course of subsequent cycles across the night, suggesting that 1) autonomic changes precede neural sleep stage changes, and that 2) the the sympathovagal balance shifts to a prevailing vagal influence across the night, related to the organism's regeneration during sleep. Indeed, a lack of vagal activation to counteract sympathetic dominance can lead to disrupted sleep quality. In patients with primary insomnia, increases of LF HRV are observed across the night, whilst acute stress blunts nocturnal parasympathetic modulation and interferes with sleep depth (Hall et al., 2004; Bonnet & Arand, 1997). Likewise, in individuals with alcohol dependence, reduction of HF HRV during the waking period predicted decrease in amount of SWS, EEG delta power and

subjective report of sleep quality, leading to increased morning measures of sleepiness and fatigue (Irwin, 2006).

8.2 Experiment 2: Functional connectivity of the basal ganglia network during NREM sleep

The basal ganglia's role in sleep has only recently received attention in the literature, and less is understood about the mechanisms through which it regulates and influences sleep-wake behaviour in humans. The basal ganglia are functionally connected to optimize beaviour and to regulate vigilance during the waking state. It is connected to the amygdala, thalamus and the cerebral cortex, and is strongly connected to midbrain dopaminergic neurons. The current study revealed the spatial profile of striatal and pallidal functional connectivity during sleep, based on the proposed model in which a dorsostriatal-pallido-cortical loop regualtes sleep-wake behaviour and cortical activation (Lazarus, Huang, Lu, Urade, & Chen, 2012). The putamen and caudate are hypothesized to project to the external globus pallidus, which in turn projects to the cerebral cortex directly or through the mediodorsal thalamic nucleus.

Evidence suggest that the striatum and the globus pallidus play different roles in the regulation of sleep-wake behavior. While the medium spiny neurons (MSNs) of the striatum show irregular firing patterns during wakefulness, during slow wave sleep they display firing patterns associated with the hyperpolarazed 'off' and depolarized 'on' states resulting from rhythmic fluctuation of the membrane potential (Lazarus et al., 2012). Neurotoxic lesions to the basal ganglia also show that bilateral lesions in the striatum reduce total wake time, and a disturbance in both sleep and wakefulness. Neurons of the globus pallidus, in contrast, show firing patterns that are most active in wakefulness and REM sleep, and less active in slow wave sleep. Lesioning to the globus pallidus leads to an increase in total wake time, and fragmentation of NREM sleep, in contrast to the effects on the striatum.

Sleep-wake behavior is predicted by a striato-pallido-cortical loop, in which the caudate and putamen project to the globus pallidus, which then activates the cerebral cortex

directly or via the mediodorsal thalamic nucleus of the thalamus. This model suggests that GABAergic neurons in the globus pallidus modulate activity of layer V pyramidal neurons and interneurons in the cerebral cortex, thereby suppressing cortical activity and promoting sleep. Disinhibition by lesioning the neurons in the globus pallidus, or by dopamine input, as in Parkinson's disease patients, therefore leads to disrupted sleep promotion through cortical activation (Lazarus et al., 2012).

8.2.1 Technical considerations

The current results support the main hypothesis that the caudate/putamen are antagonistic to the globus pallidus in the regulation of sleep-wake behavior. This was demonstrated in the increases and decreases in functional connectivity strength between the each basal ganglia subregion node to the rest of the brain, depending on the depth of sleep, and relative to the waking state.

Resting state functional connectivity determined with bivariate correlation between a seed region and the rest of the brain commonly uncovers the functional anatomy of a network. Changes in magnitude of coactivation between brain regions remain difficult to interpret. The observed changes in correlation strength(s) between two or more regions during waking task performance may be caused by a linear superpositioning of the spontaneous and task-evoked activity (Arfanakis et al., 2000; Fox & Raichle, 2007). However, the current results reflect changes in correlation structure due to fluctuations in BOLD signal associated with modulation of coherence in electrophysiological signal. The measured differences in functional connectivity capture changes in spontaneous activity, rather than task-specific activity.

Coactivation strength changes may also indicate synaptic facilitation and depression that truly re-organizes the correlation structure of spontaneous BOLD activity (Fox & Raichle, 2007). This may suggest synaptic pruning of basal ganglia network, consistent with the role of NREM sleep in synaptic homeostasis (Tononi, 2009), especially in motor learning (Gais et al., 2008; Walker, Liston, et al., 2002; Walker, 2005) and emotional memory consolidation (Hu, Stylos-Allan, & Walker, 2006; Sterpenich et al., 2007).

8.3 Experiment 3: Frequency-dependent modulation of the BOLD signal using tACS

The way in which different EEG frequencies affect the global cortical activity pattern can be understood by using simultaneous imaging techniques such as EEG-fMRI, and show that different global EEG frequencies are associated with activity in different brain regions. Concurrent tACS-fMRI can similarly be used to understand whether brain oscillations play a fundamental role in cognitive processing, rather than being an epiphenomenon of cortical information processing (Herrmann, Neuling, Rach, & Strüber, 2012). For example, by selectively interfering an oscillatory activity associated with a cognitive function, this function should theoretically also be altered, and an altered BOLD activation pattern should be observed relative to when no stimulation is delivered.

The global cortical effects of tACS can therefore be measured with concurrent tACS-fMRI to indirectly assess the validity of activation pattern changes related to EEG frequency changes, such as those observed in sleep-fMRI studies. Previous studies have shown that tDCS can alter the BOLD signal during and after stimulation (Saiote, Turi, Paulus, & Antal, 2013). However, no study using concurrent tACS-fMRI has been published, and it remains uncertain whether tACS can efficiently modulate the EEG to induce changes in cortical activation observable in the BOLD signal.

In Experiment 3, tACS was delivered at four different frequencies to V1, while the resting EEG was manipulated by instructing the participants to have their eyes open or closed. The results show that the visual area V4 was differentially activated by each frequency, and that the direction of BOLD signal change (increase or decrease) depended on the resting EEG frequency as well. In humans, V4 receives direct input from V1, as well as feedforward input from V2, and sends signals to the inferior temporal gyrus as part of the ventral stream of visual processing. Its function has been largely studied in the macaque monkey, but human studies have shown its involvement in selective attention and visual object recognition (Hayden & Gallant, 2013; Ipata, Gee, & Goldberg, 2012). Stimulation of the primary visual cortex at different frequencies selectively alter the activity of V4, suggesting that the resting EEG of the brain can affect cognitive functions such as

selective attention, and more broadly its ability to selectively extract visual features from global percepts, regardless of whether the modulated domains are driven by bottom-up or top-down processes (Roe et al., 2012).

8.3.1 Technical considerations

The after-effects of tACS are known to be affected by stimulation parameters, such as electrode size, stimulation intensity and duration, current density, the type of alternating current (e.g. sinusoidal, sawtooth), the timing of the stimulation (e.g. in relation to the ongoing oscillatory phase, or before, during or after a behavioral task performance), as well as electrode placement (Faria, Hallett, & Miranda, 2011; Antal et al., 2008; Zaehle, Rach, & Herrmann, 2010; Pirulli, Fertonani, & Miniussi, 2013; Bikson, Rahman, & Datta, 2012). However, less has been studied about the effects of stimulation parameters on cortical activation *during* stimulation. In addition, the activation state of neuronal populations are state-dependent, and the neural impact of tACS may be influenced by the initial activation state of the brain regions, depending on whether the subject is at rest or engaged in a task (Silvanto, Muggleton, & Walsh, 2008). For example, studies using TMS have revealed that sleep, learning, expectancy and alcohol have different effects on the motor system (Kähkönen et al., 2001; Nikulin, Kičić, Kähkönen, & Ilmoniemi, 2003; Lee, Siebner, Rowe, & Rizzo, 2003), and that resting EEG activity influences the perceptual and cognitive impact of both TMS and tACS (Romei, Gross, & Thut, 2010; Kanai et al., 2010), and but less is understood about the state-dependent effects of tACS on cortical activation, especially as detected by the BOLD signal. Outstanding questions such as:

1. How does stimulation at different frequency affect the functional connectivity between cortical structures?
2. How do individual differences in resting EEG or brain structure interact with different stimulation parameters to affect stimulation efficacy?
3. Can tACS affect neuronal activity even if a behavioral effect is not observed?

can be better addressed in future studies by increasing the spatial accuracy of the stimulation target (Edwards, Cortes, Datta, & Minhas, 2013), targeting structures with well defined functional networks within the experimental context (e.g. the PCC of the DMN during resting state), and combining imaging methods (fMRI or EEG) with stimulation at the same time for more direct physiological investigation.

Appendix A

Subject sleep statistics

Sleep Statistics Definitions and Explanations

SPT Sleep period time (elapsed time from sleep onset through last epoch of sleep).

TDT Total dark time (elapsed time from lights out to lights on).

TST Total sleep time (duration of time spent in Stages 1, 2, 3, 4 and REM during SPT).

NREM Duration of time in Stages 1, 2, 3, 4.

SW Slow wave sleep (Stages 3, 4).

All sleep tabulated from within SPT

Sleep Onset The time from the epoch of lights out until the first epoch of 3 contiguous epochs of sleep.

Wake After Sleep Onset Wake time after sleep onset during SPT.

Wake After Final Awakening Elapsed time spent awake between the final epoch of sleep and lights on.

Sleep Before Sleep Onset Any transient sleep occurring between lights off and sleep onset.

All Stage Latencies Elapsed time to first epoch of specified stage (from either lights off or sleep onset, as specified).

NREM-REM Cycle definitions per the modified criterion of Feinberg and Floyd (1979) as in Aeschbach and Borbély (1993)

NREM-REM Cycle Succession of NREM period of at least 15 minutes duration by a REM period of at least 5 minutes duration. No minimum duration for the first or last REM period.

NREM Period Time interval between first occurance of Stage 2 and the first epoch of the next REM period.

REM Period Time interval between two consecutive NREM periods or that between the last NREM period and final awakening.

NREM/REM Segments Number of uninterrupted periods of NREM/REM during a NREM/REM period.

All other sleep statistics per Carskadon, MA, Rechtschaffen, A. Monitoring and Staging Human Sleep. In: Principles and Practices of Sleep Medicine 4th Edition, pgs. 1359-1377. Ed: Kryger, MH, Roth, T, Dement, WC. Philadelphia, PA : Elsevier Saunders, 2005.

*** Subject 01: Sleep Stats ***

Notes:
Scoring window: 30 secs

Lights OUT: 04:23:01.420
Lights ON: 05:50:17.336

Sleep onset epoch: 3 (relative to record start: 3)
Final awakening epoch: 172 (relative to record start: 172)
First scored epoch relative to record start: 1

Last stage of sleep: MT
Awake at lights on? Yes

Sleep Percentages

	Epochs	Minutes	%TDT	%SPT	%TST
Total dark time:	174	87.0			
Sleep period time:	170	85.0	97.70		
Total sleep time:	134	67.0	77.01	78.82	
Sleep before sleep onset:	1	0.5	0.57		
Wake after sleep onset:	23	11.5	13.22	13.53	17.16
Wake after final awakening:	1	0.5	0.57	0.59	0.75
Total wake time	26	13.0	14.94	15.29	19.40
Stage 1	63	31.5	36.21	37.06	47.01
Stage 2	71	35.5	40.80	41.76	52.99
Stage 3	0	0.0	0.00	0.00	0.00
Stage 4	0	0.0	0.00	0.00	0.00
REM	0	0.0	0.00	0.00	0.00
MT	13	6.5	7.47	7.65	9.70
NREM	134	67.0	77.01	78.82	100.00
SW	0	0.0	0.00	0.00	0.00

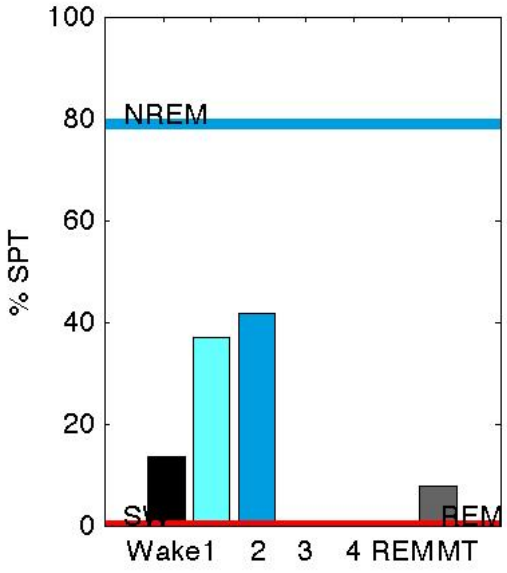

Sleep Latencies

	Epochs	Minutes
lights out to sleep onset	2	1.0
lights out to Stage 1	2	1.0
lights out to Stage 2	4	2.0
lights out to Stage 3	NaN	NaN
lights out to Stage 4	NaN	NaN
lights out to REM	NaN	NaN
Sleep onset to Stage 1	0	0.0
Sleep onset to Stage 2	2	1.0
Sleep onset to Stage 3	NaN	NaN
Sleep onset to Stage 4	NaN	NaN
Sleep onset to REM	NaN	NaN

NREM Period Stats (min)

	1
Wake:	11.50
Stage 1:	30.50
Stage 2:	35.50
Stage 3:	-
Stage 4:	-
REM:	-
MT:	6.50
SW:	-
Total Time:	84.00
Segments:	1

NREM-REM Cycle Stats (min)

.

REM Period Stats (min)

Segments:

Last REM to final awakening: NaN
Last REM to lights on: NaN

Full Hypnogram:

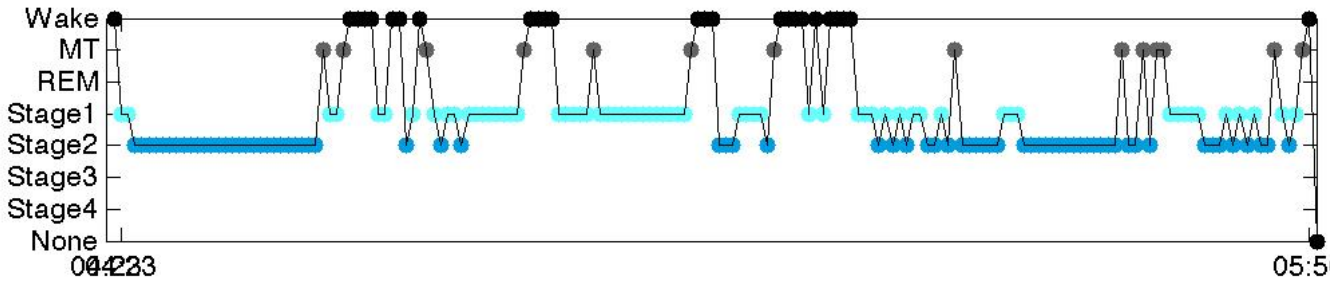

Full Transition Table:

From\To	**Wake**	**Stage 1**	**Stage 2**	**Stage 3**	**Stage 4**	**REM**	**MT**
Wake:	**16**	6	2	0	0	0	1
Stage 1:	4	**39**	15	0	0	0	5
Stage 2:	0	13	**51**	0	0	0	7
Stage 3:	0	0	0	**0**	0	0	0
Stage 4:	0	0	0	0	**0**	0	0
REM:	0	0	0	0	0	**0**	0
MT:	5	5	3	0	0	0	**1**

SW Collapsed Hypnogram:

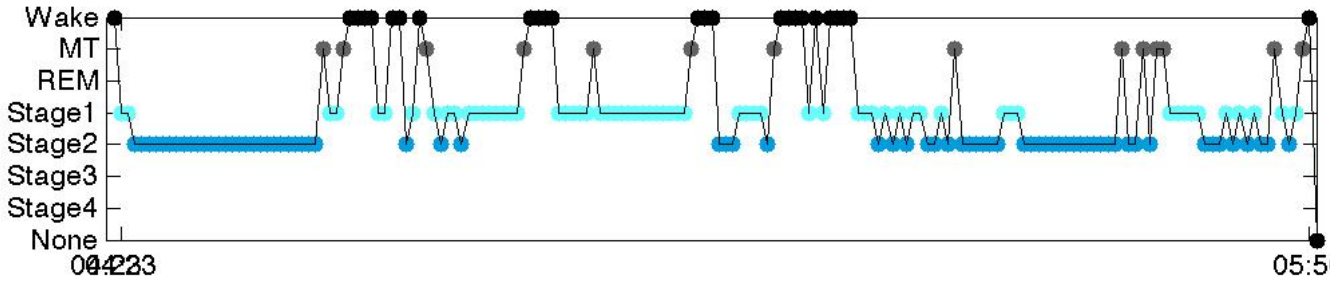

SW Collapsed Transition Table:

From\To	**Wake**	**Stage 1**	**Stage 2**	**SW**	**REM**	**MT**
Wake:	**16**	6	2	0	0	1
Stage 1:	4	**39**	15	0	0	5
Stage 2:	0	13	**51**	0	0	7
SW:	0	0	0	**0**	0	0
REM:	0	0	0	0	**0**	0

*** Subject 02: Sleep Stats ***

Notes:
Scoring window: 30 secs

Lights OUT: 03:33:11.380
Lights ON: 05:04:34.132

Sleep onset epoch: 2 (relative to record start: 2)
Final awakening epoch: 181 (relative to record start: 181)
First scored epoch relative to record start: 1

Last stage of sleep: MT
Awake at lights on? No

Sleep Percentages

	Epochs	Minutes	%TDT	%SPT	%TST
Total dark time:	182	91.0			
Sleep period time:	180	90.0	98.90		
Total sleep time:	125	62.5	68.68	69.44	
Sleep before sleep onset:	1	0.5	0.55		
Wake after sleep onset:	32	16.0	17.58	17.78	25.60
Wake after final awakening:	0	0.0	0.00	0.00	0.00
Total wake time	33	16.5	18.13	18.33	26.40
Stage 1	53	26.5	29.12	29.44	42.40
Stage 2	51	25.5	28.02	28.33	40.80
Stage 3	16	8.0	8.79	8.89	12.80
Stage 4	5	2.5	2.75	2.78	4.00
REM	0	0.0	0.00	0.00	0.00
MT	23	11.5	12.64	12.78	18.40
NREM	125	62.5	68.68	69.44	100.00
SW	21	10.5	11.54	11.67	16.80

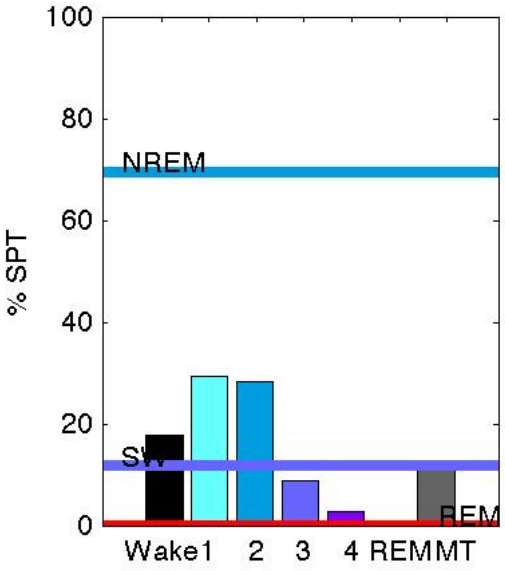

Sleep Latencies

	Epochs	Minutes
lights out to sleep onset	1	0.5
lights out to Stage 1	1	0.5
lights out to Stage 2	4	2.0
lights out to Stage 3	42	21.0
lights out to Stage 4	48	24.0
lights out to REM	NaN	NaN
Sleep onset to Stage 1	0	0.0
Sleep onset to Stage 2	3	1.5
Sleep onset to Stage 3	41	20.5
Sleep onset to Stage 4	47	23.5
Sleep onset to REM	NaN	NaN

NREM Period Stats (min)

	1
Wake:	16.00
Stage 1:	25.00
Stage 2:	25.50
Stage 3:	8.00
Stage 4:	2.50
REM:	-
MT:	11.50
SW:	10.50
Total Time:	88.50
Segments:	1

NREM-REM Cycle Stats (min)

.

REM Period Stats (min)

Segments:

Last REM to final awakening: NaN
Last REM to lights on: NaN

Full Hypnogram:

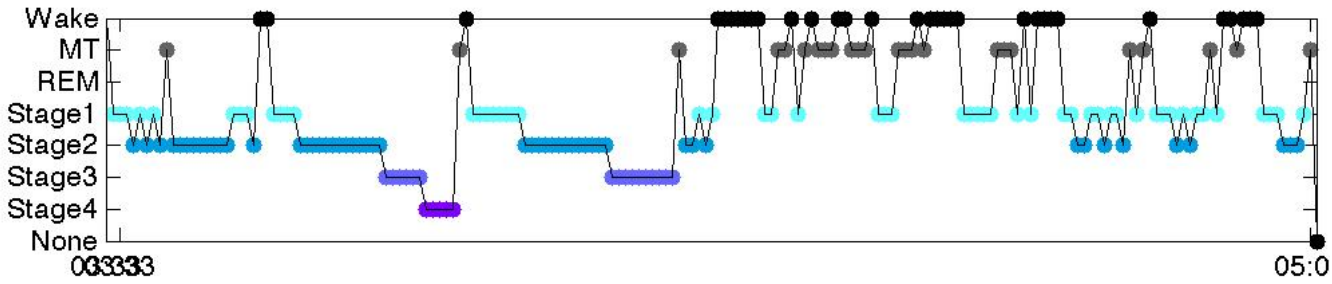

Full Transition Table:

From\To	**Wake**	**Stage 1**	**Stage 2**	**Stage 3**	**Stage 4**	**REM**	**MT**
Wake:	**18**	11	0	0	0	0	4
Stage 1:	4	**29**	13	0	0	0	7
Stage 2:	1	10	**36**	2	0	0	2
Stage 3:	0	0	0	**14**	1	0	1
Stage 4:	0	0	0	0	**4**	0	1
REM:	0	0	0	0	0	**0**	0
MT:	9	3	2	0	0	0	**9**

SW Collapsed Hypnogram:

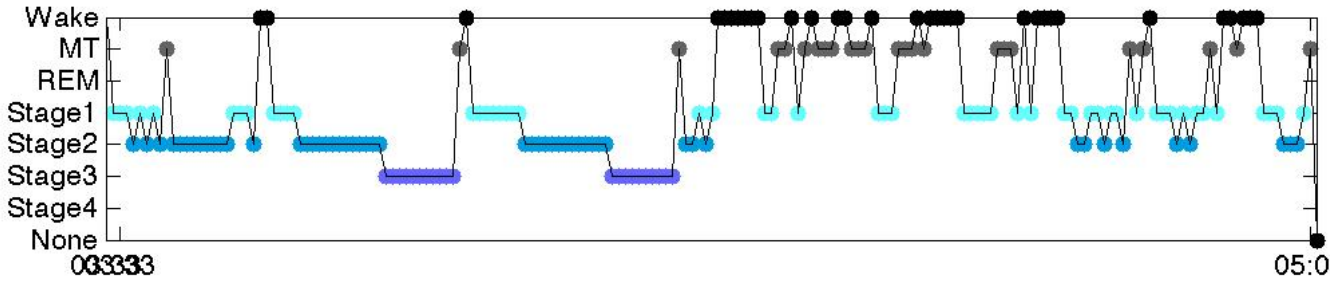

SW Collapsed Transition Table:

From\To	**Wake**	**Stage 1**	**Stage 2**	**SW**	**REM**	**MT**
Wake:	**18**	11	0	0	0	4
Stage 1:	4	**29**	13	0	0	7
Stage 2:	1	10	**36**	2	0	2
SW:	0	0	0	**19**	0	2
REM:	0	0	0	0	**0**	0

*** Subject 03: Sleep Stats ***

Notes:
Scoring window: 30 secs

Lights OUT: 03:30:28.788
Lights ON: 04:46:32.356

Sleep onset epoch: 9 (relative to record start: 9)
Final awakening epoch: 147 (relative to record start: 147)
First scored epoch relative to record start: 1

Last stage of sleep: MT
Awake at lights on? Yes

Sleep Percentages

	Epochs	Minutes	%TDT	%SPT	%TST
Total dark time:	152	76.0			
Sleep period time:	139	69.5	91.45		
Total sleep time:	125	62.5	82.24	89.93	
Sleep before sleep onset:	1	0.5	0.66		
Wake after sleep onset:	12	6.0	7.89	8.63	9.60
Wake after final awakening:	4	2.0	2.63	2.88	3.20
Total wake time	24	12.0	15.79	17.27	19.20
Stage 1	9	4.5	5.92	6.47	7.20
Stage 2	60	30.0	39.47	43.17	48.00
Stage 3	15	7.5	9.87	10.79	12.00
Stage 4	41	20.5	26.97	29.50	32.80
REM	0	0.0	0.00	0.00	0.00
MT	2	1.0	1.32	1.44	1.60
NREM	125	62.5	82.24	89.93	100.00
SW	56	28.0	36.84	40.29	44.80

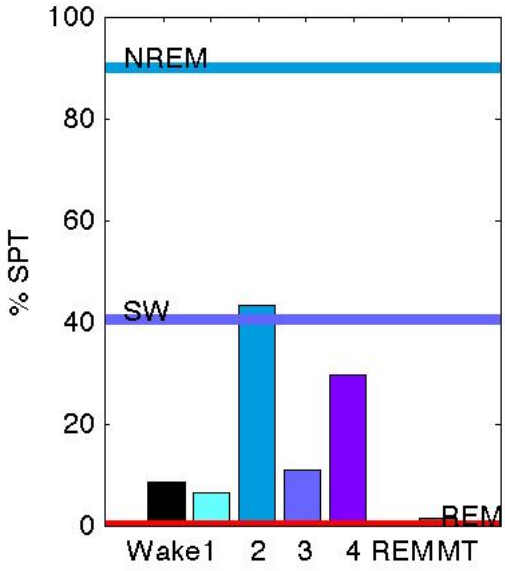

Sleep Latencies

	Epochs	Minutes
lights out to sleep onset	8	4.0
lights out to Stage 1	8	4.0
lights out to Stage 2	11	5.5
lights out to Stage 3	33	16.5
lights out to Stage 4	38	19.0
lights out to REM	NaN	NaN
Sleep onset to Stage 1	0	0.0
Sleep onset to Stage 2	3	1.5
Sleep onset to Stage 3	25	12.5
Sleep onset to Stage 4	30	15.0
Sleep onset to REM	NaN	NaN

NREM Period Stats (min)

	1
Wake:	6.00
Stage 1:	3.00
Stage 2:	30.00
Stage 3:	7.50
Stage 4:	20.50
REM:	-
MT:	1.00
SW:	28.00
Total Time:	68.00
Segments:	1

NREM-REM Cycle Stats (min)

.

REM Period Stats (min)

Segments:

Last REM to final awakening: NaN
Last REM to lights on: NaN

Full Hypnogram:

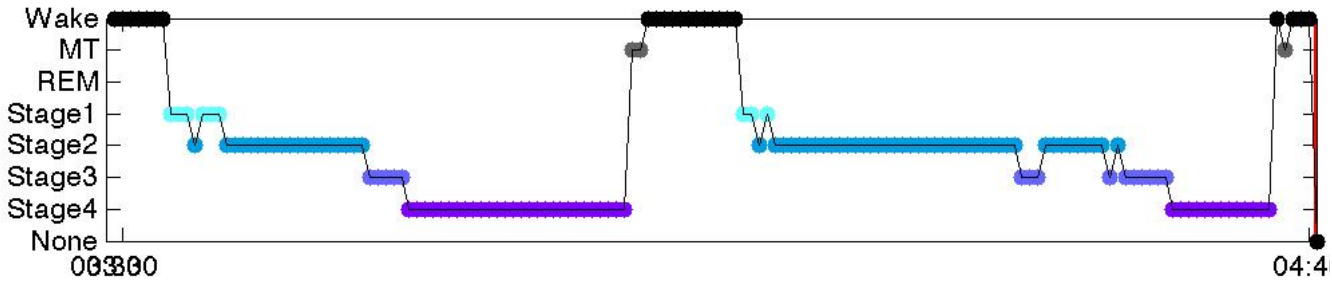

Full Transition Table:

From\To	**Wake**	**Stage 1**	**Stage 2**	**Stage 3**	**Stage 4**	**REM**	**MT**
Wake:	**20**	2	0	0	0	0	1
Stage 1:	0	**5**	4	0	0	0	0
Stage 2:	0	2	**54**	4	0	0	0
Stage 3:	0	0	2	**11**	2	0	0
Stage 4:	1	0	0	0	**39**	0	1
REM:	0	0	0	0	0	**0**	0
MT:	2	0	0	0	0	0	**1**

SW Collapsed Hypnogram:

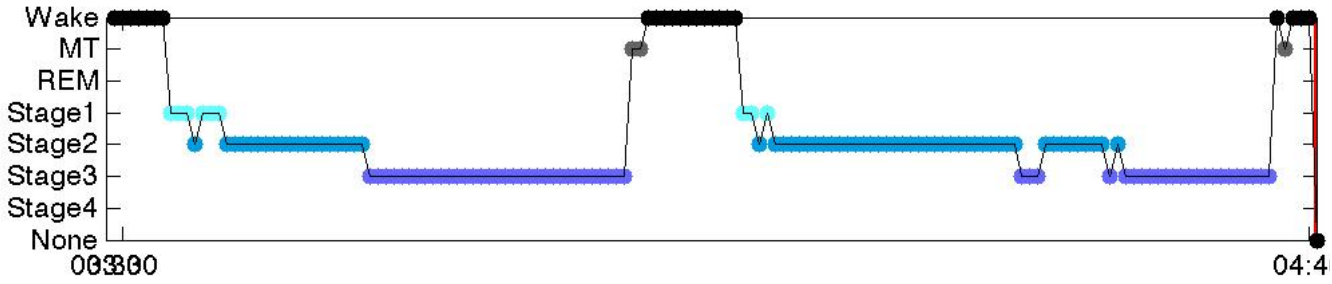

SW Collapsed Transition Table:

From\To	**Wake**	**Stage 1**	**Stage 2**	**SW**	**REM**	**MT**
Wake:	**20**	2	0	0	0	1
Stage 1:	0	**5**	4	0	0	0
Stage 2:	0	2	**54**	4	0	0
SW:	1	0	2	**52**	0	1
REM:	0	0	0	0	**0**	0

*** Subject 04: Sleep Stats ***

Notes:
Scoring window: 30 secs

Lights OUT: 03:45:16.655
Lights ON: 05:33:01.243

Sleep onset epoch: 3 (relative to record start: 3)
Final awakening epoch: 215 (relative to record start: 215)
First scored epoch relative to record start: 1

Last stage of sleep: Stage 2
Awake at lights on? No

Sleep Percentages

	Epochs	Minutes	%TDT	%SPT	%TST
Total dark time:	215	107.5			
Sleep period time:	213	106.5	99.07		
Total sleep time:	209	104.5	97.21	98.12	
Sleep before sleep onset:	1	0.5	0.47		
Wake after sleep onset:	0	0.0	0.00	0.00	0.00
Wake after final awakening:	0	0.0	0.00	0.00	0.00
Total wake time	2	1.0	0.93	0.94	0.96
Stage 1	7	3.5	3.26	3.29	3.35
Stage 2	96	48.0	44.65	45.07	45.93
Stage 3	40	20.0	18.60	18.78	19.14
Stage 4	66	33.0	30.70	30.99	31.58
REM	0	0.0	0.00	0.00	0.00
MT	4	2.0	1.86	1.88	1.91
NREM	209	104.5	97.21	98.12	100.00
SW	106	53.0	49.30	49.77	50.72

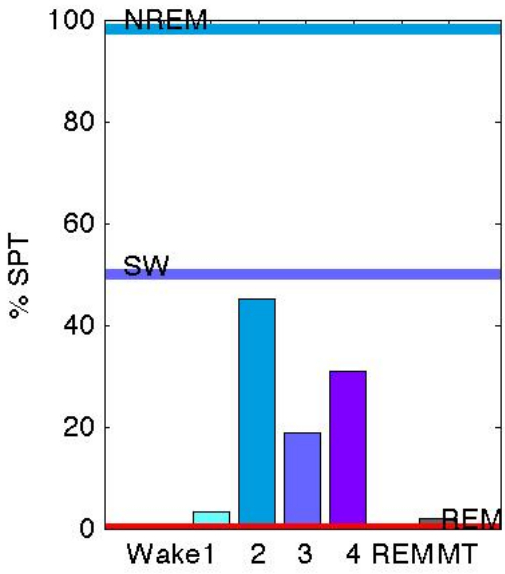

Sleep Latencies

	Epochs	Minutes
lights out to sleep onset	2	1.0
lights out to Stage 1	2	1.0
lights out to Stage 2	3	1.5
lights out to Stage 3	15	7.5
lights out to Stage 4	25	12.5
lights out to REM	NaN	NaN
Sleep onset to Stage 1	0	0.0
Sleep onset to Stage 2	1	0.5
Sleep onset to Stage 3	13	6.5
Sleep onset to Stage 4	23	11.5
Sleep onset to REM	NaN	NaN

NREM Period Stats (min)

	1
Wake:	-
Stage 1:	3.00
Stage 2:	48.00
Stage 3:	20.00
Stage 4:	33.00
REM:	-
MT:	2.00
SW:	53.00
Total Time:	106.00
Segments:	1

NREM-REM Cycle Stats (min)

.

REM Period Stats (min)

Segments:

Last REM to final awakening: NaN
Last REM to lights on: NaN

Full Hypnogram:

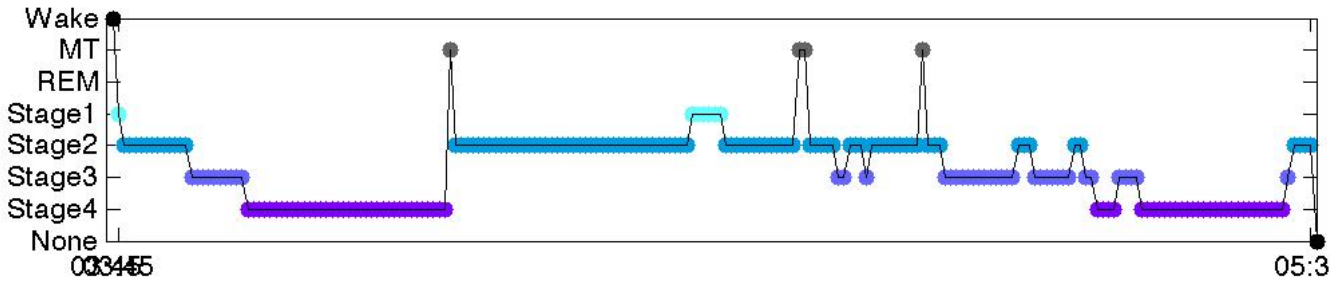

Full Transition Table:

From\To	**Wake**	**Stage 1**	**Stage 2**	**Stage 3**	**Stage 4**	**REM**	**MT**
Wake:	**1**	1	0	0	0	0	0
Stage 1:	0	**5**	2	0	0	0	0
Stage 2:	0	1	**86**	6	0	0	2
Stage 3:	0	0	5	**32**	3	0	0
Stage 4:	0	0	0	2	**63**	0	1
REM:	0	0	0	0	0	**0**	0
MT:	0	0	3	0	0	0	**1**

SW Collapsed Hypnogram:

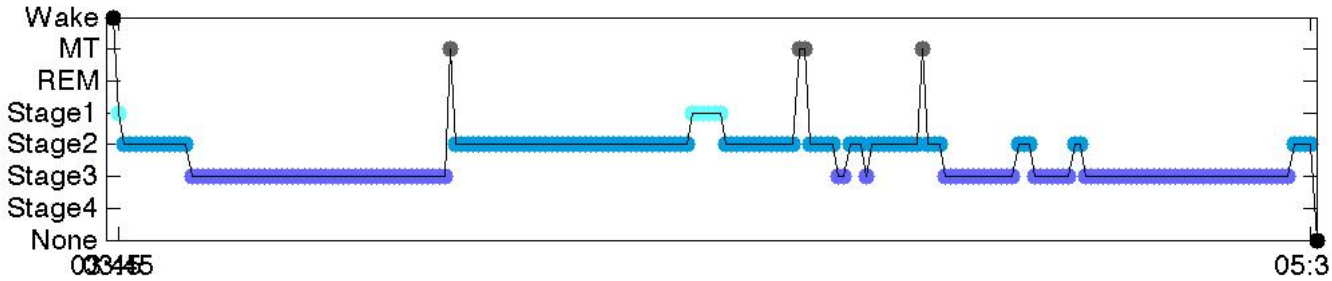

SW Collapsed Transition Table:

From\To	**Wake**	**Stage 1**	**Stage 2**	**SW**	**REM**	**MT**
Wake:	**1**	1	0	0	0	0
Stage 1:	0	**5**	2	0	0	0
Stage 2:	0	1	**86**	6	0	2
SW:	0	0	5	**100**	0	1
REM:	0	0	0	0	**0**	0

*** Subject 05: Sleep Stats ***

Notes:
Scoring window: 30 secs

Lights OUT: 03:41:18.377
Lights ON: 05:22:54.069

Sleep onset epoch: 4 (relative to record start: 4)
Final awakening epoch: 201 (relative to record start: 201)
First scored epoch relative to record start: 1

Last stage of sleep: MT
Awake at lights on? Yes

Sleep Percentages

	Epochs	Minutes	%TDT	%SPT	%TST
Total dark time:	203	101.5			
Sleep period time:	198	99.0	97.54		
Total sleep time:	190	95.0	93.60	95.96	
Sleep before sleep onset:	1	0.5	0.49		
Wake after sleep onset:	3	1.5	1.48	1.52	1.58
Wake after final awakening:	1	0.5	0.49	0.51	0.53
Total wake time	7	3.5	3.45	3.54	3.68
Stage 1	11	5.5	5.42	5.56	5.79
Stage 2	137	68.5	67.49	69.19	72.11
Stage 3	28	14.0	13.79	14.14	14.74
Stage 4	2	1.0	0.99	1.01	1.05
REM	12	6.0	5.91	6.06	6.32
MT	5	2.5	2.46	2.53	2.63
NREM	178	89.0	87.68	89.90	93.68
SW	30	15.0	14.78	15.15	15.79

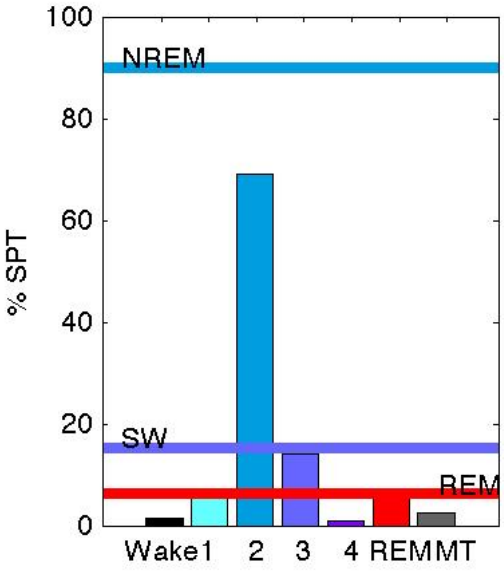

Sleep Latencies

	Epochs	Minutes
lights out to sleep onset	3	1.5
lights out to Stage 1	3	1.5
lights out to Stage 2	9	4.5
lights out to Stage 3	79	39.5
lights out to Stage 4	103	51.5
lights out to REM	121	60.5
Sleep onset to Stage 1	0	0.0
Sleep onset to Stage 2	6	3.0
Sleep onset to Stage 3	76	38.0
Sleep onset to Stage 4	100	50.0
Sleep onset to REM	118	59.0

NREM-REM Cycle Stats (min) NREM Period Stats (min) REM Period Stats (min)

	1
Wake:	1.50
Stage 1:	2.50
Stage 2:	39.00
Stage 3:	13.50
Stage 4:	1.00
REM:	6.00
MT:	2.50
SW:	14.50
Total Time:	66.00
.	

	1	2
Wake:	1.50	-
Stage 1:	2.50	-
Stage 2:	35.50	29.50
Stage 3:	13.50	0.50
Stage 4:	1.00	-
REM:	-	-
MT:	2.00	-
SW:	14.50	0.50
Total Time:	56.00	30.00
Segments:	1	1

	1
Wake:	-
Stage 1:	-
Stage 2:	3.50
Stage 3:	-
Stage 4:	-
REM:	6.00
MT:	0.50
SW:	-
Total Time:	10.00
Segments:	2

Last REM to final awakening: 30.5
Last REM to lights on: 31.0

Full Hypnogram:

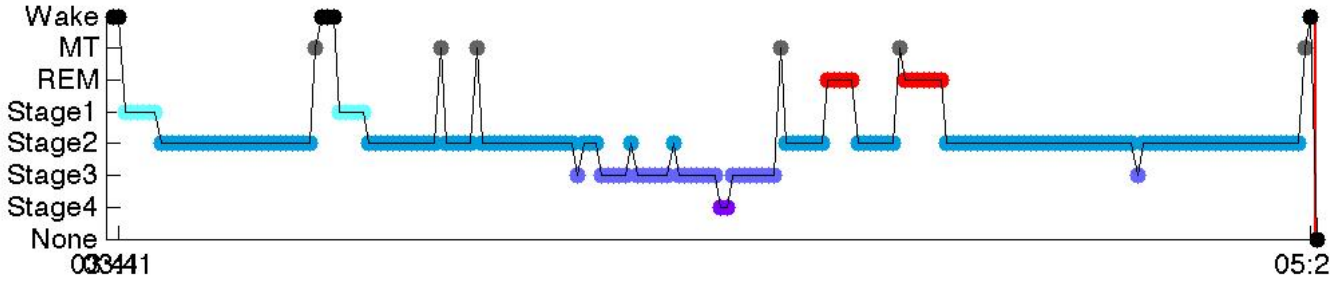

Full Transition Table:

From\To	**Wake**	**Stage 1**	**Stage 2**	**Stage 3**	**Stage 4**	**REM**	**MT**
Wake:	**4**	2	0	0	0	0	0
Stage 1:	0	**9**	2	0	0	0	0
Stage 2:	0	0	**126**	5	0	1	5
Stage 3:	0	0	4	**22**	1	0	1
Stage 4:	0	0	0	1	**1**	0	0
REM:	0	0	2	0	0	**10**	0
MT:	2	0	3	0	0	1	**0**

SW Collapsed Hypnogram:

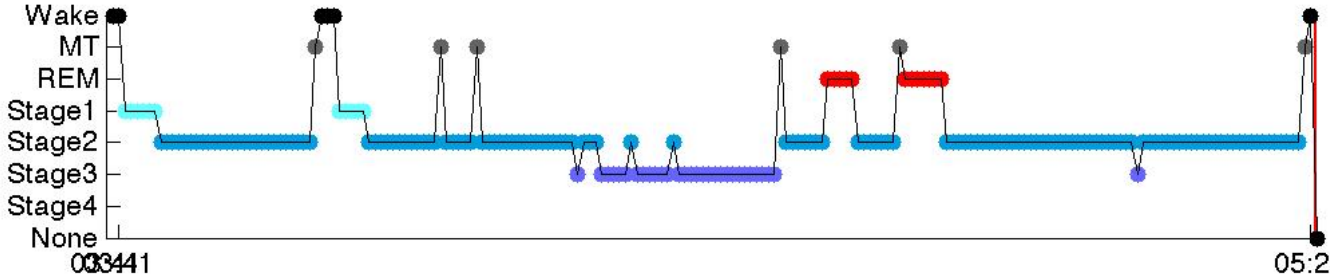

SW Collapsed Transition Table:

From\To	**Wake**	**Stage 1**	**Stage 2**	**SW**	**REM**	**MT**
Wake:	**4**	2	0	0	0	0
Stage 1:	0	**9**	2	0	0	0
Stage 2:	0	0	**126**	5	1	5
SW:	0	0	4	**25**	0	1
REM:	0	0	2	0	**10**	0

*** Subject 06: Sleep Stats ***

Notes:
Scoring window: 30 secs

Lights OUT: 03:34:58.204
Lights ON: 05:06:10.436

Sleep onset epoch: 13 (relative to record start: 13)
Final awakening epoch: 182 (relative to record start: 182)
First scored epoch relative to record start: 1

Last stage of sleep: Stage 2
Awake at lights on? No

Sleep Percentages

	Epochs	Minutes	%TDT	%SPT	%TST
Total dark time:	182	91.0			
Sleep period time:	170	85.0	93.41		
Total sleep time:	160	80.0	87.91	94.12	
Sleep before sleep onset:	1	0.5	0.55		
Wake after sleep onset:	8	4.0	4.40	4.71	5.00
Wake after final awakening:	0	0.0	0.00	0.00	0.00
Total wake time	20	10.0	10.99	11.76	12.50
Stage 1	11	5.5	6.04	6.47	6.88
Stage 2	109	54.5	59.89	64.12	68.12
Stage 3	35	17.5	19.23	20.59	21.88
Stage 4	5	2.5	2.75	2.94	3.12
REM	0	0.0	0.00	0.00	0.00
MT	2	1.0	1.10	1.18	1.25
NREM	160	80.0	87.91	94.12	100.00
SW	40	20.0	21.98	23.53	25.00

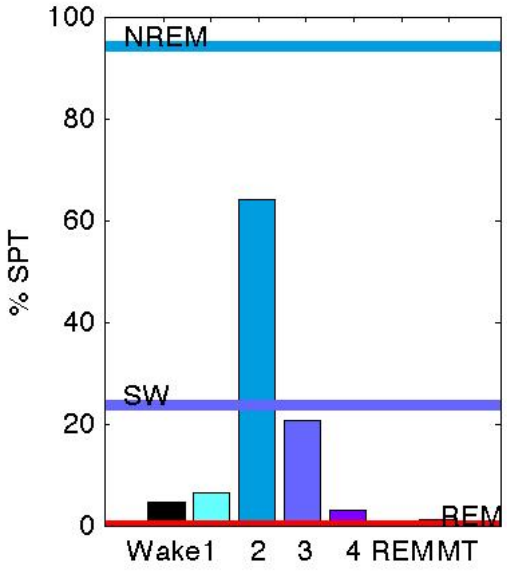

Sleep Latencies

	Epochs	Minutes
lights out to sleep onset	12	6.0
lights out to Stage 1	12	6.0
lights out to Stage 2	16	8.0
lights out to Stage 3	53	26.5
lights out to Stage 4	146	73.0
lights out to REM	NaN	NaN
Sleep onset to Stage 1	0	0.0
Sleep onset to Stage 2	4	2.0
Sleep onset to Stage 3	41	20.5
Sleep onset to Stage 4	134	67.0
Sleep onset to REM	NaN	NaN

NREM Period Stats (min)

	1
Wake:	4.00
Stage 1:	3.50
Stage 2:	54.50
Stage 3:	17.50
Stage 4:	2.50
REM:	-
MT:	1.00
SW:	20.00
Total Time:	83.00
Segments:	1

NREM-REM Cycle Stats (min)

.

REM Period Stats (min)

Segments:

Last REM to final awakening: NaN
Last REM to lights on: NaN

Full Hypnogram:

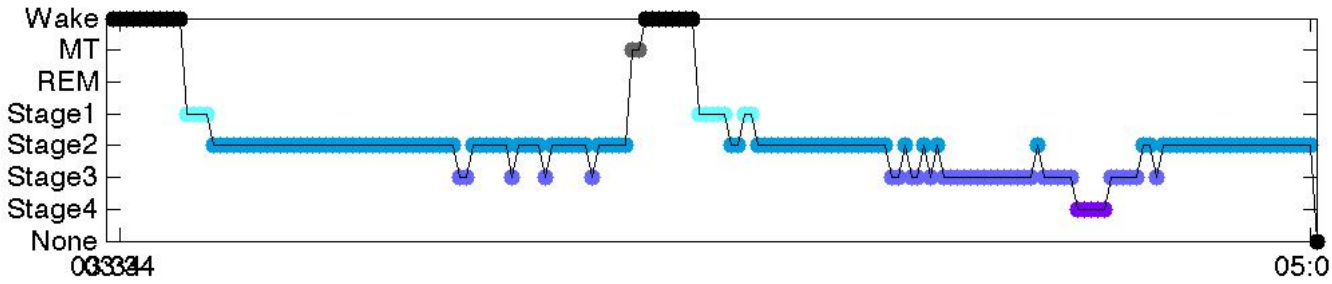

Full Transition Table:

From\To	**Wake**	**Stage 1**	**Stage 2**	**Stage 3**	**Stage 4**	**REM**	**MT**
Wake:	**18**	2	0	0	0	0	0
Stage 1:	0	**8**	3	0	0	0	0
Stage 2:	0	1	**96**	10	0	0	1
Stage 3:	0	0	10	**24**	1	0	0
Stage 4:	0	0	0	1	**4**	0	0
REM:	0	0	0	0	0	**0**	0
MT:	1	0	0	0	0	0	**1**

SW Collapsed Hypnogram:

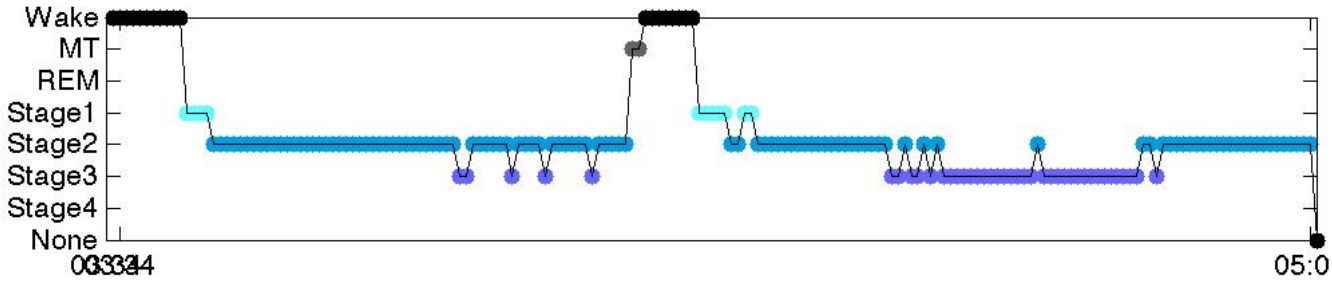

SW Collapsed Transition Table:

From\To	**Wake**	**Stage 1**	**Stage 2**	**SW**	**REM**	**MT**
Wake:	**18**	2	0	0	0	0
Stage 1:	0	**8**	3	0	0	0
Stage 2:	0	1	**96**	10	0	1
SW:	0	0	10	**30**	0	0
REM:	0	0	0	0	**0**	0

*** Subject 07: Sleep Stats ***

Notes:
Scoring window: 30 secs

Lights OUT: 03:46:12.410
Lights ON: 05:23:05.474

Sleep onset epoch: 11 (relative to record start: 11)
Final awakening epoch: 193 (relative to record start: 193)
First scored epoch relative to record start: 1

Last stage of sleep: Stage 1
Awake at lights on? No

Sleep Percentages

	Epochs	Minutes	%TDT	%SPT	%TST
Total dark time:	193	96.5			
Sleep period time:	183	91.5	94.82		
Total sleep time:	113	56.5	58.55	61.75	
Sleep before sleep onset:	1	0.5	0.52		
Wake after sleep onset:	69	34.5	35.75	37.70	61.06
Wake after final awakening:	0	0.0	0.00	0.00	0.00
Total wake time	79	39.5	40.93	43.17	69.91
Stage 1	18	9.0	9.33	9.84	15.93
Stage 2	95	47.5	49.22	51.91	84.07
Stage 3	0	0.0	0.00	0.00	0.00
Stage 4	0	0.0	0.00	0.00	0.00
REM	0	0.0	0.00	0.00	0.00
MT	1	0.5	0.52	0.55	0.88
NREM	113	56.5	58.55	61.75	100.00
SW	0	0.0	0.00	0.00	0.00

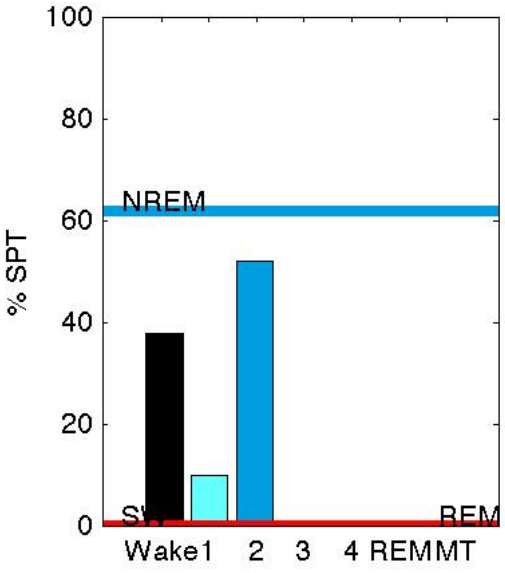

Sleep Latencies

	Epochs	Minutes
lights out to sleep onset	10	5.0
lights out to Stage 1	10	5.0
lights out to Stage 2	18	9.0
lights out to Stage 3	NaN	NaN
lights out to Stage 4	NaN	NaN
lights out to REM	NaN	NaN
Sleep onset to Stage 1	0	0.0
Sleep onset to Stage 2	8	4.0
Sleep onset to Stage 3	NaN	NaN
Sleep onset to Stage 4	NaN	NaN
Sleep onset to REM	NaN	NaN

NREM Period Stats (min)

	1
Wake:	34.50
Stage 1:	5.00
Stage 2:	47.50
Stage 3:	-
Stage 4:	-
REM:	-
MT:	0.50
SW:	-
Total Time:	87.50
Segments:	1

NREM-REM Cycle Stats (min)

.

REM Period Stats (min)

Segments:

Last REM to final awakening: NaN
Last REM to lights on: NaN

Full Hypnogram:

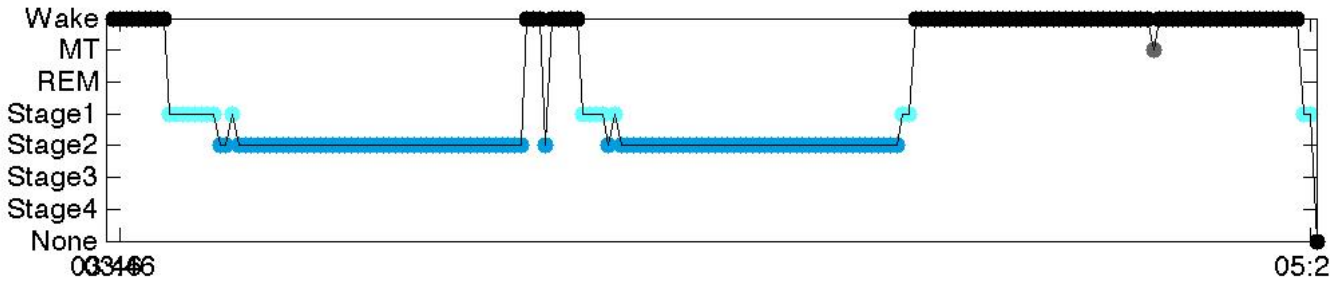

Full Transition Table:

From\To	**Wake**	**Stage 1**	**Stage 2**	**Stage 3**	**Stage 4**	**REM**	**MT**
Wake:	**74**	3	1	0	0	0	1
Stage 1:	1	**12**	4	0	0	0	0
Stage 2:	2	3	**90**	0	0	0	0
Stage 3:	0	0	0	**0**	0	0	0
Stage 4:	0	0	0	0	**0**	0	0
REM:	0	0	0	0	0	**0**	0
MT:	1	0	0	0	0	0	**0**

SW Collapsed Hypnogram:

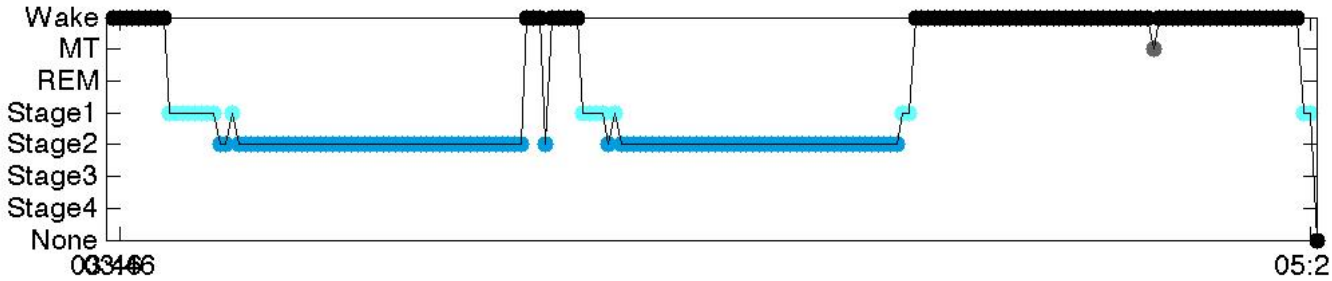

SW Collapsed Transition Table:

From\To	**Wake**	**Stage 1**	**Stage 2**	**SW**	**REM**	**MT**
Wake:	**74**	3	1	0	0	1
Stage 1:	1	**12**	4	0	0	0
Stage 2:	2	3	**90**	0	0	0
SW:	0	0	0	**0**	0	0
REM:	0	0	0	0	**0**	0

*** Subject 09: Sleep Stats ***

Notes:
Scoring window: 30 secs

Lights OUT: 03:41:25.221
Lights ON: 05:22:16.285

Sleep onset epoch: 5 (relative to record start: 5)
Final awakening epoch: 201 (relative to record start: 201)
First scored epoch relative to record start: 1

Last stage of sleep: Stage 4
Awake at lights on? No

Sleep Percentages

	Epochs	Minutes	%TDT	%SPT	%TST
Total dark time:	201	100.5			
Sleep period time:	197	98.5	98.01		
Total sleep time:	192	96.0	95.52	97.46	
Sleep before sleep onset:	1	0.5	0.50		
Wake after sleep onset:	2	1.0	1.00	1.02	1.04
Wake after final awakening:	0	0.0	0.00	0.00	0.00
Total wake time	6	3.0	2.99	3.05	3.12
Stage 1	25	12.5	12.44	12.69	13.02
Stage 2	59	29.5	29.35	29.95	30.73
Stage 3	32	16.0	15.92	16.24	16.67
Stage 4	64	32.0	31.84	32.49	33.33
REM	12	6.0	5.97	6.09	6.25
MT	3	1.5	1.49	1.52	1.56
NREM	180	90.0	89.55	91.37	93.75
SW	96	48.0	47.76	48.73	50.00

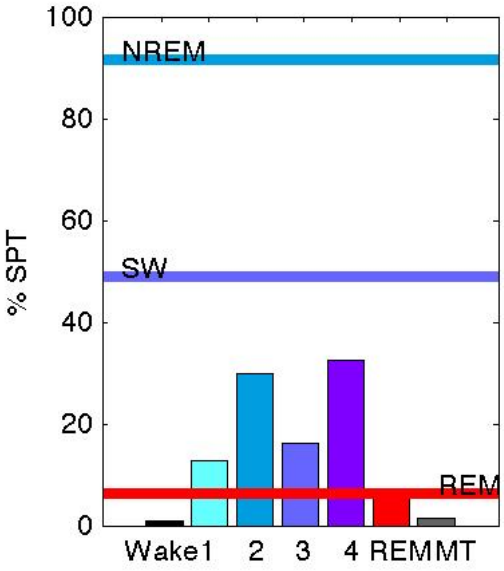

Sleep Latencies

	Epochs	Minutes
lights out to sleep onset	4	2.0
lights out to Stage 1	4	2.0
lights out to Stage 2	19	9.5
lights out to Stage 3	31	15.5
lights out to Stage 4	41	20.5
lights out to REM	124	62.0
Sleep onset to Stage 1	0	0.0
Sleep onset to Stage 2	15	7.5
Sleep onset to Stage 3	27	13.5
Sleep onset to Stage 4	37	18.5
Sleep onset to REM	120	60.0

NREM-REM Cycle Stats (min) NREM Period Stats (min) REM Period Stats (min)

	1
Wake:	-
Stage 1:	6.00
Stage 2:	20.50
Stage 3:	9.50
Stage 4:	18.00
REM:	6.00
MT:	0.50
SW:	27.50
Total Time:	60.50
.	

	1	2
Wake:	-	-
Stage 1:	4.00	-
Stage 2:	20.50	9.00
Stage 3:	9.50	6.50
Stage 4:	18.00	14.00
REM:	-	-
MT:	0.50	1.00
SW:	27.50	20.50
Total Time:	52.50	30.50
Segments:	1	1

	1
Wake:	-
Stage 1:	2.00
Stage 2:	-
Stage 3:	-
Stage 4:	-
REM:	6.00
MT:	-
SW:	-
Total Time:	8.00
Segments:	1

Last REM to final awakening: 32.5
Last REM to lights on: 32.5

Full Hypnogram:

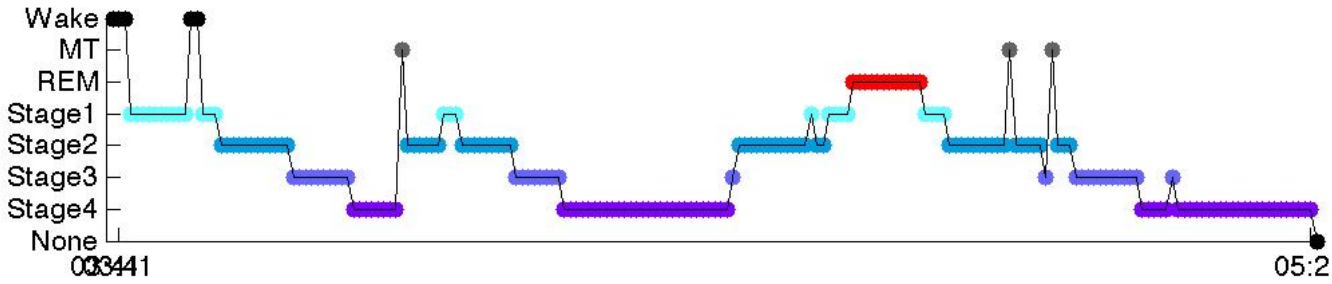

Full Transition Table:

From\To	**Wake**	**Stage 1**	**Stage 2**	**Stage 3**	**Stage 4**	**REM**	**MT**
Wake:	**4**	2	0	0	0	0	0
Stage 1:	1	**19**	4	0	0	1	0
Stage 2:	0	3	**51**	4	0	0	1
Stage 3:	0	0	1	**26**	4	0	1
Stage 4:	0	0	0	2	**60**	0	1
REM:	0	1	0	0	0	**11**	0
MT:	0	0	3	0	0	0	**0**

SW Collapsed Hypnogram:

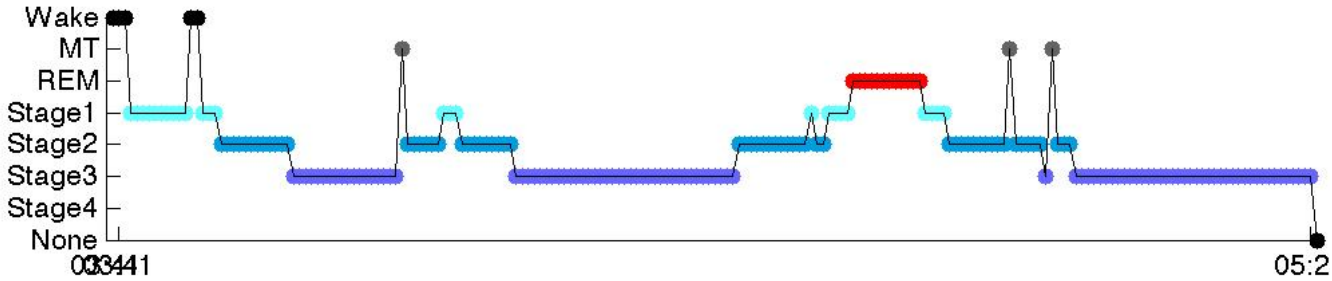

SW Collapsed Transition Table:

From\To	**Wake**	**Stage 1**	**Stage 2**	**SW**	**REM**	**MT**
Wake:	**4**	2	0	0	0	0
Stage 1:	1	**19**	4	0	1	0
Stage 2:	0	3	**51**	4	0	1
SW:	0	0	1	**92**	0	2
REM:	0	1	0	0	**11**	0

*** Subject 10: Sleep Stats ***

Notes:
Scoring window: 30 secs

Lights OUT: 03:26:18.332
Lights ON: 05:07:00.472

Sleep onset epoch: 10 (relative to record start: 10)
Final awakening epoch: 201 (relative to record start: 201)
First scored epoch relative to record start: 1

Last stage of sleep: Stage 1
Awake at lights on? No

Sleep Percentages

	Epochs	Minutes	%TDT	%SPT	%TST
Total dark time:	201	100.5			
Sleep period time:	192	96.0	95.52		
Total sleep time:	184	92.0	91.54	95.83	
Sleep before sleep onset:	1	0.5	0.50		
Wake after sleep onset:	0	0.0	0.00	0.00	0.00
Wake after final awakening:	0	0.0	0.00	0.00	0.00
Total wake time	9	4.5	4.48	4.69	4.89
Stage 1	14	7.0	6.97	7.29	7.61
Stage 2	88	44.0	43.78	45.83	47.83
Stage 3	33	16.5	16.42	17.19	17.93
Stage 4	28	14.0	13.93	14.58	15.22
REM	21	10.5	10.45	10.94	11.41
MT	8	4.0	3.98	4.17	4.35
NREM	163	81.5	81.09	84.90	88.59
SW	61	30.5	30.35	31.77	33.15

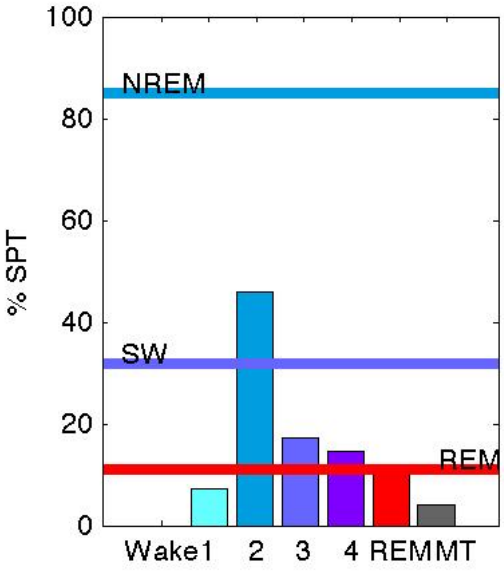

Sleep Latencies

	Epochs	Minutes
lights out to sleep onset	9	4.5
lights out to Stage 1	9	4.5
lights out to Stage 2	14	7.0
lights out to Stage 3	35	17.5
lights out to Stage 4	93	46.5
lights out to REM	153	76.5
Sleep onset to Stage 1	0	0.0
Sleep onset to Stage 2	5	2.5
Sleep onset to Stage 3	26	13.0
Sleep onset to Stage 4	84	42.0
Sleep onset to REM	144	72.0

NREM-REM Cycle Stats (min) NREM Period Stats (min) REM Period Stats (min)

	1
Wake:	-
Stage 1:	4.50
Stage 2:	44.00
Stage 3:	16.50
Stage 4:	14.00
REM:	10.50
MT:	4.00
SW:	30.50
Total Time:	93.50
.	

	1
Wake:	-
Stage 1:	1.00
Stage 2:	35.00
Stage 3:	16.50
Stage 4:	14.00
REM:	-
MT:	3.00
SW:	30.50
Total Time:	69.50
Segments:	1

	1
Wake:	-
Stage 1:	3.50
Stage 2:	9.00
Stage 3:	-
Stage 4:	-
REM:	10.50
MT:	1.00
SW:	-
Total Time:	24.00
Segments:	2

Last REM to final awakening: 12.5
Last REM to lights on: 12.5

Full Hypnogram:

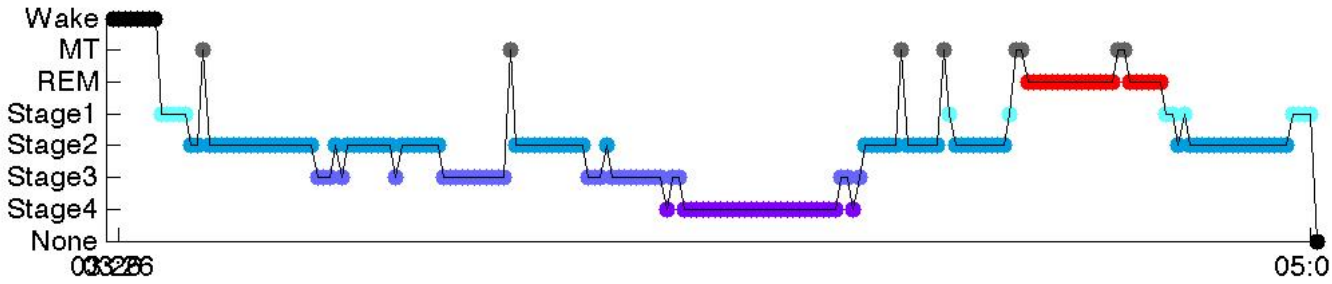

Full Transition Table:

From\To	**Wake**	**Stage 1**	**Stage 2**	**Stage 3**	**Stage 4**	**REM**	**MT**
Wake:	**8**	1	0	0	0	0	0
Stage 1:	0	**8**	4	0	0	0	1
Stage 2:	0	3	**76**	6	0	0	3
Stage 3:	0	0	5	**24**	3	0	1
Stage 4:	0	0	0	3	**25**	0	0
REM:	0	1	0	0	0	**19**	1
MT:	0	1	3	0	0	2	**2**

SW Collapsed Hypnogram:

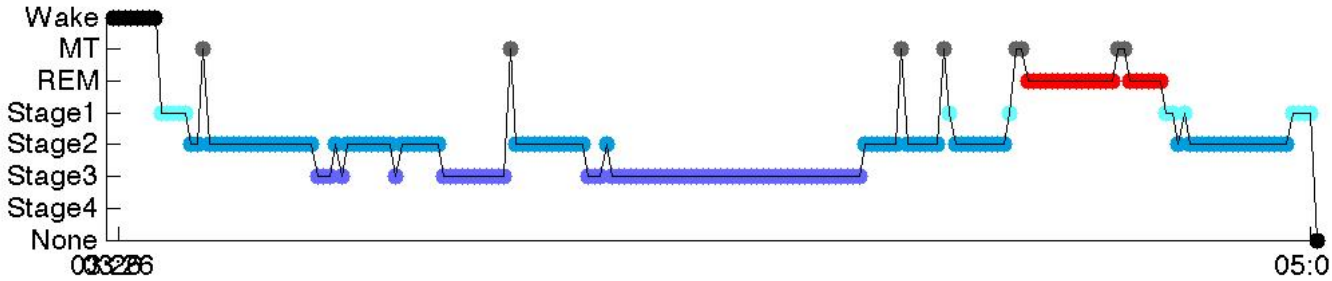

SW Collapsed Transition Table:

From\To	**Wake**	**Stage 1**	**Stage 2**	**SW**	**REM**	**MT**
Wake:	**8**	1	0	0	0	0
Stage 1:	0	**8**	4	0	0	1
Stage 2:	0	3	**76**	6	0	3
SW:	0	0	5	**55**	0	1
REM:	0	1	0	0	**19**	1

Appendix B

Questionnaires

APPENDIX XIV: BERLIN QUESTIONNAIRE

SLEEP EVAUATION IN PRIMARY CARE

1. Complete the following:

Height_____ Age_____

Weight_____ Male/Female _____

2. Do you snore?

- ❑ Yes
- ❑ no
- ❑ don't know

If you snore:

3. Your snoring is?
   - ❑ slightly louder than breathing
   - ❑ as loud as talking
   - ❑ louder than talking
   - ❑ very loud. Can be heard in adjacent rooms

4. How often do you snore?
   - ❑ nearly everyday
   - ❑ 3-4 times a week
   - ❑ 1-2 time a week
   - ❑ 1-2 times a month
   - ❑ never or nearly never

5. Has your snoring ever bothered other people?
   - ❑ Yes
   - ❑ No

6. Has anyone noticed that you quit breathing during your sleep?
   - ❑ Nearly every day
   - ❑ 3-4 times a week
   - ❑ 1-2 times a week
   - ❑ 1-2 times a month
   - ❑ never or nearly never

Scoring Questions: Any answer within box outline is a positive respone

Scoring Categories:
Category 1 is positive with 2 or more positive responses to questions 2-6❑
Category 2 is positive with 2 or more positive responses to questions 7-9❑
Category 3 is positive with 1positive responses &/or a BMI>30

Final Result: 2 or more possible categories indictes a high likelihood of sleep disordered breathing.

7 How often do you feel tired or fatigued after sleep?
   - ❑ nearly every day
   - ❑ 3-4 times a week
   - ❑ 1-2 times a week
   - ❑ 1-2 times a month
   - ❑ never or nearly never

8. During your waketime, do you feel tired fatigued or not up to par?
   - ❑ nearly every day
   - ❑ 3-4 times a week
   - ❑ 1-2 times a week
   - ❑ 1-2 times a month
   - ❑ never or nearly never

9. Have you ever nodded off or fallen asleep while driving a vehicle?
   - ❑ Yes
   - ❑ No

   If yes, how often does it occur?
   - ❑ nearly every day
   - ❑ 3-4 times a week
   - ❑ 1-2 times a week
   - ❑ 1-2 times a month
   - ❑ never or nearly never

10. Do you have high blood pressure?
    - ❑ Yes
    - ❑ No
    - ❑ Don't know

BMI:

Initials:_____

ID #:_____

DUKE STRUCTURED INTERVIEW FOR SLEEP DISORDERS

CHECKLIST OF UNUSUAL EVENTS AND BEHAVIORS OCCURRING DURING SLEEP

Have you ever had or do you currently have (i.e. past month) any of the following symptoms? Please check the appropriate box (current or past) for all that apply.

CURRENT (past month)	PAST	SYMPTOMS
		Recurrent disturbing dreams
		Night terrors (abrupt awakening with feelings of fright and confusion)
		Sleepwalking
		Strange sensory experiences upon awakening or falling asleep
		Memory changes or bizarre behaviors during the night
		Confusion and difficulty coming to your senses when awakened from sleep
		Painful leg cramps during sleep
		Paralysis or inability to move while in bed
		Behaviors that are aggressive to others or dangerous to yourself during sleep
		Acting out your dreams
		Grinding your teeth during sleep
		Eating/drinking during sleep
		Groaning during sleep
		Loud noises in your head upon awakening or falling asleep
		Bedwetting

The Epworth Sleepiness Scale

Subject Code:_____ Date: _____

How likely are you to fall asleep in the following situations, in contrast to feeling just tired? This refers to your usual way of life in recent times. Even if you have not done some of these things recently, try to work out how they would have affected you. Use the following scale to choose the *most appropriate number* for each situation:

0 = would ***never*** doze
1 = ***slight*** chance of dozing
2 = ***moderate*** chance of dozing
3 = ***high*** chance of dozing

SITUATION	CHANCE OF DOZING
Sitting and Reading	_____
Watching TV	_____
Sitting inactive in a public place (e.g. in a theater or a meeting)	_____
As a passenger in a car without a break for an hour	_____
Lying down in the afternoon when circumstances permit	_____
Sitting and talking with someone	_____
Sitting quietly after lunch without alcohol	_____
In a car, while stopped for a few minutes in traffic	_____

Participant ID: _____ DATE: _____ TIME: _____

KAROLINSKA SLEEPINESS SCALE

Choose the number of the description that best fits your current state:

1 Extremely alert

2

3 Alert

4

5 Neither alert nor sleepy

6

7 Sleepy—but no difficulty remaining awake

8

9 Extremely sleepy—fighting sleep

Munich ChronoType Questionnaire (MCTQ)

Please enter your age, gender, etc.. This information is important for our evaluations

Age: _____ **female** **male** **Height** _____ **Weight** _____

On work days ...

I have to get up at... _____o'clock

I need... _____min to wake up

I regularly wake up... before the alarm with the alarm

From... _____o'clock I am fully awake

At around... _____o'clock, I have an energy dip

On nights before workdays, I go to bed at _____o'clock...

... and it then takes me... _____min to fall asleep

If I get the chance, I like to take a siesta/nap ...

correct I then sleep for..._____ min

not correct I would feel terrible afterwards

On free days (please only judge normal free days, i.e., without parties etc.) ...

My dream would be to sleep until... _____o'clock

I normally wake up at... _____o'clock

If I wake up at around the normal (workday) alarm time, I try to get back to sleep...

correct not correct

if I get back to sleep, I sleep for another... _____min

I need ... _____min to wake up

From... _____o'clock I am fully awake

At around... _____o'clock, I have an energy dip

On nights before free days, I go to bed at... _____o'clock...

... and it then takes me... _____min to fall asleep

If I get the chance, I like to take a siesta/nap ...

correct I then sleep for..._____ min

not correct I would feel terrible afterwards

---

once I am in bed, I would like to read for ... _____ min, ...

... but generally fall asleep after no more than ... _____ min.

I prefer to sleep in a completely dark room correct not correct

I wake up more easily when morning light shines into my room correct not correct

---

How long per day do you spend on average outside (really outside) exposed to day light?

On work days: ___ hrs. ___min. On free days: ___ hrs. ___min.

Self assessment

After you have answered the preceding questions, you should have a feeling to which chronotype (time-of-day-type) you belong to. If for example, you like (and manage) to sleep quite a bit longer on free days than on workdays, or if you cannot get out of bed on Monday mornings, even without a Sunday-night-party, then you are more a late type. If, however, you regularly wake up and feel perky once you jump out of bed, and if you would rather go to bed early than to an evening concert then you are an early type. In the following questions, you should categorise yourself and your family members.

Please tick only one possibility!

Description of categories:

extreme	early type = 0
moderate	early type = 1
slight	early type = 2
	normal type = 3
slight	late type = 4
moderate	late type = 5
extreme	late type = 6

I am...	0	1	2	3	4	5	6
as a child, I was ...	0	1	2	3	4	5	6
as a teenager, I was ...	0	1	2	3	4	5	6

In case you are older than 65: in the middle of my life, I was ...

	0	1	2	3	4	5	6
My parents are/were...							
Mother ...	0	1	2	3	4	5	6
Father ...	0	1	2	3	4	5	6

My siblings are/were ... (please underline Brother or Sister)

Brother/Sister	0	1	2	3	4	5	6
Brother/Sister	0	1	2	3	4	5	6
Brother/Sister	0	1	2	3	4	5	6
Brother/Sister	0	1	2	3	4	5	6
Brother/Sister	0	1	2	3	4	5	6
Brother/Sister	0	1	2	3	4	5	6
Brother/Sister	0	1	2	3	4	5	6

My partner (girl/boy friend, spouse, significant other) is/was ...

	0	1	2	3	4	5	6

The Morningness-Eveningness Questionnaire

As in "Horne JA and Osteberg O, 1976"

Instructions:

1. Please read each question very carefully before answering.
2. Answer ALL questions.
3. Answer questions in numerical order.
4. Each question should be answered independently of others. Do NOT go back and check your answers.
5. All questions have a selection of answers. For each question place a cross alongside ONE answer only. Some questions have a scale instead of a selection of answers. Place a cross at the appropriate point along the scale.
6. Please answer each question as honestly as possible. Both your answers and the results will be kept, in strict confidence.
7. Please feel free to make any comments in the section provided below each question

Scoring:

- For questions 3,4,5,6,7,8,9,11,12,13,14,15,16 and 19, the appropriate score for each response is displayed besides t he answer box.
- For questions 1,2,10 and 18, the cross made along each scale is referred to the appropriate score value range below the scale.
- For question 17 the most extreme cross on the right hand side is taken as the reference point and the appropriate score value range below this point is take.
- The scores are added together and the sum converted into a five point Morningness-Eveningness scale:

    - Definitely Morning Type:
      70-86
    - Moderately Morning Type:
      59-69
    - Neither Type:
      42-58
    - Moderately Evening Type:
      31-41
    - Definitely Evening Type:
      16-30

The Questionnaire, with scores for each choice:

1. Considering only your own "feeling best" rhythm, at what time would you get up if you were entirely free to plan your day?

__:__ (scale in original)

05:00-06:30 = 5
06:30-07:45 = 4
07:45-09:45 = 3
09:45-11:00 = 2
11:00-12:00 = 1

2. Considering only your own "feeling best" rhythm, at what time would you go to bed if you were entirely free to plan your evening?

__:__ (scale in original)

20:00-21:00 = 5
21:00-22:15 = 4
22:15-00:30 = 3
00:30-02:45 = 2
02:45-03:00 = 1

3. If there is a specific time at which you have to get up in the morning, to what extent are you dependent on being woken up by an alarm clock?

Not at all dependent	___	4
Slightly dependent	___	3
Fairly dependent	___	2
Very dependent	___	1

4. Assuming adequate environmental conditions, how easy is it do you find getting up in the mornings?

Not at all easy	___	1
Not very easy	___	2
Fairly easy	___	3
Very easy	___	4

5. How alert do you feel during the first half hour after having woken in the mornings?

Not at all alert	___	1
Slightly alert	___	2
Fairly alert	___	3
Very alert	___	4

6. How is your appetite during the first half-hour after having woken in the mornings?

Very poor	___	1
Fairly poor	___	2
Fairly good	___	3
Very good	___	4

7. During the first half-hour after having woken in the morning how tired do you feel?

Very tired	___	1
Fairly tired	___	2
Fairly refreshed	___	3
Very refreshed	___	4

8. When you have no commitments the next day, at what time do you go to bed compared to your usual bedtime?

Seldom or never later	___	4
Less than one hour later	___	3
1-2 hours later	___	2
More than two hours later	___	1

9. You have decided to engage in some physical exercise. A friend suggests that you do this one hour twice a week and the best time for him is between 7.0-8.0 AM. Bearing in mind nothing else but your own "feeling best" rhythm How do you think you would perform?

Would be on good form	___	4
Would be on reasonable form	___	3
Would find it difficult	___	2
Would find it very difficult	___	1

10. At what time in the evening do you feel tired and as a result in need of sleep?

__:__ (scale in original)

20:00-21:00 = 5
21:00-22:15 = 4
22:15-00:45 = 3
00:45-02:00 = 2
02:00-03:00 = 1

11. You wish to be at your peak performance for a test which you know is going to be mentally exhausting and lasting for two hours. You are entirely free to plan your day and considering only your "feel best" rhythm which ONE of the four testing times would you choose?

08:00 – 10:00	___	6
11:00 – 13:00	___	4
15:00 – 17:00	___	2
19:00 – 21:00	___	0

12. If you went to bed at 23:00 at what level of tiredness would you be?

Not at all tired	___	0
A little tired	___	2
Fairly tired	___	3
Very tired	___	5

13. For some reason you have gone to bed several hours later then usual, but there is no need to get up at any particular time the next morning. Which ONE of the following events are you most likely to experience?

Will wake up at usual time and will NOT fall asleep	___	4
Will wake up at usual time and will dose thereafter	___	3
Will wake up at usual time but will fall asleep again	___	2
Will NOT wake up until later than usual	___	1

14. One night you have to remain awake between 04:00 – 06:00 in order to carry out a night watch. You have no commitments the next day. Which ONE of the following alternatives will suit you best?

Would NOT go to bed until watch was over	___	1
Would take a nap before and sleep after	___	2
Would take a good sleep before and nap after	___	3
Would take ALL sleep before watch	___	4

15. You have to do two hours of hard physical work. You are entirely free to plan your day and considering only your own "feeling best" rhythm which ONE of the following times would you choose?

08:00 – 10:00	___	4
11:00 – 13:00	___	3
15:00 – 17:00	___	2
19:00 – 21:00	___	1

16. You have decided to engage in hard physical exercise. A friend suggests that you do this for one hour twice a week and the best time for him is between 22:00 – 23:00. Bearing in mind nothing else but your own "feeling best" rhythm how well do you think you would perform?

Would be on good form	___	1
Would be on reasonable form	___	2
Would find it difficult	___	3
Would find it very difficult	___	4

17. Suppose that you can choose your own work hours. Assume that you worked a FIVE hour day (including breaks) and that your job was interesting and paid by results. Which FIVE CONSECTIVE HOURS would you select?

0 1 2 3 4 5 6 7 8 9 10 11 12 13 14 15 16 17 18 19 20 21 22 23 0

Midnight Noon Midnight

0-3 = 1
4-7 = 5
8 = 4
9-13 = 3
14-16 = 2
17-0 =1

18. At what point of the day do you think that you reach your "feeling best" peak?

0 1 2 3 4 5 6 7 8 9 10 11 12 13 14 15 16 17 18 19 20 21 22 23 0

Midnight Noon Midnight

0-4 = 1
5-7 = 5
8-9 = 4
10–16 = 3
17–21 = 2
22-0 = 1

19. One hears about "morning" and "evening" types of people. Which ONE of these types do you consider yourself to be?

Definitely a "morning" type	___	6
Rather more a "morning" than an "evening" type	___	4
Rather more an "evening" than a "morning" type	___	2
Definitely an "evening" type	___	0

Participant ID: _____ CONDITION: _____ DATE: _____ TIME: _____

For each of the following personal attributes, indicate which description best describes how you feel:

1: *Very slightly / not al all* **2:** *A little* **3:** *Moderately* **4:** *Quite a bit* **5:** *Extremely*

- _____ Interested
- _____ Distressed
- _____ Excited
- _____ Upset
- _____ Strong
- _____ Guilty
- _____ Scared
- _____ Hostile
- _____ Enthusiastic
- _____ Proud
- _____ Irritable
- _____ Alert
- _____ Ashamed
- _____ Inspired
- _____ Nervous
- _____ Angry
- _____ Determined
- _____ Attentive
- _____ Jittery
- _____ Sad
- _____ Afraid
- _____ Happy
- _____ Active

APPENDIX XII: PITTSBURGH SLEEP QUALITY INDEX (PSQI)

ID: _____ DATE _____

Pittsburgh Sleep Quality Index (PSQI)

Instructions: The following questions relate to your usual sleep habits during the past month ***only***. Your answers should indicate the most accurate reply for the *majority* of days and nights in the past month. Please answer all questions.

	Not during the past month	Once a week	Twice a week	Three times a week or more
1. During the past month, how often have you had trouble sleeping because you…				
a. cannot get to sleep within 30 minutes	❑	❑	❑	❑
b. wake up in the middle of the night or early morning	❑	❑	❑	❑
c. have to get up to use the bathroom	❑	❑	❑	❑
d. cannot breathe comfortably	❑	❑	❑	❑
e. cough or snore loudly	❑	❑	❑	❑
f. feel too cold	❑	❑	❑	❑
g. feel too hot	❑	❑	❑	❑
h. have bad dreams	❑	❑	❑	❑
i. have pain	❑	❑	❑	❑
j. other reason(s) for poor sleep, please describe here: _____ _____	❑	❑	❑	❑
2. During the past month, how often have you taken medicine (either prescription or "over the counter") to help you sleep?	❑	❑	❑	❑
3. During the past month, how often have you had trouble staying awake while driving, eating meals, or engaging in social activity?	❑	❑	❑	❑

APPENDIX XII: PITTSBURGH SLEEP QUALITY INDEX (PSQI)

4. During the past month, how would you rate your sleep quality overall?

Very Good	**Fairly Good**	**Fairly Bad**	**Very Bad**
❑	❑	❑	❑

5. During the past month, how much of a problem has it been for you to keep up enough enthusiasm to get things done?

No problem at all	**Only a very slight problem**	**Somewhat of a problem**	**A very big problem**
❑	❑	❑	❑

6. During the past month:

a) What time have you usually gone to bed at night? **USUAL BED TIME** _____

b) How long (in minutes) has it usually taken you to fall asleep each night? **NUMBER OF MINUTES** _____

c) When have you usually gotten up in the morning? **USUAL WAKE UP TIME** _____

d) How many hours of *actual sleep* did you get at night? **(This may be different than the number of hours you spend in bed.)** **HOURS OF SLEEP PER NIGHT** _____

7. Do you have a bed partner or roommate?

No bed partner or roommate	**Partner/roommate in another room**	**Partner in same room, different bed**	**Partner in same bed**
❑	❑	❑	❑

APPENDIX XII: PITTSBURGH SLEEP QUALITY INDEX (PSQI)

8. If you have a roommate or bed partner, ask him/her how often in the past month you have had....	Not during the past month	Once a week	Twice a week	Three times a week or more
a. loud snoring	❑	❑	❑	❑
b. long pauses between breaths while asleep	❑	❑	❑	❑
c. leg(s) twitching or jerking while you sleep	❑	❑	❑	❑
d. episodes of disorientation or confusion during sleep	❑	❑	❑	❑
e. other reasons for poor sleep, please describe here: _____ _____	❑	❑	❑	❑

Appendix I: Health Screening form

Screening Questionnaire

"I'd like to ask you some questions about your physical and mental health, your sleep patterns, medications you might be taking, and your use of drugs and alcohol. All information you provide here will be confidential. It's important that you be completely honest so that we can correctly determine whether it is safe and appropriate for you to participate in this study."

Date of Birth:

Phone No:

Gender:

Are you left or right handed?_____

Are you currently taking any prescription or over-the-counter medications?_____

Do you currently have any medical problems? (allergies)_____

Do you have any past history of substance abuse? _____

Have you ever been diagnosed with a mental illness? _____

Have you ever experience a head injury? _____

Have you ever had a psychotic episode, suicidal tendency, or major depression?_____

Have you ever been diagnosed with or treated for elevated anxiety?_____

Have you ever been treated with antidepressants? _____

Do you have normal or corrected to normal vision? _____

Have you ever been diagnosed with or treated for claustrophobia? _____

Have you traveled across time zones in the past month, if so where? _____

How often do you consume caffeine and how much do you consume? _____

Have you worked on night rotating shifts within the last year? _____

Have you ever been diagnosed with or treated for a sleep problem? _____

When do you usually go to bed and get up? Bedtime _____ Rise time _____

In an average week, how often do either of these times differ by more than 2 hours? _____

Do you fall asleep easily?_____

On average, how long does it take you to fall asleep?_____

How deeply do you sleep? (light, medium, deep)

Do you usually feel well rested? _____

How many times during the night do you wake up?_____

Do you normally have trouble falling back asleep?_____

How many hours do you usually sleep per night?_____

Have you ever sought help for a sleep disorder?_____

Have you ever experienced any of the following during your sleep?: Snoring that disturbs others--Choking--Sleep walking--Stop breathing--Gasping--Using the bathroom often--Coughing fits--Grinding or clenching teeth--Tightness in chest--Sleep through alarms--Leg twitches or kicks. _____
If Yes, please state which_____

Do you have any dietary restrictions (e.g. vegan, vegetarian or other restricted diet)? _____

Do you have any food allergies and if so what are they? _____

Participant ID: _____ DATE: _____ TIME: _____

STAI-TRAIT

A number of statements which people have used to describe themselves are given below. Read each statement and then write down the appropriate number to the right of the statement to indicate how you **GENERALLY** feel. Do not spend too much time on any one statement but give the answer which seems to describe how you GENERALLY FEEL. Answer each statement using the following scale.

1 = Not at all **2 = Somewhat** **3 = Moderately so** **4 = Very much so**

(1 to 4)

1.	I feel pleasant.	
2.	I feel nervous and restless.	
3.	I feel satisfied with myself.	
4.	I wish I could be as happy as others seem to be.	
5.	I feel like a failure.	
6.	I feel rested.	
7.	I am “calm, cool and collected”.	
8.	I feel that difficulties are piling up so that I cannot overcome them.	
9.	I worry too much over something that really doesn’t matter.	
10.	I am happy.	
11.	I have disturbing thoughts.	
12.	I lack self-confidence.	
13.	I feel secure.	
14.	I make decisions easily.	
15.	I feel inadequate.	
16.	I am content.	
17.	Some unimportant thought runs through my mind and bothers me.	
18.	I take disappointments so keenly that I can’t put them out of my mind	
19.	I am a steady person.	
20.	I get in a state of tension or turmoil as I think over my recent concerns and interests.	

Participant ID: _____ DATE: _____ TIME: _____

STAI-STATE

A number of statements which people have used to describe themselves are given below. Read each statement and then write down the appropriate number to the right of the statement to indicate how you feel RIGHT NOW, that is, AT THIS MOMENT. Answer each statement using the following scale.

1 = Not at all **2 = Somewhat** **3 = Moderately so** **4 = Very much so**

(1 to 4)

1.	I feel calm.	
2.	I feel secure.	
3.	I am tense.	
4.	I feel strained.	
5.	I feel at ease.	
6.	I feel upset.	
7.	I am presently worrying over possible misfortunes.	
8.	I feel that difficulties are piling up so that I cannot overcome them.	
9.	I feel satisfied.	
10.	I feel comfortable.	
11.	I feel self-confident.	
12.	I feel nervous.	
13.	I am jittery.	
14.	I feel indecisive.	
15.	I am relaxed.	
16.	I feel content.	
17.	I am worried.	
18.	I feel confused.	
19.	I feel steady.	
20.	I feel pleasant.	

PARTICIPANT ID: _____ DATE: _____

STANFORD SLEEPINESS SCALE

Choose the number of the description that best fits your current state:

1 feeling active and vital; alert; wide awake
2 functioning at a high level, but not at peak; able to concentrate
3 relaxed; awake; not at full alertness; responsive
4 a little foggy, not at peak; let down
5 fogginess; beginning to lose interest in remaining awake; slowed down
6 sleepiness; prefer to be lying down; fighting sleep, woozy
7 almost in reverie; sleep onset soon; lost struggle to remain awake
X asleep

References

Achard, S. S., Salvador, R. R., Whitcher, B. B., Suckling, J. J., & Bullmore, E. E. (2006, January). A resilient, low-frequency, small-world human brain functional network with highly connected association cortical hubs. *Audio, Transactions of the IRE Professional Group on*, *26*(1), 63–72.

Adrien, J. (2002, October). Neurobiological bases for the relation between sleep and depression. *Sleep Medicine Reviews*, *6*(5), 341–351.

Aeschbach, D., & Borbély, A. (1993, June). All-night dynamics of the human sleep EEG. *Journal of Sleep Research*, *2*(2), 70–81.

Allen, P. J., Josephs, O., & Turner, R. (2000, August). A Method for Removing Imaging Artifact from Continuous EEG Recorded during Functional MRI. *NeuroImage*, *12*(2), 230–239.

Allen, P. J., Polizzi, G., Krakow, K., Fish, D. R., & Lemieux, L. (1998, October). Identification of EEG events in the MR scanner: the problem of pulse artifact and a method for its subtraction. *NeuroImage*, *8*(3), 229–239.

Amzica, F., & Steriade, M. (1997, October). The K-complex: its slow (. *Neurology*, *49*(4), 952–959.

Anderer, P., Klösch, G., Gruber, G., Trenker, E., Pascual-Marqui, R. D., Zeitlhofer, J., ... Saletu, B. (2001). Low-resolution brain electromagnetic tomography revealed simultaneously active frontal and parietal sleep spindle sources in the human cortex. *Neuroscience*, *103*(3), 581–592.

Andrade, K. C., Spoormaker, V. I., Dresler, M., Wehrle, R., Holsboer, F., Samann, P. G., & Czisch, M. (2011). Sleep spindles and hippocampal functional connectivity in human NREM sleep. *The Journal of Neuroscience*, *31*(28), 10331–10339.

Angelakis, E., Liouta, E., Andreadis, N., Leonardos, A., Ktonas, P., Stavrinou, L. C., ... Sakas, D. E. (2013, January). Neuroscience Letters. *Neuroscience Letters*, *533*, 39–43.

Antal, A., Bikson, M., Datta, A., Lafon, B., Dechent, P., Parra, L. C., & Paulus, W. (2012, October). Imaging artifacts induced by electrical stimulation during conventional fMRI of the brain. *NeuroImage*.

Antal, A., Boros, K., Poreisz, C., Chaieb, L., Terney, D., & Paulus, W. (2008, April). Comparatively weak after-effects of transcranial alternating current stimulation (tACS) on cortical excitability in humans. *Brain Stimulation*, *1*(2), 97–105.

Antal, A., Paulus, W., & Nitsche, M. A. (2011). Electrical stimulation and visual network plasticity. *Restorative Neurology and Neuroscience*, *29*(6), 365–374.

Arfanakis, K., Cordes, D., Haughton, V. M., Moritz, C. H., Quigley, M. A., & Meyerand, M. E. (2000, October). Combining independent component analysis and correlation analysis to probe interregional connectivity in fMRI task activation datasets. *Magnetic resonance imaging*, *18*(8), 921–930.

Aserinsky, E., & Kleitman, N. (1953, September). Regularly occurring periods of eye motility, and concomitant phenomena, during sleep. *Science*, *118*(3062), 273–274.

Barnes, K. A., Cohen, A. L., Power, J. D., Nelson, S. M., Dosenbach, Y. B. L., Miezin, F. M., ... Schlaggar, B. L. (2010). Identifying Basal Ganglia divisions in individuals using resting-state functional connectivity MRI. *Frontiers in System Neuroscience*, *4*, 18.

Bassett, D. S. D., & Bullmore, E. E. (2006, December). Small-world brain networks. *Neuroscientist*, *12*(6), 512–523.

Battaglia, F. P., Sutherland, G. R., & McNaughton, B. L. (2004, November). Hippocampal sharp wave bursts coincide with neocortical "up-state" transitions. *Learning & Memory*, *11*(6), 697–704.

Baudewig, J., Nitsche, M. A., & Paulus, W. (2001). Regional modulation of BOLD MRI responses to human sensorimotor activation by transcranial direct current stimulation. *Magnetic Resonance in ....*

Berger, H. (1929). Über das elektrenkephalogramm des menschen. *European Archives of Psychiatry and Clinical ....*

Berger, R. (1961, September). Tonus of Extrinsic Laryngeal Muscles during Sleep and Dreaming. *Science*, *134*(3482), 840.

Bergmann, T. O., Mölle, M., Diedrichs, J., Born, J., & Siebner, H. R. (2012, February). Sleep spindle-related reactivation of category-specific cortical regions after learning face-scene associations. *NeuroImage*, *59*(3), 2733–2742.

Bikson, M., Datta, A., & Elwassif, M. (2009, June). Establishing safety limits for transcranial direct current stimulation. *Clinical Neurophysiology*, *120*(6), 1033–1034.

Bikson, M., Rahman, A., & Datta, A. (2012, July). Computational models of transcranial direct current stimulation. *Clinical EEG and neuroscience : official journal of the EEG and Clinical Neuroscience Society (ENCS)*, *43*(3), 176–183.

Birchler-Pedross, A., Schröder, C. M., Münch, M., Knoblauch, V., Blatter, K., Schnitzler-Sack, C., ... Cajochen, C. (2009, June). Subjective well-being is modulated by circadian phase, sleep pressure, age, and gender. *Journal of biological rhythms*, *24*(3), 232–242.

Bódizs, R., Sverteczki, M., Lázár, A. S., & Halász, P. (2005, March). Human parahippocampal activity: non-REM and REM elements in wake-sleep transition. *Brain research bulletin*, *65*(2), 169–176.

Bonnet, M. H., & Arand, D. L. (1997, May). Heart rate variability: sleep stage, time of night, and arousal influences. *Electroencephalography and Clinical Neurophysiology*, *102*(5), 390–396.

Boroojerdi, B., Prager, A., Muellbacher, W., & Cohen, L. G. (2000, April). Reduction of human visual cortex excitability using 1-Hz transcranial magnetic stimulation. *Neurology*, *54*(7), 1529–1531.

Boucousis, S. M., Beers, C. A., Cunningham, C. J. B., Gaxiola-Valdez, I., Pittman, D. J., Goodyear, B. G., & Federico, P. (2012, November). Feasibility of an intracranial EEG-fMRI protocol at 3T: risk assessment and image quality. *NeuroImage*, *63*(3), 1237–1248.

Brading, A. (1999). The autonomic nervous system and its effectors.

Brignani, D., Ruzzoli, M., Mauri, P., & Miniussi, C. (2013, February). Is Transcranial Alternating Current Stimulation Effective in Modulating Brain Oscillations? *PLoS*

ONE, *8*(2), e56589.

Bullmore, E., & Sporns, O. (2009, February). Complex brain networks: graph theoretical analysis of structural and functional systems. *Nature Reviews Neuroscience*, *10*(3), 186–198.

Busek, P., Vanková, J., Opavský, J., Salinger, J., & Nevsímalová, S. (2005). Spectral analysis of the heart rate variability in sleep. *Physiological research / Academia Scientiarum Bohemoslovaca*, *54*(4), 369–376.

Buzsáki, G. (1996, March). The hippocampo-neocortical dialogue. *Cerebral cortex (New York, N.Y. : 1991)*, *6*(2), 81–92.

Cantero, J. L., Atienza, M., Stickgold, R., Kahana, M. J., Madsen, J. R., & Kocsis, B. (2003, November). Sleep-dependent theta oscillations in the human hippocampus and neocortex. *Journal of Neuroscience*, *23*(34), 10897–10903.

Carskadon, M. A. (2000). Monitoring and staging human sleep. *... of sleep ...*.

Cauda, F., D'Agata, F., Sacco, K., Duca, S., Geminiani, G., & Vercelli, A. (2011, March). Functional connectivity of the insula in the resting brain. *NeuroImage*, *55*(1), 8–23.

Chaieb, L., Paulus, W., & Antal, A. (2011). Evaluating Aftereffects of Short-Duration Transcranial Random Noise Stimulation on Cortical Excitability. *Neural Plasticity*, *2011*, 1–5.

Chersi, F., Ferrari, P. F., & Fogassi, L. (2011). Neuronal chains for actions in the parietal lobe: a computational model. *PLoS ONE*, *6*(11), e27652.

Chikama, M., McFarland, N. R., Amaral, D. G., & Haber, S. N. (1997, December). Insular cortical projections to functional regions of the striatum correlate with cortical cytoarchitectonic organization in the primate. *The Journal of Neuroscience*, *17*(24), 9686–9705.

Corsi-Cabrera, M., Guevara, M. A., & del Río-Portilla, Y. (2008, October). Brain activity and temporal coupling related to eye movements during REM sleep: EEG and MEG results. *Brain Research*, *1235*, 82–91.

Craig, A. D. (2009, January). How do you feel–now? The anterior insula and human awareness. *Nature Reviews Neuroscience*, *10*(1), 59–70.

Crawford, J. R., & Henry, J. D. (2004, August). The Positive and Negative Affect

Schedule (PANAS): Construct validity, measurement properties and normative data in a large non-clinical sample. , 1–22.

Critchley, H. D. (2009, August). Psychophysiology of neural, cognitive and affective integration: fMRI and autonomic indicants. *International journal of psychophysiology : official journal of the International Organization of Psychophysiology*, *73*(2), 88–94.

Critchley, H. D., Wiens, S., Rotshtein, P., Öhman, A., & Dolan, R. J. (2004, January). Neural systems supporting interoceptive awareness. *Nature neuroscience*, *7*(2), 189–195.

Damasio, A. (2003, October). Feelings of emotion and the self. *Annals of the New York Academy of Sciences*, *1001*, 253–261.

Damasio, A., Grabowski, T., Bechara, A., Damasio, H., Ponto, L., Parvizi, J., & Hichwa, R. (2000, October). Subcortical and cortical brain activity during the feeling of self-generated emotions. *Nature neuroscience*, *3*(10), 1049–1056.

Dang-Vu, T. T., Schabus, M., Desseilles, M., Albouy, G., Boly, M., Darsaud, A., ... Maquet, P. (2008, September). Spontaneous neural activity during human slow wave sleep. *PNAS*, *105*(39), 15160–15165.

Datta, S. (2000, November). Avoidance task training potentiates phasic pontine-wave density in the rat: A mechanism for sleep-dependent plasticity. *Journal of Neuroscience*, *20*(22), 8607–8613.

Datta, S., Mavanji, V., Ulloor, J., & Patterson, E. H. (2004, February). Activation of phasic pontine-wave generator prevents rapid eye movement sleep deprivation-induced learning impairment in the rat: a mechanism for sleep-dependent plasticity. *Journal of Neuroscience*, *24*(6), 1416–1427.

De Gennaro, L., & Ferrara, M. (2003, October). Sleep spindles: an overview. *Sleep Medicine Reviews*, *7*(5), 423–440.

De Havas, J. A., Parimal, S., Soon, C. S., & Chee, M. W. L. (2012, January). Sleep deprivation reduces default mode network connectivity and anti-correlation during rest and task performance. *NeuroImage*, *59*(2), 1745–1751.

De Hert, M., van Eyck, D., & De Nayer, A. (2006, March). Metabolic abnormalities associated with second generation antipsychotics: fact or fiction? Development of

guidelines for screening and monitoring. *International clinical psychopharmacology*, *21 Suppl 2*, S11–5.

Diekelmann, S., & Born, J. (2010, March). Slow-wave sleep takes the leading role in memory reorganization. *Nature Reviews Neuroscience*, *11*(3), 218–218.

Diekelmann, S., Born, J., & Wagner, U. (2010, April). Sleep enhances false memories depending on general memory performance. *Behavioural Brain Research*, *208*(2), 425–429.

Diekelmann, S., Wilhelm, I., & Born, J. (2009, October). The whats and whens of sleep-dependent memory consolidation. *Sleep Medicine Reviews*, *13*(5), 309–321.

Di Martino, A., Scheres, A., Margulies, D. S., Kelly, A. M. C., Uddin, L. Q., Shehzad, Z., ... Milham, M. P. (2008, March). Functional Connectivity of Human Striatum: A Resting State fMRI Study. *Cerebral Cortex*, *18*(12), 2735–2747.

Dimitriadis, S. I., Laskaris, N. A., Del Rio-Portilla, Y., & Koudounis, G. C. (2009, September). Characterizing dynamic functional connectivity across sleep stages from EEG. *Brain Topography*, *22*(2), 119–133.

Dinges, D. F., Pack, F., Williams, K., & Gillen, K. A. (1997). Cumulative sleepiness, mood disturbance and psychomotor vigilance performance decrements during aweek of sleep restricted to 4-5 hours per night. *Sleep: Journal of ....*

Donner, T. H., & Siegel, M. (2011, May). A framework for local cortical oscillation patterns. *Trends in Cognitive Sciences*, *15*(5), 191–199.

Duncan, J., & Owen, A. M. (2000, October). Common regions of the human frontal lobe recruited by diverse cognitive demands. *Trends in Neurosciences*, *23*(10), 475–483.

Edwards, D., Cortes, M., Datta, A., & Minhas, P. (2013). Physiological and modeling evidence for focal transcranial electrical brain stimulation in humans: a basis for high-definition tDCS. *NeuroImage*.

Ekman, P. P., Levenson, R. W. R., & Friesen, W. V. W. (1983, September). Autonomic nervous system activity distinguishes among emotions. *Science*, *221*(4616), 1208–1210.

Elsenbruch, S., Harnish, M. J., & Orr, W. C. (1999, December). Heart rate variability during waking and sleep in healthy males and females. *Sleep*, *22*(8), 1067–1071.

Factor, S. A., McAlarney, T., Sanchez-Ramos, J. R., & Weiner, W. J. (1990). Sleep disorders and sleep effect in Parkinson's disease. *Movement disorders : official journal of the Movement Disorder Society*, *5*(4), 280–285.

Faria, P., Hallett, M., & Miranda, P. C. (2011, November). A finite element analysis of the effect of electrode area and inter-electrode distance on the spatial distribution of the current density in tDCS. *Journal of Neural Engineering*, *8*(6), 066017.

Fedorov, A., Chibisova, Y., Szymaszek, A., Alexandrov, M., Gall, C., & Sabel, B. A. (2010). Non-invasive alternating current stimulation induces recovery from stroke. *Restorative Neurology and Neuroscience*, *28*(6), 825–833.

Fedorov, A., Jobke, S., Bersnev, V., Chibisova, A., Chibisova, Y., Gall, C., & Sabel, B. A. (2011, October). Restoration of vision after optic nerve lesions with noninvasive transorbital alternating current stimulation: a clinical observational study. *Brain Stimulation*, *4*(4), 189–201.

Feinberg, I., & Floyd, T. C. (1979, May). Systematic trends across the night in human sleep cycles. *Psychophysiology*, *16*(3), 283–291.

Ferri, R., Rundo, F., Bruni, O., Terzano, M. G., & Stam, C. J. (2007, February). Small-world network organization of functional connectivity of EEG slow-wave activity during sleep. *Clinical neurophysiology : official journal of the International Federation of Clinical Neurophysiology*, *118*(2), 449–456.

Fox, M. D., & Raichle, M. E. (2007, September). Spontaneous fluctuations in brain activity observed with functional magnetic resonance imaging. *Nature Reviews Neuroscience*, *8*(9), 700–711.

Franzen, P., Buysse, D., Dahl, R. E., Thompson, W., & Siegle, G. J. (2009, March). Sleep deprivation alters pupillary reactivity to emotional stimuli in healthy young adults. *Biological Psychology*, *80*(3), 300–305.

Franzen, P., Siegle, G. J., & Buysse, D. (2008, March). Relationships between affect, vigilance, and sleepiness following sleep deprivation. *Journal of Sleep Research*, *17*(1), 34–41.

Fröhlich, F., & McCormick, D. A. (2010, July). Endogenous electric fields may guide neocortical network activity. *Neuron*, *67*(1), 129–143.

Gais, S., Köster, S., Sprenger, A., Bethke, J., Heide, W., & Kimmig, H. (2008, November). Sleep is required for improving reaction times after training on a procedural visuo-motor task. *Neurobiology of Learning and Memory*, *90*(4), 610–615.

Geyer, S., Luppino, G., Ekamp, H., & Zilles, K. (2005, September). The macaque inferior parietal lobule: cytoarchitecture and distribution pattern of serotonin 5-HT1A binding sites. *Anatomy and Embryology*, *210*(5-6), 353–362.

Gillin, J. C., Buchsbaum, M., Wu, J., Clark, C., & Bunney, W. (2001). Sleep deprivation as a model experimental antidepressant treatment: findings from functional brain imaging. *Depression and anxiety*, *14*(1), 37–49.

Gujar, N., McDonald, S. A., Nishida, M., & Walker, M. P. (2010, December). A Role for REM Sleep in Recalibrating the Sensitivity of the Human Brain to Specific Emotions. *Cerebral Cortex*, *21*(1), 115–123.

Gujar, N., Yoo, S. S., Hu, P., & Walker, M. P. (2011, March). Sleep Deprivation Amplifies Reactivity of Brain Reward Networks, Biasing the Appraisal of Positive Emotional Experiences. *Journal of Neuroscience*, *31*(12), 4466–4474.

Hall, M., Vasko, R., Buysse, D., Ombao, H., Chen, Q., Cashmere, J. D., ... Thayer, J. F. (2004, January). Acute stress affects heart rate variability during sleep. *Psychosomatic Medicine*, *66*(1), 56–62.

Harvey, A. G., Jones, C., & Schmidt, D. A. (2003, May). Sleep and posttraumatic stress disorder: a review. *Clinical Psychology Review*, *23*(3), 377–407.

Hayden, B. Y., & Gallant, J. L. (2013). Working memory and decision processes in visual area v4. *Front Neurosci*, *7*, 18.

Hegde, P., Jayakrishnan, H. R., Chattarji, S., Kutty, B. M., & Laxmi, T. R. (2011, March). Chronic stress-induced changes in REM sleep on θ oscillations in the rat hippocampus and amygdala. *Brain Research*, *1382*, 155–164.

Herrmann, C. S., Neuling, T., Rach, S., & Strüber, D. (2012, August). Modulation of EEG oscillations via transcranial alternating current stimulation. *Biomedizinische Technik. Biomedical engineering*.

Hobson, J. A., & Pace-Schott, E. F. (2002, September). The cognitive neuroscience of sleep: neuronal systems, consciousness and learning. *Nature Reviews Neuroscience*, *3*(9), 679–693.

Hobson, J. A., & Steriade, M. (1986). Neuronal basis of behavioral state control. *Comprehensive Physiology*.

Hofle, N., Paus, T., Reutens, D., Fiset, P., Gotman, J., Evans, A. C., & Jones, B. E. (1997, June). Regional cerebral blood flow changes as a function of delta and spindle activity during slow wave sleep in humans. *The Journal of Neuroscience*, *17*(12), 4800–4808.

Horne, J. A. (1985). Sleep function, with particular reference to sleep deprivation. *Annals of clinical research*, *17*(5), 199–208.

Horovitz, S. G., Braun, A. R., Carr, W. S., Picchioni, D., Balkin, T. J., Fukunaga, M., & Duyn, J. H. (2009a, July). Decoupling of the brain's default mode network during deep sleep. *PNAS*, *106*(27), 11376–11381.

Horovitz, S. G., Braun, A. R., Carr, W. S., Picchioni, D., Balkin, T. J., Fukunaga, M., & Duyn, J. H. (2009b, July). Decoupling of the brain's default mode network during deep sleep. *PNAS*, *106*(27), 11376–11381.

Horovitz, S. G., Fukunaga, M., de Zwart, J. A., van Gelderen, P., Fulton, S. C., Balkin, T. J., & Duyn, J. H. (2008, June). Low frequency BOLD fluctuations during resting wakefulness and light sleep: A simultaneous EEG-fMRI study. *Human Brain Mapping*, *29*(6), 671–682.

Hu, P., Stylos-Allan, M., & Walker, M. P. (2006, October). Sleep Facilitates Consolidation of Emotional Declarative Memory. *Psychological Science*, *17*(10), 891–898.

Iber, C. (2007). *The AASM Manual for the Scoring of Sleep and Associated Events.*

Ioannides, A. A., Kostopoulos, G. K., Liu, L., & Fenwick, P. B. C. (2009, January). MEG identifies dorsal medial brain activations during sleep. *NeuroImage*, *44*(2), 455–468.

Ipata, A. E., Gee, A. L., & Goldberg, M. E. (2012, October). Feature attention evokes task-specific pattern selectivity in V4 neurons. *PNAS*, *109*(42), 16778–16785.

Irwin, M. R. (2006, January). Association Between Nocturnal Vagal Tone and Sleep Depth, Sleep Quality, and Fatigue in Alcohol Dependence. *Psychosomatic Medicine*, *68*(1), 159–166.

Isomura, Y., Sirota, A., Ozen, S., Montgomery, S., Mizuseki, K., Henze, D. A., & Buzsáki, G. (2006, December). Integration and segregation of activity in

entorhinal-hippocampal subregions by neocortical slow oscillations. *Neuron*, *52*(5), 871–882.

Itier, R. J., & Batty, M. (2009, June). Neural bases of eye and gaze processing: the core of social cognition. *Neuroscience and biobehavioral reviews*, *33*(6), 843–863.

James, W. (1894). UCL Single Sign-on. *Psychological Review*.

Jensen, A. L., & Durand, D. M. (2007, June). Suppression of axonal conduction by sinusoidal stimulation in rat hippocampus in vitro. *Journal of Neural Engineering*, *4*(2), 1–16.

Johnson, J. D. (2006, January). The conversational brain: Fronto-hippocampal interaction and disconnection. *Medical Hypotheses*, *67*(4), 759–764.

Jones, B. E. (2005, November). From waking to sleeping: neuronal and chemical substrates. *Trends in pharmacological sciences*, *26*(11), 578–586.

Kähkönen, S., Kesäniemi, M., Nikouline, V. V., Karhu, J., Ollikainen, M., Holi, M., & Ilmoniemi, R. J. (2001, August). Ethanol modulates cortical activity: direct evidence with combined TMS and EEG. *NeuroImage*, *14*(2), 322–328.

Kanai, R., Chaieb, L., Antal, A., Walsh, V., & Paulus, W. (2008, December). Frequency-dependent electrical stimulation of the visual cortex. *Current biology : CB*, *18*(23), 1839–1843.

Kanai, R., Paulus, W., & Walsh, V. (2010, September). Transcranial alternating current stimulation (tACS) modulates cortical excitability as assessed by TMS-induced phosphene thresholds. *Clinical Neurophysiology*, *121*(9), 1551–1554.

Kar, K., & Krekelberg, B. (2012, October). Transcranial electrical stimulation over visual cortex evokes phosphenes with a retinal origin. *Journal of Neurophysiology*, *108*(8), 2173–2178.

Kaufmann, C., Wehrle, R., Wetter, T. C., Holsboer, F., Auer, D. P., Pollmächer, T., & Czisch, M. (2006, March). Brain activation and hypothalamic functional connectivity during human non-rapid eye movement sleep: an EEG/fMRI study. *Brain : a journal of neurology*, *129*(Pt 3), 655–667.

Koike, T., Kan, S., Misaki, M., & Miyauchi, S. (2011, April). Connectivity pattern changes in default-mode network with deep non-REM and REM sleep. *Neuroscience research*, *69*(4), 322–330.

Kubota, Y., Takasu, N. N., Horita, S., Kondo, M., Shimizu, M., Okada, T., ... Toichi, M. (2011, May). Dorsolateral prefrontal cortical oxygenation during REM sleep in humans. *Brain Research*, *1389*, 83–92.

Laczó, B., Antal, A., Niebergall, R., Treue, S., & Paulus, W. (2013, July). Transcranial alternating stimulation in a high gamma frequency range applied over V1 improves contrast perception but does not modulate spatial attention. *Brain Stimulation*, 1–8.

Larson-Prior, L. J., Zempel, J. M., Nolan, T. S., Prior, F. W., Snyder, A. Z., & Raichle, M. E. (2009, March). Cortical network functional connectivity in the descent to sleep. *PNAS*, *106*(11), 4489–4494.

Laufs, H., Walker, M. C., & Lund, T. E. (2007, May). 'Brain activation and hypothalamic functional connectivity during human non-rapid eye movement sleep: an EEG/fMRI study'–its limitations and an alternative approach. *Brain : a journal of neurology*, *130*(7), e75–e75.

Lazarus, M., Huang, Z.-L., Lu, J., Urade, Y., & Chen, J.-F. (2012, December). How do the basal ganglia regulate sleep-wake behavior? *Trends in Neurosciences*, *35*(12), 723–732.

Lee, L., Siebner, H. R., Rowe, J. B., & Rizzo, V. (2003). Acute remapping within the motor system induced by low-frequency repetitive transcranial magnetic stimulation. *The Journal of ....*

Libedinsky, C., Smith, D. V., Teng, C. S., Namburi, P., Chen, V. W., Huettel, S. A., & Chee, M. W. L. (2011). Sleep deprivation alters valuation signals in the ventromedial prefrontal cortex. *Frontiers in behavioral neuroscience*, *5*, 70.

Macey, P. M., Macey, K. E., Kumar, R., & Harper, R. M. (2004, May). A method for removal of global effects from fMRI time series. *NeuroImage*, *22*(1), 360–366.

Mahon, S., Vautrelle, N., Pezard, L., Slaght, S. J., Deniau, J.-M., Chouvet, G., & Charpier, S. (2006, November). Distinct patterns of striatal medium spiny neuron activity during the natural sleep-wake cycle. *Journal of Neuroscience*, *26*(48), 12587–12595.

Mander, B. A., Santhanam, S., Saletin, J. M., & Walker, M. P. (2011, March). Wake deterioration and sleep restoration of human learning. *Current Biology*, *21*(5),

R183–R184.

Maquet, P. (2000, September). Functional neuroimaging of normal human sleep by positron emission tomography. *Journal of Sleep Research*, *9*(3), 207–231.

Maquet, P., Degueldre, C., Delfiore, G., Aerts, J., Péters, J. M., Luxen, A., & Franck, G. (1997, April). Functional neuroanatomy of human slow wave sleep. *The Journal of Neuroscience*, *17*(8), 2807–2812.

Maquet, P., Laureys, S., Peigneux, P., Fuchs, S., Petiau, C., Phillips, C., ... Cleeremans, A. (2000, August). Experience-dependent changes in cerebral activation during human REM sleep. *Nature neuroscience*, *3*(8), 831–836.

Marrosu, F., Portas, C., Mascia, M. S., Casu, M. A., Fà, M., Giagheddu, M., ... Gessa, G. L. (1995, February). Microdialysis measurement of cortical and hippocampal acetylcholine release during sleep-wake cycle in freely moving cats. *Brain Research*, *671*(2), 329–332.

Marshall, L. (2004, November). Transcranial Direct Current Stimulation during Sleep Improves Declarative Memory. *Journal of Neuroscience*, *24*(44), 9985–9992.

Marshall, L., & Born, J. (2007, October). The contribution of sleep to hippocampus-dependent memory consolidation. *Trends in Cognitive Sciences*, *11*(10), 442–450.

Marshall, L., Helgadóttir, H., Mölle, M., & Born, J. (2006, November). Boosting slow oscillations during sleep potentiates memory. *Nature*, *444*(7119), 610–613.

Massimini, M. (2005, September). Breakdown of Cortical Effective Connectivity During Sleep. *Science*, *309*(5744), 2228–2232.

Massimini, M., Ferrarelli, F., Esser, S. K., Riedner, B. A., HUBER, R., MURPHY, M., ... Tononi, G. (2007, May). Triggering sleep slow waves by transcranial magnetic stimulation. *Proceedings of the National Academy of Sciences of the United States of America*, *104*(20), 8496–8501.

Massimini, M., Huber, R., Ferrarelli, F., & Hill, S. (2004). The sleep slow oscillation as a traveling wave. *The Journal of ....*

Massimini, M., Huber, R., Ferrarelli, F., Hill, S., & Tononi, G. (2004, August). The sleep slow oscillation as a traveling wave. *Journal of Neuroscience*, *24*(31), 6862–6870.

McCarley, R. (2007). Neurobiology of REM and NREM sleep. *Sleep Medicine*.

McCormick, D. A. (1989, June). Cholinergic and noradrenergic modulation of thalamocortical processing. *Trends in Neurosciences*, *12*(6), 215–221.

McGlinchey, E. L., Talbot, L. S., Chang, K.-H., Kaplan, K. A., Dahl, R. E., & Harvey, A. G. (2011, September). The effect of sleep deprivation on vocal expression of emotion in adolescents and adults. *Sleep*, *34*(9), 1233–1241.

McKenna, B. S., Dickinson, D. L., Orff, H. J., & Drummond, S. P. A. (2007, September). The effects of one night of sleep deprivation on known-risk and ambiguous-risk decisions. *Journal of Sleep Research*, *16*(3), 245–252.

Merton, P. A., & Morton, H. B. (1980, May). Stimulation of the cerebral cortex in the intact human subject. *Nature*, *285*(5762), 227.

Mesulam, M. (2009, April). Defining Neurocognitive Networks in the BOLD New World of Computed Connectivity. *Neuron*, *62*(1), 1–3.

Meyer, B. U., Diehl, R., Steinmetz, H., Britton, T. C., & Benecke, R. (1991). Magnetic stimuli applied over motor and visual cortex: influence of coil position and field polarity on motor responses, phosphenes, and eye movements. *Electroencephalography and clinical neurophysiology. Supplement*, *43*, 121–134.

Mink, J. W. (1996, November). The basal ganglia: focused selection and inhibition of competing motor programs. *Progress in Neurobiology*, *50*(4), 381–425.

Minkel, J., Htaik, O., Banks, S., & Dinges, D. (2011). Emotional expressiveness in sleep-deprived healthy adults. *Behavioral Sleep Medicine*, *9*(1), 5–14.

Miranda, P. C., Lomarev, M., & Hallett, M. (2006). Modeling the current distribution during transcranial direct current stimulation. *Clinical Neurophysiology*.

Moliadze, V., Atalay, D., Antal, A., & Paulus, W. (2012, October). Close to threshold transcranial electrical stimulation preferentially activates inhibitory networks before switching to excitation with higher intensities. *Brain Stimulation*, *5*(4), 505–511.

Mölle, M. (2006, March). Hippocampal Sharp Wave-Ripples Linked to Slow Oscillations in Rat Slow-Wave Sleep. *Journal of Neurophysiology*, *96*(1), 62–70.

Mölle, M., Marshall, L., Gais, S., & Born, J. (2002, December). Grouping of spindle activity during slow oscillations in human non-rapid eye movement sleep. *Journal of Neuroscience*, *22*(24), 10941–10947.

Moran, J., & Desimone, R. (1985). Selective attention gates visual processing in the extrastriate cortex. *Science*.

Morrison, A. R., Sanford, L. D., & Ross, R. J. (2000, November). The amygdala: a critical modulator of sensory influence on sleep. *Biological signals and receptors*, *9*(6), 283–296.

Moruzzi, G., & Magoun, H. W. (1949, November). Brain stem reticular formation and activation of the EEG. *Electroencephalography and Clinical Neurophysiology*, *1*(4), 455–473.

Motokawa, K., & Ebe, M. (1952, July). Selective Stimulation of Color Receptors with Alternating Currents. *Science*, *116*(3004), 92–94.

Muzur, A., Pace-Schott, E. F., & Hobson, J. A. (2002, November). The prefrontal cortex in sleep. *Trends in Cognitive Sciences*, *6*(11), 475–481.

Nambu, A. (2008, December). Seven problems on the basal ganglia. *Current opinion in neurobiology*, *18*(6), 595–604.

Nikulin, V. V., Kicić, D., Kähkönen, S., & Ilmoniemi, R. J. (2003, September). Modulation of electroencephalographic responses to transcranial magnetic stimulation: evidence for changes in cortical excitability related to movement. *The European journal of neuroscience*, *18*(5), 1206–1212.

Nir, Y., Staba, R. J., Andrillon, T., Vyazovskiy, V. V., Cirelli, C., Fried, I., & Tononi, G. (2011, April). Regional slow waves and spindles in human sleep. *Neuron*, *70*(1), 153–169.

Nitsche, M. A., Antal, A., Liebetanz, D., & Lang, N. (2008). Neuroplasticity induced by transcranial direct current stimulation. *... stimulation*.

Nitsche, M. A., Cohen, L. G., Wassermann, E. M., Priori, A., Lang, N., Antal, A., ... Pascual-Leone, A. (2008, July). Transcranial direct current stimulation: State of the art 2008. *Brain Stimulation*, *1*(3), 206–223.

Nitsche, M. A., Doemkes, S., Karakose, T., Antal, A., Liebetanz, D., Lang, N., ... Paulus, W. (2007, January). Shaping the Effects of Transcranial Direct Current Stimulation of the Human Motor Cortex. *Journal of Neurophysiology*, *97*(4), 3109–3117.

Nofzinger, E. A. (2005, March). Functional neuroimaging of sleep. *Seminars in neurology*, *25*(1), 9–18.

Nofzinger, E. A., Buysse, D. J., Miewald, J. M., Meltzer, C. C., Price, J. C., Sembrat, R. C., ... Moore, R. Y. (2002, May). Human regional cerebral glucose metabolism during non-rapid eye movement sleep in relation to waking. *Brain : a journal of neurology*, *125*(Pt 5), 1105–1115.

Ohayon, M. M., & Shapiro, C. M. (2000, November). Sleep disturbances and psychiatric disorders associated with posttraumatic stress disorder in the general population. *Comprehensive Psychiatry*, *41*(6), 469–478.

Ozen, S., Sirota, A., Belluscio, M. A., Anastassiou, C. A., Stark, E., Koch, C., & Buzsáki, G. (2010, August). Transcranial electric stimulation entrains cortical neuronal populations in rats. *Journal of Neuroscience*, *30*(34), 11476–11485.

Pace-Schott, E. F., & Hobson, J. A. (2002, August). The neurobiology of sleep: genetics, cellular physiology and subcortical networks. *Nature Reviews Neuroscience*, *3*(8), 591–605.

Paré, D., Collins, D. R., & Pelletier, J. G. (2002, July). Amygdala oscillations and the consolidation of emotional memories. *Trends in Cognitive Sciences*, *6*(7), 306–314.

Parent, A., & Hazrati, L. N. (1995, January). Functional anatomy of the basal ganglia. I. The cortico-basal ganglia-thalamo-cortical loop. *Brain research. Brain research reviews*, *20*(1), 91–127.

Paulus, W. (2010, July). On the difficulties of separating retinal from cortical origins of phosphenes when using transcranial alternating current stimulation (tACS). *Clinical Neurophysiology*, *121*(7), 987–991.

Payne, J. D., & Kensinger, E. A. (2011, June). Sleep Leads to Changes in the Emotional Memory Trace: Evidence from fMRI. *Journal of Cognitive Neuroscience*, *23*(6), 1285–1297.

Peigneux, P. (2003). Memory-related replay of neuronal networks during post-training sleep in humans: a different role for REM and non-REM sleep episodes?

Peigneux, P., Laureys, S., & Maquet, P. (2001). PET investigations of experience-dependant modifications during human REM sleep.

Pirulli, C., Fertonani, A., & Miniussi, C. (2013, July). The role of timing in the induction

of neuromodulation in perceptual learning by transcranial electric stimulation. *Brain Stimulation*, *6*(4), 683–689.

Poewe, W., & Högl, B. (2000, August). Parkinson's disease and sleep. *Current opinion in neurology*, *13*(4), 423–426.

Postuma, R. B. (2005, December). Basal Ganglia Functional Connectivity Based on a Meta-Analysis of 126 Positron Emission Tomography and Functional Magnetic Resonance Imaging Publications. *Cerebral Cortex*, *16*(10), 1508–1521.

Qiu, M.-H., Vetrivelan, R., Fuller, P. M., & Lu, J. (2010, February). Basal ganglia control of sleep-wake behavior and cortical activation. *European Journal of Neuroscience*, *31*(3), 499–507.

Raichle, M. E., MacLeod, A. M., & Snyder, A. Z. (2001). A default mode of brain function. In *Proceedings of the ....*

Raichle, M. E. M., & Snyder, A. Z. A. (2007, September). A default mode of brain function: a brief history of an evolving idea. *NeuroImage*, *37*(4), 1083–1089.

Rasch, B., & Born, J. (2013, April). About sleep's role in memory. *Physiological reviews*, *93*(2), 681–766.

Rauchs, G., Feyers, D., Landeau, B., Bastin, C., Luxen, A., Maquet, P., & Collette, F. (2011, February). Sleep contributes to the strengthening of some memories over others, depending on hippocampal activity at learning. *Journal of Neuroscience*, *31*(7), 2563–2568.

Rechtschaffen, A., & Kales, A. (1968a). A manual of standardized terminology, techniques and scoring system for sleep stages of human subjects.

Rechtschaffen, A., & Kales, A. (1968b). A manual of standardized terminology, techniques, and scoring systems for sleep stages of human subjects.

Robertson, E. M. (2005, July). Off-Line Learning and the Primary Motor Cortex. *Journal of Neuroscience*, *25*(27), 6372–6378.

Roe, A. W., Chelazzi, L., Connor, C. E., Conway, B. R., Fujita, I., Gallant, J. L., ... Vanduffel, W. (2012, April). Toward a unified theory of visual area V4. *Neuron*, *74*(1), 12–29.

Romei, V., Driver, J., Schyns, P. G., & Thut, G. (2011, February). Rhythmic TMS over Parietal Cortex Links Distinct Brain Frequencies to Global versus Local Visual

Processing. *Current Biology*, *21*(4), 334–337.

Romei, V., Gross, J., & Thut, G. (2010, June). On the Role of Prestimulus Alpha Rhythms over Occipito-Parietal Areas in Visual Input Regulation: Correlation or Causation? *Journal of Neuroscience*, *30*(25), 8692–8697.

Rush, S., & Driscoll, D. A. (1968, November). Current distribution in the brain from surface electrodes. *Anesthesia and analgesia*, *47*(6), 717–723.

Saiote, C., Turi, Z., Paulus, W., & Antal, A. (2013). Combining functional magnetic resonance imaging with transcranial electrical stimulation. *Frontiers in human ...*, *7*, 435.

Salih, F., Sharott, A., Khatami, R., Trottenberg, T., Schneider, G., Kupsch, A., ... Grosse, P. (2009, February). Functional connectivity between motor cortex and globus pallidus in human non-REM sleep. *The Journal of Physiology*, *587*(5), 1071–1086.

Sanes, J. N., & Donoghue, J. P. (2000). Plasticity and primary motor cortex. *Annual review of neuroscience*, *23*, 393–415.

Saper, C. B. (2002). The central autonomic nervous system: conscious visceral perception and autonomic pattern generation. *Annual review of neuroscience*, *25*, 433–469.

Schabus, M., Dang-Vu, T. T., Albouy, G., Balteau, E., Boly, M., Carrier, J., ... Maquet, P. (2007, August). Hemodynamic cerebral correlates of sleep spindles during human non-rapid eye movement sleep. *Proceedings of the National Academy of Sciences of the United States of America*, *104*(32), 13164–13169.

Schabus, M., Gruber, G., Parapatics, S., Sauter, C., Klösch, G., Anderer, P., ... Zeitlhofer, J. (2004). Sleep spindles and their significance for declarative memory consolidation. *Sleep*, *27*(8), 1479–1485.

Schacter, S., & Singer, J. E. (1962). [CITATION][C]. *Psychosomatic Medicine*.

Schröder, C. M. (2010, March). Sleep deprivation and emotion recognition. *Sleep*, *33*(3), 281–282.

Schroeder, M. J., & Barr, R. E. (2001, November). Quantitative analysis of the electroencephalogram during cranial electrotherapy stimulation. *Clinical neurophysiology : official journal of the International Federation of Clinical Neurophysiology*,

112(11), 2075–2083.

Schutter, D. J. L. G., & Hortensius, R. (2010, July). Clinical Neurophysiology. *Clinical Neurophysiology*, *121*(7), 1080–1084.

Sejnowski, T. J. (2006, February). Network Oscillations: Emerging Computational Principles. *Journal of Neuroscience*, *26*(6), 1673–1676.

Silvanto, J., Muggleton, N., & Walsh, V. (2008, December). State-dependency in brain stimulation studies of perception and cognition. *Trends in Cognitive Sciences*, *12*(12), 447–454.

Spoormaker, V. I., Czisch, M., Maquet, P., & Jancke, L. (2011, September). Large-scale functional brain networks in human non-rapid eye movement sleep: insights from combined electroencephalographic/functional magnetic resonance imaging studies. *Philosophical Transactions of the Royal Society A: Mathematical, Physical and Engineering Sciences*, *369*(1952), 3708–3729.

Spoormaker, V. I., Schroter, M. S., Gleiser, P. M., Andrade, K. C., Dresler, M., Wehrle, R., ... Czisch, M. (2010, August). Development of a Large-Scale Functional Brain Network during Human Non-Rapid Eye Movement Sleep. *Journal of Neuroscience*, *30*(34), 11379–11387.

Steriade, M. (2001). Impact of network activities on neuronal properties in corticothalamic systems. *Journal of Neurophysiology*.

Steriade, M., Curró Dossi, R., & Contreras, D. (1993, September). Electrophysiological properties of intralaminar thalamocortical cells discharging rhythmic (approximately 40 HZ) spike-bursts at approximately 1000 HZ during waking and rapid eye movement sleep. *Neuroscience*, *56*(1), 1–9.

Steriade, M., & McCarley, R. (2005). Brain control of wakefulness and sleep.

Sterpenich, V., Albouy, G., Boly, M., Vandewalle, G., Darsaud, A., Balteau, E., ... Gais, S. (2007). Sleep-related hippocampo-cortical interplay during emotional memory recollection. *PLoS biology*, *5*(11), e282.

Stickgold, R., & Walker, M. (2004). To sleep, perchance to gain creative insight? *Trends in Cognitive Sciences*.

Stickgold, R., & Walker, M. P. (2007, June). Sleep-dependent memory consolidation and reconsolidation. *Sleep Medicine*, *8*(4), 331–343.

Talati, A., & Hirsch, J. (2005). Functional specialization within the medial frontal gyrus for perceptual go/no-go decisions based on "what," "when," and "where" related information: an fMRI study. *Journal of Cognitive Neuroscience*.

Thom, N., Johnson, D. C., Flagan, T., Simmons, A. N., Kotturi, S., Van Orden, K. F., ... Paulus, M. P. (2012, November). Detecting Emotion in Others: Increased Insula and Decreased Medial Prefrontal Cortex Activation During Emotion Processing in Elite Adventure Racers. *Social Cognitive and Affective Neuroscience*.

Thut, G., & Miniussi, C. (2009, April). New insights into rhythmic brain activity from TMS–EEG studies. *Trends in Cognitive Sciences*, *13*(4), 182–189.

Thut, G., Veniero, D., Romei, V., Miniussi, C., Schyns, P., & Gross, J. (2011, July). Rhythmic TMS Causes Local Entrainment of Natural Oscillatory Signatures. *Current Biology*, *21*(14), 1176–1185.

Tononi, G. (2009). Slow wave homeostasis and synaptic plasticity. *Journal of clinical sleep medicine : JCSM : official publication of the American Academy of Sleep Medicine*, *5*(2 Suppl), S16–9.

Urbain, N., Gervasoni, D., Soulière, F., Lobo, L., Rentéro, N., Windels, F., ... Chouvet, G. (2000, September). Unrelated course of subthalamic nucleus and globus pallidus neuronal activities across vigilance states in the rat. *The European journal of neuroscience*, *12*(9), 3361–3374.

Ushimaru, M., Ueta, Y., & Kawaguchi, Y. (2012, February). Differentiated Participation of Thalamocortical Subnetworks in Slow/Spindle Waves and Desynchronization. *Journal of Neuroscience*, *32*(5), 1730–1746.

van der Helm, E., Gujar, N., & Walker, M. P. (2010, March). Sleep deprivation impairs the accurate recognition of human emotions. *Sleep*, *33*(3), 335–342.

van der Helm, E., & Walker, M. P. (2012). Sleep and Affective Brain Regulation. *Social and Personality ....*

van der Helm, E., Yao, J., Dutt, S., Rao, V., Saletin, J. M., & Walker, M. P. (2011, November). REM Sleep Depotentiates Amygdala Activity to Previous Emotional Experiences. *Current Biology*, 1–4.

Vanderwolf, C. H., & Stewart, D. J. (1988, April). Thalamic control of neocortical activation: a critical re-evaluation. *Brain research bulletin*, *20*(4), 529–538.

Venkatraman, V., Huettel, S. A., Chuah, L. Y. M., Payne, J. W., & Chee, M. W. L. (2011, March). Sleep Deprivation Biases the Neural Mechanisms Underlying Economic Preferences. *Journal of Neuroscience*, *31*(10), 3712–3718.

Vetrivelan, R., Qiu, M.-H., Chang, C., & Lu, J. (2010). Role of Basal Ganglia in Sleep–Wake Regulation: Neural Circuitry and Clinical Significance. *Frontiers in Neuroanatomy*, *4*.

Wach, C., Krause, V., Moliadze, V., Paulus, W., Schnitzler, A., & Pollok, B. (2013, March). Behavioural Brain Research. *Behavioural Brain Research*, *241*, 1–6.

Wagner, U., Gais, S., & Born, J. (2001, March). Emotional memory formation is enhanced across sleep intervals with high amounts of rapid eye movement sleep. *Learning & Memory*, *8*(2), 112–119.

Walker, M. P. (2005). A refined model of sleep and the time course of memory formation. *The Behavioral and brain sciences*, *28*(1), 51–64; discussion 64–104.

Walker, M. P. (2010, December). In Sleep Lost, Emotions Become Unrecognized: Commentary on Minkel et al.'s, "Emotional Expressiveness in Sleep-Deprived Healthy Adults". *Behavioral Sleep Medicine*, *9*(1), 15–17.

Walker, M. P., Brakefield, T., Morgan, A., Hobson, J. A., & Stickgold, R. (2002, July). Practice with sleep makes perfect: sleep-dependent motor skill learning. *Neuron*, *35*(1), 205–211.

Walker, M. P., Liston, C., Hobson, J. A., & Stickgold, R. (2002). Cognitive flexibility across the sleep-wake cycle: REM-sleep enhancement of anagram problem solving. *Brain research Cognitive brain research*, *14*(3), 317–324.

Walker, M. P., Stickgold, R., Alsop, D., Gaab, N., & Schlaug, G. (2005). Sleep-dependent motor memory plasticity in the human brain. *Neuroscience*, *133*(4), 911–917.

Walker, M. P., & van der Helm, E. (2009). Overnight therapy? The role of sleep in emotional brain processing. *Psychological Bulletin*, *135*(5), 731–748.

Watson, D., Clark, L. A., & Tellegen, A. (1988, June). Development and validation of brief measures of positive and negative affect: the PANAS scales. *Journal of personality and social psychology*, *54*(6), 1063–1070.

Watson, R. T., Valenstein, E., & Heilman, K. M. (1981, August). Thalamic neglect. Possible role of the medial thalamus and nucleus reticularis in behavior. *Archives*

of Neurology, *38*(8), 501–506.

Wehrle, R., Kaufmann, C., Wetter, T. C., Holsboer, F., Auer, D. P., Pollmächer, T., & Czisch, M. (2007, February). Functional microstates within human REM sleep: first evidence from fMRI of a thalamocortical network specific for phasic REM periods. *European Journal of Neuroscience*, *25*(3), 863–871.

Wilhelm, I., Diekelmann, S., & Born, J. (2008, April). Sleep in children improves memory performance on declarative but not procedural tasks. *Learning & Memory*, *15*(5), 373–377.

Wu, J. C., Buchsbaum, M. S., Hershey, T. G., & Hazlett, E. (1991). PET in generalized anxiety disorder. *Biological ...*.

Yoo, S.-S., Gujar, N., Hu, P., Jolesz, F. A., & Walker, M. P. (2007, October). The human emotional brain without sleep — a prefrontal amygdala disconnect. *Current Biology*, *17*(20), R877–R878.

Zaehle, T. (2009). Inter- and intra-individual covariations of hemodynamic and oscillatory gamma responses in the human cortex. *Frontiers in Human Neuroscience*, *3*.

Zaehle, T., Rach, S., & Herrmann, C. S. (2010, November). Transcranial Alternating Current Stimulation Enhances Individual Alpha Activity in Human EEG. *PLoS ONE*, *5*(11), e13766.

Zaghi, S., Acar, M., Hultgren, B., Boggio, P. S., & Fregni, F. (2010, May). Noninvasive Brain Stimulation with Low-Intensity Electrical Currents: Putative Mechanisms of Action for Direct and Alternating Current Stimulation. *The Neuroscientist*, *16*(3), 285–307.

Zaki, J., Davis, J. I., & Ochsner, K. N. (2012, August). Overlapping activity in anterior insula during interoception and emotional experience. *NeuroImage*, *62*(1), 493–499.

Zepelin, H., & Rechtschaffen, A. (1974). Mammalian sleep, longevity, and energy metabolism. *Brain, behavior and evolution*, *10*(6), 425–470.

Zohar, D., Tzischinsky, O., Epstein, R., & Lavie, P. (2005, January). The effects of sleep loss on medical residents' emotional reactions to work events: a cognitive-energy model. *Sleep*, *28*(1), 47–54.